Catal. Sci. Technol. 2015, DOI: 10.1039/c4cy01682c.

Sporopollenin as an Efficient Green Support for Covalent Immobilization of a Lipase

Stefânia P. de Souza,[a] Jonathan Bassut, [a] Heiddy V. Marquez, [a] Ivaldo I. Junior, [a] Leandro S. M. Miranda,[a] Youkui Huang,[b] Grahame Mackenzie,[b] Andrew N. Boa,*[b] Rodrigo O. M. A. de Souza*[a]

a- Biocatalysis and Organic Synthesis Group, Chemistry Institute, Federal University of Rio de Janeiro, Brazil, CEP21941909

b- Department of Chemistry, University of Hull, Cottingham Road, Kingston upon Hull, HU6 7RX, UK

Abstract

Sporopollenin exine capsules (SECs), derived from the spores of *Lycopodium clavatum*, have been functionalised with 1,*n*-diamines and the resulting aminoalkyl microcapsules used to immobilize *Candida antarctica* lipase B (Cal B) *via* a glutaradehyde-based diimine covalent linker. The supported enzyme efficiently catalyzes the esterification of oleic acid with ethanol. Initial rates using the SEC-CalBs were comparable to the commercial enzyme Novozym 435, but displayed up to 20-fold higher specific activity. The supported enzymes could also be recycled and after four cycles displayed only a modest decrease in conversions. In a kinetic resolution the SEC-CalBs efficiently acetylated *rac*-1-phenylethanol, with conversions up to 37% after 5 hours and product enantiomeric excesses of >99%. Related to this, the dynamic resolution of *rac*-1-phenylethylamine, in the presence of Pd-$BaSO_4$ and ammonium formate, led to the acetylated amine with a 94% conversion and >99% ee.

Introduction

Enzymes may be considered the greenest catalysts that can be used for selective transformations in organic chemistry since they are biocompatible, biodegradable and derived from renewable resources. Besides that, enzyme-catalyzed reactions often require mild conditions leading to the desired products with high chemo-, regio- and enantioselectivity.[1-3]

Great advances have been obtained in this area during recent years with the advent of protein engineering enabling the production of enzymes with enhanced stability, selectivity, activity and substrate specificity.[4-9] However, the industrial applications of such enzymes are still restricted since most of them are lacking in terms of recovery efficiency and operational stability.[10-13]

One strategy that can be used to increase recovery efficiency and operational stability is enzyme immobilization. Attachment of an enzyme to a carrier can be done in different ways, amongst which are adsorption, covalent binding, entrapment and cross-linking of the enzyme to the carrier.[14, 15] The new biocatalyst obtained after immobilization has additional features that can help on process development such as low or no allergenicity, convenient handling, easy separation from product, minimal or no protein contamination in the product. In some cases, the immobilization protocol can improve enzyme performance and thus increase catalyst productivity and determine the enzyme cost per Kg of product.[16-21] In this way, the use of cheap and readily available supports is crucial for the development of economically feasible biocatalyst processes.

Spores are produced by non-seed bearing plants, for example ferns and mosses, as part of the process of reproduction. The diameter of a spore is typically within the range of 5 μm (Myosotis, forget-me-not) to 250 μm (*Cucurbita*, pumpkin); however, the particles from any particular species of plant are monodispersed and highly uniform in size and morphology. They are roughly spherical in shape and contain surface architectural features that are specific to the particular species of plant.[22] The wall of a spore particle contains two layers.[23-25] The inner layer, or intine, is made largely of cellulose, and the outer layer is made up of the polymer sporopollenin. The structure of sporopollenin is not known in detail, but it is known to possess lignin-like characteristics and contains cross-linked lipids and cinnamic acid derivatives.[26] The lack of definitive knowledge of its structure is in part due to sporopollenin's chemical and physical robustness; it is hard to degrade unless strongly oxidizing conditions are used.[22, 27, 28] However, this particular property means that the genetic material contained within the spore can be removed easily to leave behind an empty shell, or microcapsule, which retains the same morphology and similar size of the parent spore.[29-31] The highly uniform

sporopollenin exine capsules (SECs) are capable of encapsulating a large variety of substances with potential uses in a wide range of applications such as drug delivery,[30, 32] foods[33] and cosmetics.[34]

Lycopodium clavatum was chosen for this study since the spores can be sourced in bulk quantities from various suppliers in several countries around the world, thus making them a viable renewable and sustainable raw material. A long-established protocol for the extraction of SECs from *L. clavatum* spores involves sequential treatment with acetone, potassium hydroxide and phosphoric acid.[30, 35, 36] This extraction produces a SEC that is free of protein on the basis of nitrogen combustion elemental analysis, MALDI-TOF-MS and ESI-QqToF-MS.[30] Surface functional groups on the SEC are known to include carboxylic acids,[31, 37] alcohols[38] and phenols,[39] and the foremost of these have been shown to be a useful point of derivatisation of the SECs through formation of an amide link.[37, 40, 41] Such functional group availability and variety open several potential opportunities to use SECs as conjugates and solid supports. For the present study, SECs from *L. clavatum* spores were envisaged as a particularly attractive candidate as a solid support for enzyme catalysis since not only do they have sites in sufficient quantity for attachment it was also known that the SECs are not deleterious to the activity of enzymes but are extremely stable to a wide range of digestive enzymes.[29, 42-44] In addition, batch variability of SECs from *L. clavatum* spores is minimal since they are incredibly consistent in chemical composition, size, and morphology seemingly irrespective of where in the world the bulk spores are sourced.[22, 28]

Previously SECs have been used to encapsulate the lipase from *Candida rugosa* by simple adsorption[42] and also as part of a siloxane-based gel matrix.[45] In this work, SECs extracted from *L. clavatum* were derivatised using a sequence of permethylation of the alcohol, phenol and acid groups on the surface of the exines, followed by amination

of the resulting methyl ester functions using a range of aliphatic 1,*n*-diamines. This generated a range of hydrophobic SECs with pendant aminoalkyl chains. Six different types of these functionalized SECs were used as supports for the covalent immobilization of lipase B of *Candida antarctica* (CaL B). For this purpose, an amino function from the functionalized support was reacted with glutaraldehyde and then covalently bonded to the lipase. It was anticipated that covalent attachment would provide greater stability for the enzyme without the need for a gel-matrix co-encapsulant, Also, recognizing that these enzymes work most efficiently at hydrophobic-hydrophilic interfaces, we anticipated that the hydrophobic surface of the SECs, resulting from permethylation could facilitate lipase-catalysed reactions. The new immobilized biocatalyst was applied to the kinetic resolution of *sec*-phenylethanol and dynamic resolution of *rac*-1-phenylethylamine.

Materials and Methods

Preparation of amino functionalized sporopollenin exine capsules (SECs).

1. **Extraction of sporopollenin exine capsules from raw spores:**

Spores (125 g) from *L. clavatum* L. (27 μm type, from Unikem - Denmark) were stirred in acetone (375 cm^3) with heating under reflux for 4 h. The 'defatted' spores were recovered by filtration and then dried under vacuum. The spores were then stirred under reflux with 6% KOH (560 cm^3) for 6 h at 80 °C. Then the KOH solution was refreshed and heating was continued for a further 6 h at 80 °C. After cooling, the spores were recovered by filtration and washed with hot water until the filtrate was neutral and uncoloured. The spores were then dried under vacuum overnight. Next the particles were then suspended in *ortho*-phosphoric acid (85%, 600 cm^3) and stirred under reflux for 7 days at reflux. The acid-hydrolyzed spores were recovered by filtration, washed successively with water (5 × 200 cm^3), acetone (200 cm^3), HCl (2 M, 200 cm^3), NaOH (2 M, 200 cm^3), water (5×200 cm^3), acetone (200 cm^3) and finally ethanol (2×200 cm^3). The

particles were recovered by filtration and dried under vacuum overnight to a constant weight. Elemental combustion analysis (Carlo Erba EA 1108 CHNS analyzer – supplied by Fisons) revealed the exines were nitrogen-free.

2. Methylation of sporopollenin exine capsules

To a stirred suspension of sporopollenin exine capsules (20 g) in acetone (300 cm^3) was added anhydrous powdered potassium carbonate (110 g). Dimethyl sulfate (38.0 cm^3) was added in portions over 10 mins at RT. After the addition was complete the mixture was heated at reflux for 3 h. After cooling, the mixture was filtered and the exine capsules washed with ethyl acetate (3 × 100 cm^3). Water (3 × 100 cm^3) was added to dissolve potassium carbonate, filtered and then the exine capsules washed with methanol (3 × 100 cm^3) and DCM (3 × 100 cm^3), before being dried under vacuum overnight to a constant weight.

3. Amination of methylated sporopollenin exine capsules

Typical procedure: The methylated sporopollenin exine capsules (2 g) and 1,6-diaminohexane (18.0 cm^3, 0.134 mmol) were suspended in xylene (30 cm^3) and the mixture was heated under reflux for 2 h with stirring and using a Dean-Stark trap. After cooling, the aminated sporopollenin exine capsules were filtered (sinter porosity grade 4), and washed successively with xylene (3 × 30 cm^3), HCl (2 M, 2 × 20 cm^3) and NaOH (2 M, 2 × 20 cm^3). The solid was then washed with deionised water (5 × 200 cm^3) until the conductivity of the filtrate was less than 20μS cm^{-1}. Finally the aminated sporopollenin exine capsules were washed successively with methanol (3 × 30 cm^3) and DCM (3 × 30 cm^3) and the particles were then dried to a constant weight under vacuum overnight.

SECs with other linker groups were prepared using the appropriate 1,*n*-diamine, and different loading levels were achieved by extending the reaction time or quantity of amine added. The total loading of nitrogen was determined by elemental combustion

analysis, and the free amine content was calculated as being half of the total nitrogen content (Table 1).

Immobilization conditions

For each support, proportional volumes of glutaraldehyde (25%) were calculated taking into account the loading of free amino groups present on the surface. The required amount was added to 20 ml of phosphate buffer, pH 7.0, and the system was stirred for 2 h at 40 °C, followed by filtering under vacuum and drying over night at ambient temperature. The final supports were subjected to the following lipase immobilization process: 1 mL of the enzyme solution (8.7 mg/mL, measured by the Bradford method) was dissolved in 3 mL of 0.025 mM phosphate buffer pH 7.0, and added to support (1 g) The mixture was agitated for 2 h at 40 °C using a flask shaker, before being filtered and dried under vacuum and drying over night at ambient temperature. Immobilization efficiency was evaluated by the difference between initial amount of enzyme added and that in the supernatant after filtration of the SEC-immobilized enzymes.

Esterification Reactions

The immobilized lipases (10 mg of support in 1 mL of reaction media) were evaluated in an esterification reaction between oleic acid and ethanol (1:1 – 100 mM in n-heptane) at different temperatures. The reactions were performed in cryotubes under 200 rpm of agitation on a shaker. Samples (10 μL) were collected after 1 h. For calculation of the initial reaction velocities, reaction times were varied from 5, 10, 15, 20, and 30 min. For thermal stability, reactions were investigated at 50 – 70 °C. All quantifications were done by GC-MS analysis.

GC-MS analysis

The GC-MS analysis was performed by using modified method from EN 14105. Reaction products were transformed into more volatile silylated derivatives by treatment with *N*-methyl-*N*-trimethysilyltrifluoroacetamide (MSTFA). All GC-MS measurements were carried out in duplicate (Dizge & Keskinler; 2008) using a DB 5–HT (Agilent, J & W. Scientific®, USA) capillary column (10 m x 0.32 mm x 0.1μm). 1μl of this sample was then injected into Shimadzu CG2010 gas chromatograph.

Kinetic Resolution

rac-1-Phenylethanol (1 mmol, 122 mg), vinyl acetate (1 mol. eq.) as acyl donor, and 18 mg (15% w/w) of the corresponding immobilized enzyme were reacted in cyclohexane (3 mL) for 2 h, 4 h, and 5 h at 60 °C. Enantiomeric excess values (ee) were determined by chiral GC analysis (chiral column Betadex-325).

Dynamic Resolutions

rac-1-Phenylethylamine (0.3 mmol), methyl methoxyacetate (2 eq.), 5% Pd supported on $BaSO_4$ (30 mol%), molecular sieves (375 mg), Na_2CO_3 (12 mg), ammonium formate (30 mg, 1.5 eq.), 30 mg (94 mg/mmol of substrate) of the corresponding immobilized enzyme, and biphenyl (30 mg) as internal standard were reacted in toluene (3 mL). Reactions were carried out in closed 4 mL vials (equipped with a gas bubbler) for 17 h at 70 ºC. Enantiomeric excesses were determined by GC equipped with a chiral column CP-Chirasil-Dex CB. A GC-MS was used to identify by-products and to determine the relative amount of *rac*-1-phenylethylamine, *N*-(1-phenylethyl)acetamide and reaction by products.

Thermo gravimetric analysis

The TG curves were obtained in a thermogravimetric module, coupled in a thermal analyzer, both manufactured by Netzsch®. Thermogravimetric measurements were performed using a platinum sample holder containing about 10 mg of each

immobilized enzyme. Each sample was heated from 35 to 600 °C at 10 °C.min^{-1}, under atmosphere of synthetic air and N_2, both with a flow rate of 60 mL.min^{-1}

Infrared analysis

Analysis by infrared spectroscopy used a Shimadzu 8300 FTIR spectrophotometer. The spectrum was obtained with 32 scans and with 4 cm^{-1} of resolution. For the analysis, 10 mg of sample was placed in sample collector to form tablets of approximately 2 mm of thick and 5 mm in diameter, without KBr addition.

Scanning electron microscopy (SEM) analysis

All supported enzymes had their structure analysed by scanning electron microscopy (SEM) using a Zeiss EVO® 50H microscope. All micrographs were obtained from the fractured surfaces of SECs coated with gold, prepared using a Shimadzu® sputter equipment. For this, each sample was placed in a sample holder on carbon tape and were metallized under vacuum. After preparation, the samples were placed under the microscope and bombarded by an electron beam interacting with the sample's atoms. From the interaction between the electron beam and the sample and radiation that were used to form a magnified image of the sample were produced.

Results and Discussion

The amination reactions generated a range of aminoalkyl-functionalized spores, with a range of different loadings of free amine as determined by elemental analysis. All supports were subjected to an enzyme immobilization protocol for 2 hours and samples were named with a prefix SP (sporopollenin) and the number of carbon atoms in the

amino spacer group (C2, C4, C6, C8, C10, C12). An additional number was used to differentiate samples with the same linker group but differing amine loadings. The samples SP_C0 (extracted SECs) and SP_C0_1 (methylated SECs) contained no amino linker attached and were used to evaluate the non-covalent adsorption of the enzyme to the polymeric structure of sporopollenin. The immobilized enzymes were also characterized by DTG, Infrared and SEM. BET was also used but natural values of sporopollenins are very small, ranging between 3–4 m^2/g, and after immobilization the BET values dropped by one third (see supporting information for further details).

After immobilization, all biocatalysts were evaluated for their immobilization efficiency, initial rate ($mM.min^{-1}$) and specific activity (U/mg). Results of immobilization efficiency are expressed in percentage and amount of protein linked to the support (Table 1).

Table 1: Immobilization efficiency, measured by the Bradford method.

Biocatalyst	Amino Group Loading (mmol/g)	Immobilization Eficiency (%)	Amount of Protein (mg/g of support)	Initial rate ($mM \cdot min^{-1}$)	Specific activity (U/mg)
SP_C0	---	4.2	0.37	3.44	2604.0
SP_C0_1	---	26.4	2.31	3.24	403.1
SP_C2	1.11	6.9	0.6	6.36	1988.0
SP_C4	1.47	7.5	0.65	4.53	1790.0
SP_C6	0.9	7.2	0.63	4.10	1733.3
SP_C6_1	1.3	1.4	0.12	2.83	2793.2
SP_C6_2	0.91	5.6	0.49	3.86	1983.0
SP_C6_3	0.85	0.9	0.07	1.78	1842.7
SP_C6_4	0.45	9.7	0.84	2.86	895.2
SP_C8	1.12	7.1	0.62	3.65	1582.2

SP_C10	0.68	7.6	0.66	3.87	1746.0
SP_C12	1.05	8.2	0.71	2.69	1465.0

As shown on Table 1, all sporopollenin supports presented very low protein loading even for those supports where the loading of amino groups were higher, such as SP_C4. Nevertheless, very good initial rates and specific activities were obtained. All the immobilized enzymes obtained in this study presented specific activities 10 fold higher then Novozym 435 and in some cases, such as SP_C0 and SP_C6_1, the specific activity was more then 20 times higher. It is important to note that no conversion was observed in control experiments performed with sporopollenin only.

A comparison between the sporopollenin-immobilized enzymes and Novozym 435, the most used widely available immobilized enzyme, is shown in Figure 1. Novozym 435 has an initial rate of 6.73 $mM.min^{-1}$ and a specific activity of 121 U/mg, and according to desorption studies this commercial enzyme has 35 mg of protein adsorbed for each gram of support. The immobilized enzyme SP_C2 was the one that displayed an initial rate closest to that of Novozym 435, and this sample had a very high specific activity since a very low protein loading was obtained. Other enzymes such as SP_C4 and SP_C6 also performed well leading to good initial rates.

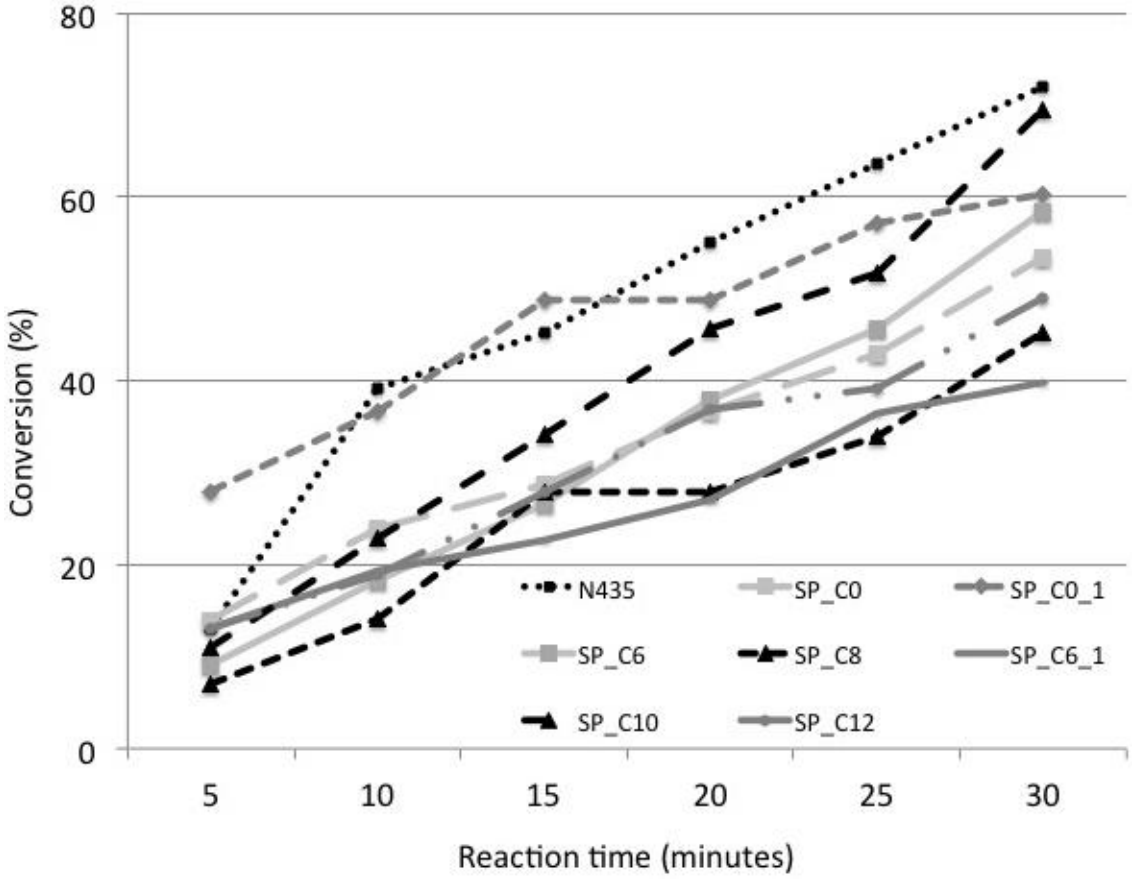
80
60
40
20
0
Conversion (%)
5
10
15
20
25
30
Reaction time (minutes)
N435
SP_C0
SP_C0_1
SP_C6
SP_C8
SP_C6_1
SP_C10
SP_C12

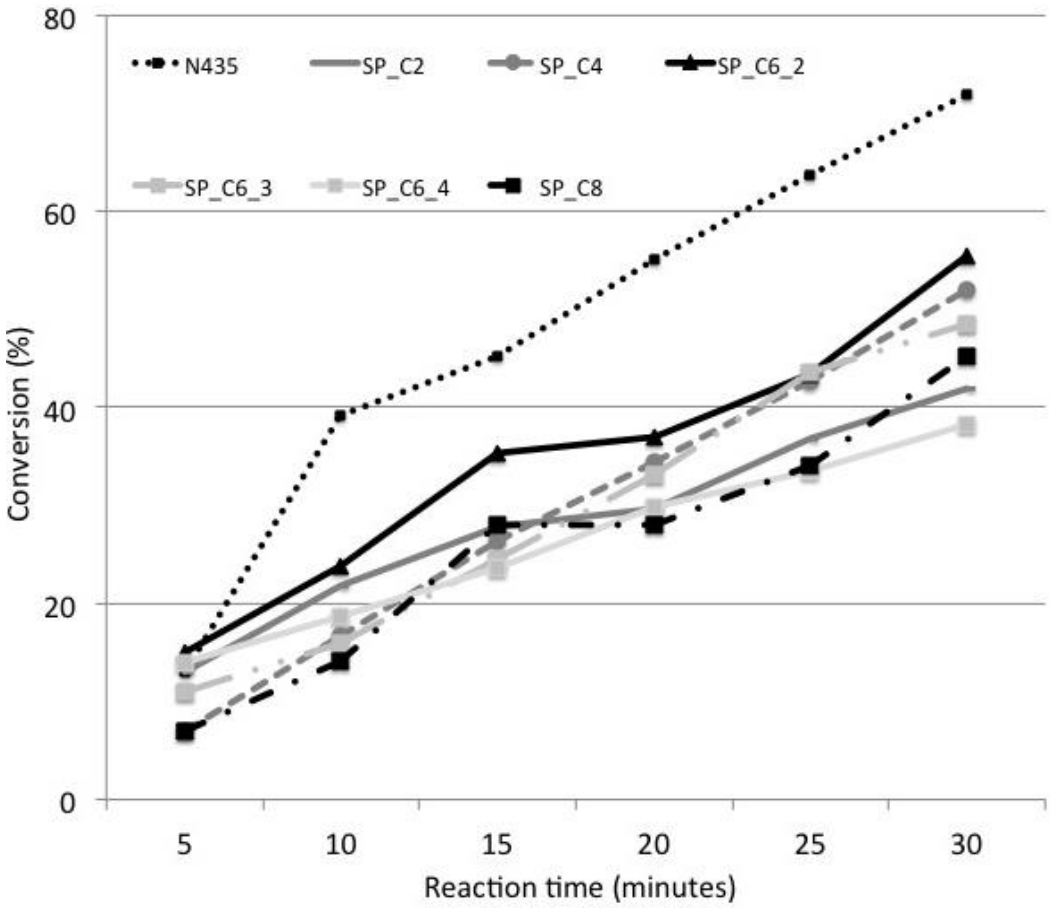
80
60
40
20
0
Conversion (%)
5
10
15
20
25
30
Reaction time (minutes)
N435
SP_C2
SP_C4
SP_C6_2
SP_C6_3
SP_C6_4
SP_C8

Figure 1: Kinetic analysis of the esterification of oleic acid, comparing Novozym 435 with the new immobilized biocatalysts. For clarity the data has been split across two graphs, each one showing the Novozym 435 as comparator.

In the first instance, according to previous work of our group, we decided to evaluate the esterification potential and thermal stability of all new biocatalysts in comparison to the commercial lipase Novozym 435 (N435). In this experiment, all reactions were studied over the course of 1 hour as described in Table 2

Table 2: Showing conversions in the esterification reaction between oleic acid and ethanol at different temperatures.

	Temperature			
Biocatalyst	40 °C	50 °C	60 °C	70 °C
N435	86	81	81	79
SP_C0	71	65	65	69
SP_C0_1	71	71	70	69
SP_C2	72	66	63	59
SP_C4	79	80	77	79
SP_C6	83	75	77	78
SP_C6_1	70	68	64	69
SP_C6_2	71	66	64	64
SP_C6_3	73	67	78	77
SP_C6_4	68	65	64	82
SP_C8	71	72	74	79

SP_C10	85	82	77	77
SP_C12	70	70	67	70

Reaction conditions: The immobilized lipases (10 mg of support in 1 mL of reaction media) were evaluated in an esterification reaction between oleic acid and ethanol (1:1 – 100 mM in *n*-heptane) at different temperatures. Reactions were performed in cryotubes under 200 rpm of agitation on a shaker.

In general, all new biocatalysts showed good conversions, comparable to Novozym 435, during the studied time and temperature. SP_C4, SP_C6 and SP_C10 presented very good conversions and thermal stabilities with results very close to those obtained with Novozyme 435. Interestingly, the SP_C6_4 immobilized enzyme showed increased conversion at higher temperature. The highest conversion at 70 °C was observed only for two enzymes SP_C6_4 and SP_C8 and this could be related to an increase on thermal stability of the enzyme by the sporopollenin support. However, it is important also to note that there are variations in the conversions for all of the samples of immobilized enzyme, and that these do not uniformly change with temperature.

Another important feature of any immobilized biocatalyst is the recyclability. All immobilized sporopollenin enzymes were subjected to recycling studies (50 °C) in order to evaluate the recyclability compared to the commercially available enzyme immobilized Novozym 435. The results are presented in Table 3.

Table 3: Recycling of immobilized biocatalysts used in the esterification of oleic acid.

	Recycles			
Biocatalyst	R1	R2	R3	R4
N435	81	85	84	79
SP_C0	65	61	67	65
SP_C0_1	70	66	65	62

SP_C2	63	61	59	56
SP_C4	77	74	75	71
SP_C6	77	57	51	43
SP_C6_C1	64	68	68	65
SP_C6_2	64	62	65	58
SP_C6_3	78	55	49	39
SP_C6_4	64	42	34	22
SP_C8	74	70	50	48
SP_C10	77	80	75	69
SP_C12	67	56	48	47

Reaction conditions: The immobilized lipases (10 mg of support in 1 mL of reaction media) were evaluated in an esterification reaction between oleic acid and ethanol (1:1 – 100 mM in n-heptane) at 50ºC. The reactions were performed in cryotubes under 200 rpm of agitation on a shaker. After reaction completion, the immobilized enzyme was filtered under vacuum and dried over night before the next run.

Most of the immobilized enzymes presented consistent recyclability results under the conditions studied, SP_C4 and SP_C10 being the best ones. The immobilized enzyme SP_C6, which showed very good thermal stability, showed a dramatic decrease in reaction conversion after the first run. The same happened with SP_C6_4 and SP_C6_3, and we believe this simply reflects variations in different batches of the amino supported exines rather than being a factor of the immobilised enzyme itself. Results were repeated three times with a maximum variation of 2% on conversion for the same batch of supports. Other batches were also tested and presented same behaviour. From the pratical point of view is difficult to recycle this immobilized biocatalyst because of the low density of sporopollenin. It is important to point out that SEM analysis of the immobilized biocatalyst before and after recycling experiments presented no change on enzyme support.

The results presented so far shows that these enzymes are able to perform an esterification reaction with good conversion, in some cases similar to Novozyme 435. However, for the development of organic chemistry protocols the most important feature is selectivity. We therefore decided to use the immobilized enzymes that presented best results on esterification reactions (SP_C4, SP_C6, and SP_C10) for the development of kinetic resolutions of alcohols and dynamic resolutions of amines.

Kinetic resolution of *rac*-1-phenylethanol using the previously selected enzymes was carried out over a period of 5 hours (Table 4). Samples were taken at 2 h, 4 h, and 5 h for conversion and selectivity evaluation. We observed that the optimum reaction time was 4 h, whereas in 5 h there was no significant change in the conversion and selectivity. All the three enzymes were highly selective with *e.e.* values greater than 99%. Regarding the conversion, it was noted that the enzymes SP_C4, SP_C6 and SP_C10 have achieved good results comparable with those obtained with Novozym 435.

Table 4: Kinetic resolution of *rac*-1-phenylethanol catalyzed by SP_C4, SP_C6 and SP_C10 immobilized enzymes.

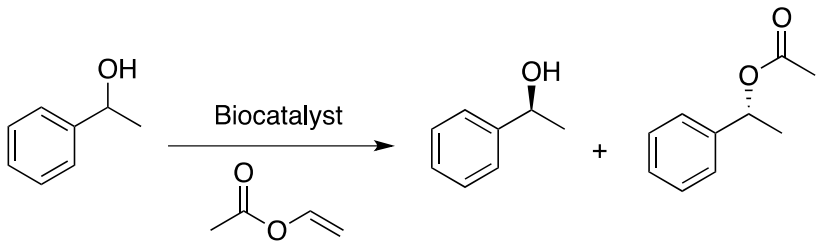

Biocatalyst	Reaction Time

	2 h		4 h		5 h	
	Conv. (%)	*e.e.*$_{prod}$	Conv. (%)	*e.e.*$_{prod}$	Conv. (%)	*e.e.*$_{prod}$
N435	51	>99	--	--	--	--
SP_C4	23	>99	26	>99	28	>99
SP_C6	28	>99	34	>99	35	>99
SP_C10	24	>99	35	>99	37	>99

Reaction conditions: *rac*-1-Phenylethanol (1 mmol), vinyl acetate (1 mol. eq.) as acyl donor, and 18 mg (15% w/w) of the corresponding immobilized enzyme were reacted in cyclohexane (3 mL) for 2 h, 4 h, and 5 h at 50 °C. Enantiomeric excess values (ee) were determined by chiral GC analysis (chiral column Betadex-325).

It is important to note that productivities of the new immobilized enzymes were 23 times higher then the commercial enzyme Novozym 435, *i.e.* SP_C4 productivity is equal to 19 mmol product. h^{-1}.mg protein^{-1} while N435 productivity equal to 0.82 mmol product h^{-1} . mg protein^{-1}. The difference observed on productivity is directed related to the amount of protein immobilized into the support.

We next evaluated the sporopollenin-immobilized enzymes in the dynamic resolution of *rac*-1-phenylethylamine (Table 5), based on a protocol already developed by our group.[46] In this protocol Pd-$BaSO_4$ is used to interconvert the amine enantiomers *via* the imine, with ammonium formate generating small quantities of hydrogen *in situ*.

Table 5: Dynamic resolution of *rac*-1-phenylethylamine catalyzed by SP_C4, SP_C6 and SP_C10 immobilized enzymes.

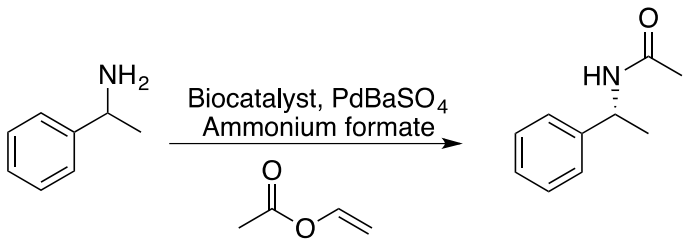

Biocatalyst	Conversion (%)	e. e. (%)
N435	87%	98
SP_C4	82%	>99
SP_C6	94%	>99
SP_C10	86%	>99

Reaction Conditions: *rac*-1-phenylethylamine (0.3 mmol), methyl methoxyacetate (2 eq.), 5% Pd supported on $BaSO_4$ (30 mol%), molecular sieves (375 mg), Na_2CO_3 (12 mg), ammonium formate (30 mg, 1.5 eq.), 30 mg (94 mg/mmol of substrate) of the corresponding immobilized enzyme, and biphenyl (30 mg) as internal standard were reacted in toluene (3 mL).

The results obtained for the dynamic resolution of *rac*-1-phenylethylamine were excellent since most immobilized enzymes presented similar results to N435, while SP_C6 have shown the highest conversion towards the desired chiral amine.

Conclusion

In conclusion we have developed new covalently immobilized lipases based on amino-functionalized sporopollenin exine capsules. These materials have very low protein loadings yet display efficient esterification, kinetic and dynamic resolution activities. The results from these new immobilized enzymes open the possibility of the development of cheap and renewable supports for enzyme immobilization in general.

Acknowledgments

The authors thank the Federal University of Rio de Janeiro, the University of Hull and the China Scholarship Council (YH) for financial support.

References

1. C. M. Clouthier and J. N. Pelletier, *Chemical Society Reviews*, 2012, **41**, 1585-1605.

2. C. C. C. R. de Carvalho, *Biotechnology Advances*, 2011, **29**, 75-83.
3. R. Wohlgemuth, *Current Opinion in Biotechnology*, 2010, **21**, 713-724.
4. U. T. Bornscheuer, G. W. Huisman, R. J. Kazlauskas, S. Lutz, J. C. Moore and K. Robins, *Nature*, 2012, **485**, 185-194.
5. J. R. Cherry and A. L. Fidantsef, *Current Opinion in Biotechnology*, 2003, **14**, 438-443.
6. R. J. Kazlauskas, *Current Opinion in Chemical Biology*, 2005, **9**, 195-201.
7. Y. Li and P. C. Cirino, *Biotechnology and Bioengineering*, 2014, **111**, 1273-1287.
8. T. Davids, M. Schmidt, D. Boettcher and U. T. Bornscheuer, *Current Opinion in Chemical Biology*, 2013, **17**, 215-220.
9. J. M. Woodley, *Current Opinion in Chemical Biology*, 2013, **17**, 310-316.
10. S. Panke, M. Held and M. Wubbolts, *Current Opinion in Biotechnology*, 2004, **15**, 272-279.
11. A. Schmid, J. S. Dordick, B. Hauer, A. Kiener, M. Wubbolts and B. Witholt, *Nature*, 2001, **409**, 258-268.
12. A. J. J. Straathof, S. Panke and A. Schmid, *Current Opinion in Biotechnology*, 2002, **13**, 548-556.
13. G.-W. Zheng and J.-H. Xu, *Current Opinion in Biotechnology*, 2011, **22**, 784-792.
14. R. A. Sheldon and S. van Pelt, *Chemical Society Reviews*, 2013, **42**, 6223-6235.
15. C. Garcia-Galan, A. Berenguer-Murcia, R. Fernandez-Lafuente and R. C. Rodrigues, *Advanced Synthesis & Catalysis*, 2011, **353**, 2885-2904.
16. D. I. Fried, F. J. Brieler and M. Froeba, *Chemcatchem*, 2013, **5**, 862-884.
17. E. Magner, *Chemical Society Reviews*, 2013, **42**, 6213-6222.
18. R. A. Sheldon, *Organic Process Research & Development*, 2011, **15**, 213-223.
19. Z. Zhou and M. Hartmann, *Topics in Catalysis*, 2012, **55**, 1081-1100.
20. Z. Zhou and M. Hartmann, *Chemical Society Reviews*, 2013, **42**, 3894-3912.
21. M. Zoumpanioti, H. Stamatis and A. Xenakis, *Biotechnology Advances*, 2010, **28**, 395-406.
22. I. Feagri and J. Iverson, in *Textbook of Pollen Analysis*, Blackwell London, 1964.
23. R. Wiermann and S. Gubatz, *International Review of Cytology*, 1992, **140**, 35-72.
24. J. R. Rowley, J. J. Skvarla and G. El-Ghazaly, *Canadian Journal of Botany-Revue Canadienne De Botanique*, 2003, **81**, 1070-1082.
25. J. Brooks and G. Shaw, *Nature*, 1968, **219**, 532.
26. P. F. Van Bergen, P. Blokker, M. E. Collinson, J. S. Sinninghe Damsté and J. W. De Leeuw, in *The Evolution of Plant Physiology. From whole plants to ecosystems.*, eds. A. R. Hemsley and I. Poole, Elsevier Academic Press, London, 2004, pp. 133-154.
27. J. Brooks and G. Shaw, *Chemical Geology*, 1972, **10**, 69-87.
28. G. Shaw, Sporopollenin, London & New York, 1971.
29. S. Barrier, A. Diego-Taboada, M. J. Thomasson, L. Madden, J. C. Pointon, J. D. Wadhawan, S. T. Beckett, S. L. Atkin and G. Mackenzie, *Journal of Materials Chemistry*, 2011, **21**, 975-981.
30. A. Diego-Taboada, L. Maillet, J. H. Banoub, M. Lorch, A. S. Rigby, A. N. Boa, S. L. Atkin and G. Mackenzie, *Journal of Materials Chemistry B*, 2013, **1**, 707-713.
31. A. Diego-Taboada, P. Cousson, E. Raynaud, Y. Huang, M. Lorch, B. P. Binks, Y. Queneau, A. N. Boa, S. L. Atkin, S. T. Beckett and G. Mackenzie, *Journal of Materials Chemistry*, 2012, **22**, 9767-9773.
32. A. Wakil, G. Mackenzie, A. Diego-Taboada, J. G. Bell and S. L. Atkin, *Lipids*, 2010, **45**, 645-649.
33. S. Barrier, A. S. Rigby, A. Diego-Taboada, M. J. Thomasson, G. Mackenzie and S. L. Atkin, *Lwt-Food Science and Technology*, 2010, **43**, 73-76.
34. S.L. Atkin, S.T. Beckett and G. Mackenzie, *WO* 2005/000280, 2005.
35. G. Shaw, in *Sporopollenin*, eds. J. Brooks, P. R. Grant, M. Muir, P. Van Gijzel and G. Shaw, Academic Press, London & New York, 1971, pp. 305-348.

36. F. Zetzsche and K. Huggler, *Justus Liebigs Annalen der Chemie*, 1928, **461**, 89-108.
37. S. Barrier, A. Lobbert, A. J. Boasman, A. N. Boa, M. Lorch, S. L. Atkin and G. Mackenzie, *Green Chemistry*, 2010, **12**, 234-240.
38. P. Fawcett, D. Green, R. Holleyhead and G. Shaw, *Grana*, 1970, **10**, 246 - 247.
39. K. Schulze Osthoff and R. Wiermann, *Journal of Plant Physiology*, 1987, **131**, 5-15.
40. G. Shaw, M. Sykes, R. W. Humble, G. Mackenzie, D. marsden and E. Pehlivan, *Reactive Polymers, Ion Exchangers, Sorbents*, 1988, **9**, 211-217.
41. R. Adamson, S. Gregson and G. Shaw, *International Journal of Peptide and Protein Research*, 1983, **22**, 560-564.
42. H. Tutar, E. Yilmaz, E. Pehlivan and M. Yilmaz, *International Journal of Biological Macromolecules*, 2009, **45**, 315-320.
43. S. Gubatz, S. Herminghaus, B. Meurer, D. Strack and R. Wiermann, *Pollen et Spores*, 1986, **28**, 347-354.
44. S. Herminghaus, S. Gubatz, S. Arendt and R. Wiermann, *Zeitschrift Für Naturforschung C-a Journal of Biosciences*, 1988, **43**, 491-500.
45. E. Yilmaz, M. Sezgin and M. Yilmaz, *Journal of Molecular Catalysis B: Enzymatic*, 2010, **62**, 162-168.
46. A. S. de Miranda, R. O. M. A. de Souza and L. S. M. Miranda, *RSC Advances*, 2014, **4**, 13620-13625.

Catal. Sci. Technol. 2015, DOI: 10.1039/c4cy01682c.

Sporopollenin as a Green and Efficient Support for Lipase Immobilization

Stefânia P. de Souza,[a] Jonathan Bassut, [a] Heiddy V. Marquez, [a] Ivaldo I. Junior, [a] Leandro S. M. Miranda,[a] Youkui Huang,[b] Grahame Mackenzie,[b] Andrew N. Boa,[b] Rodrigo O. M. A. de Souza[a]

c- Biocatalysis and Organic Synthesis Group, Chemistry Institute, Federal University of Rio de Janeiro, Brazil, CEP21941909

d- Department of Chemistry, University of Hull, Cottingham Road, Kingston-upon-Hull, HU6 7RX, UK

Supporting Information

1 . Esterification Activity

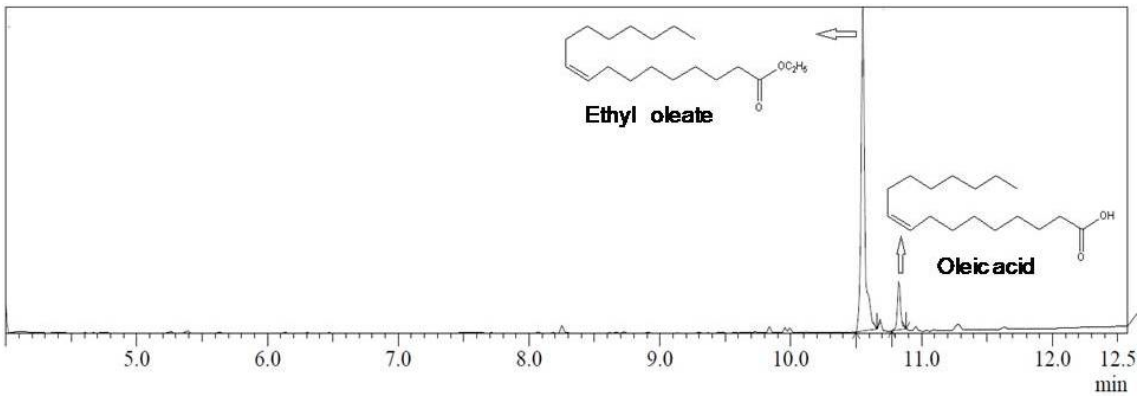

Figure S1: Esterification actitivty of Novozym 435 lipase. Experimental conditions: 10mg of support in 1mL of oleic acid and ethanol (1:1 – 100mM in n-heptane) at 40°C.

2. Kinetic Resolution Experiments

2.1 – Chromatograms of Kinetic Resolution

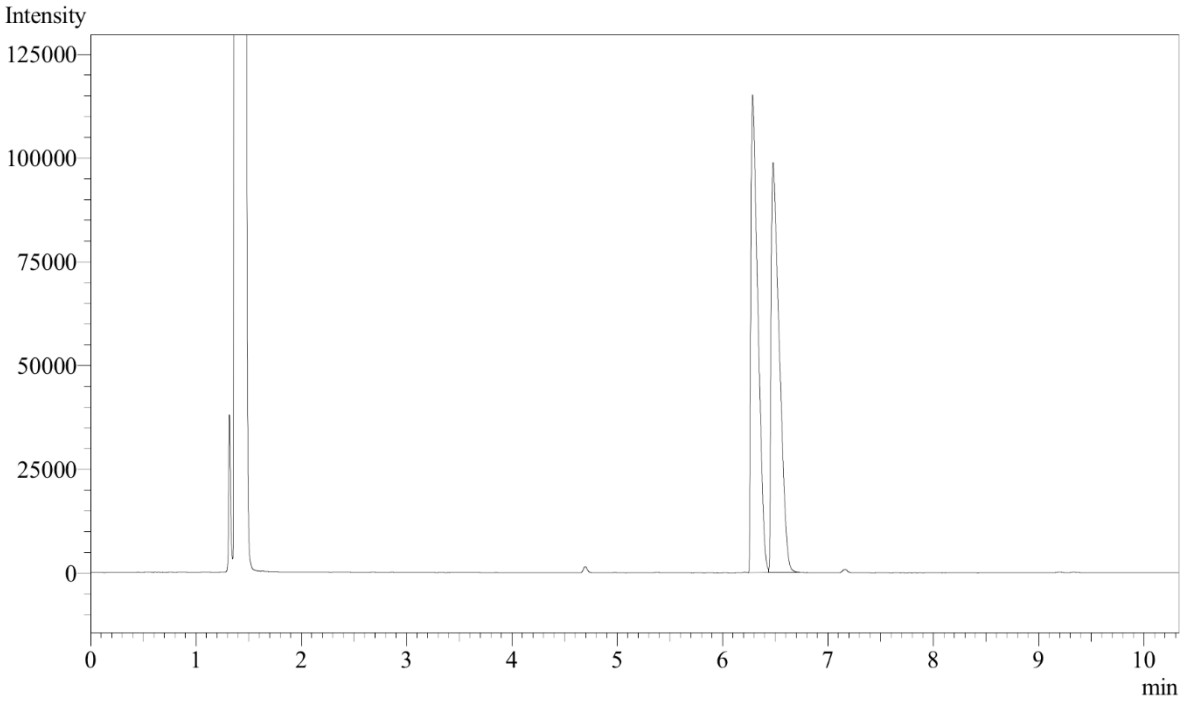

Figure S2. GC-FID of (*RS*)-1-Phenylethanol. Experimental conditions: *rac*-1-Phenylethanol (1mmol, 122mg), in cyclohexane (3 mL).

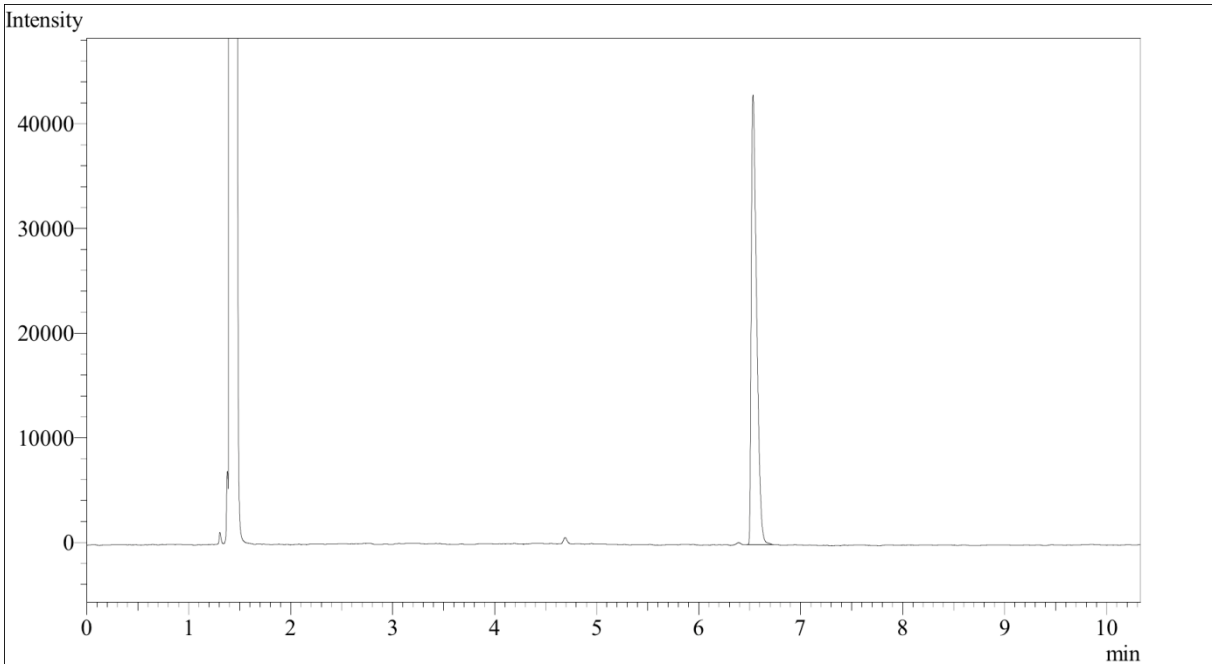

Figure S3: (*S*)-1-Phenylethanol. Experimental conditions: (S)-1-Phenylethanol (1mmol, 122mg), in cyclohexane (3 mL).

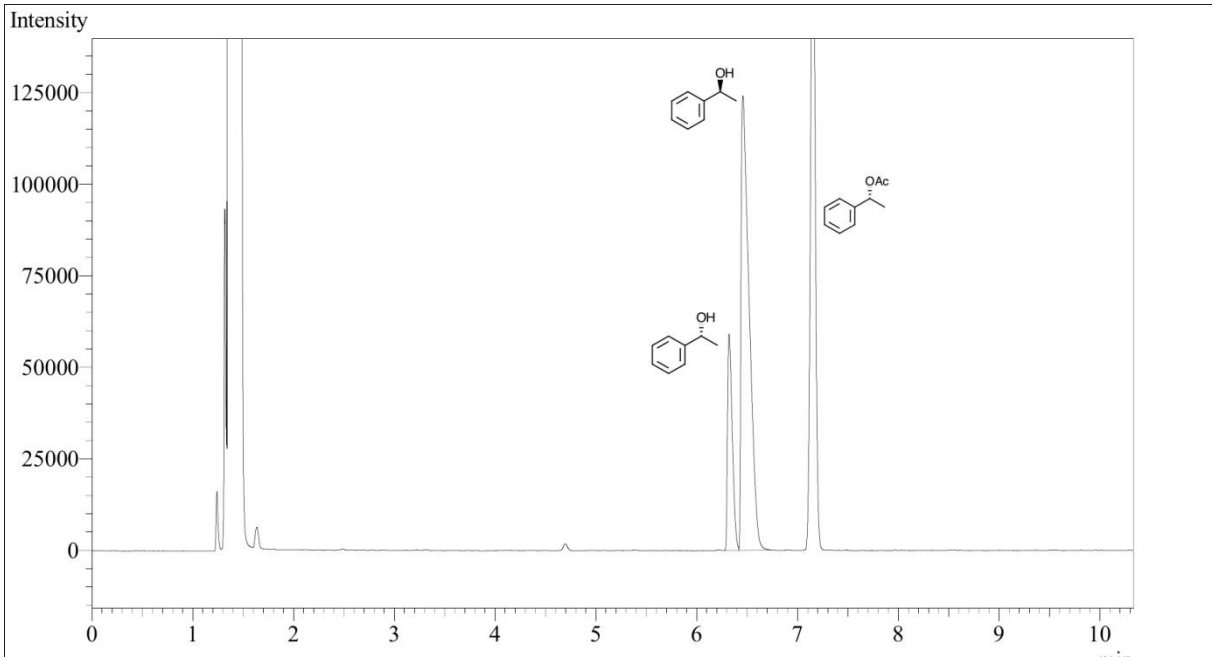

Figure S4: Kinetic Resolution of (*RS*)-1-Phenylethanol. Experimental conditions: *rac*-1-Phenylethanol (1mmol, 122mg), vinyl acetate (1eqv) as acyl donor, and 18mg (15%w/w) of Novozyme 435 in cyclohexane (3 mL) for 2 h at 60°C.

2.1.1 - Chromatograms of Kinetic Resolution in 2 Hours of Reaction

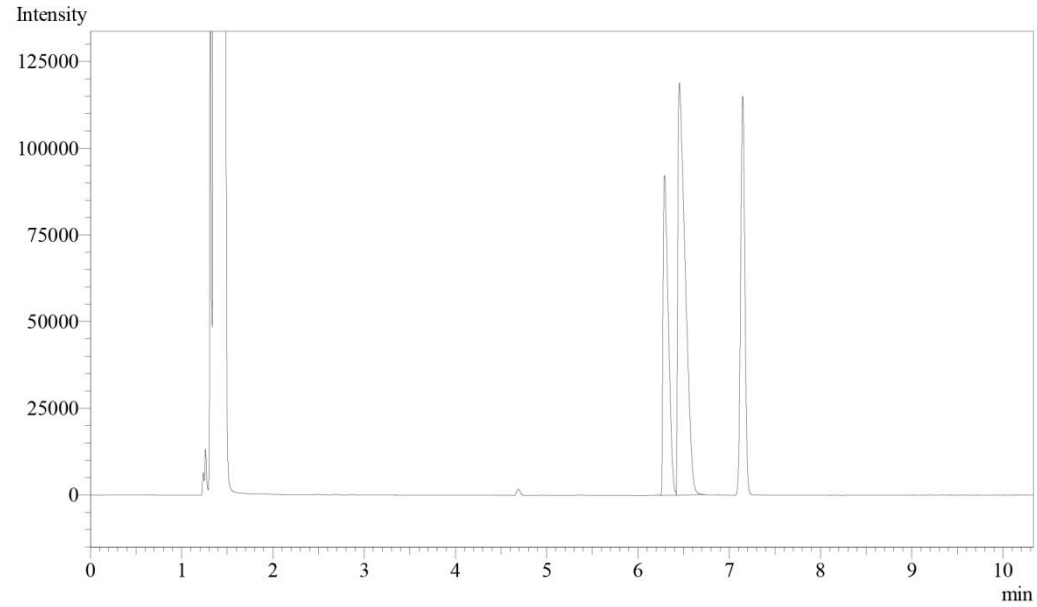

Peak#	Ret.Time	Area%
1	6,292	35,6794
2	6,455	64,3206
Total		100,0000

Figure S5. Kinetic Resolution of (*RS*)-1-Phenylethanol. Experimental conditions: *rac*-1-Phenylethanol (1mmol, 122mg), vinyl acetate (1eqv) as acyl donor, and 18mg (15%w/w) of SP_C0 in cyclohexane (3 mL) for 2 h at 60°C.

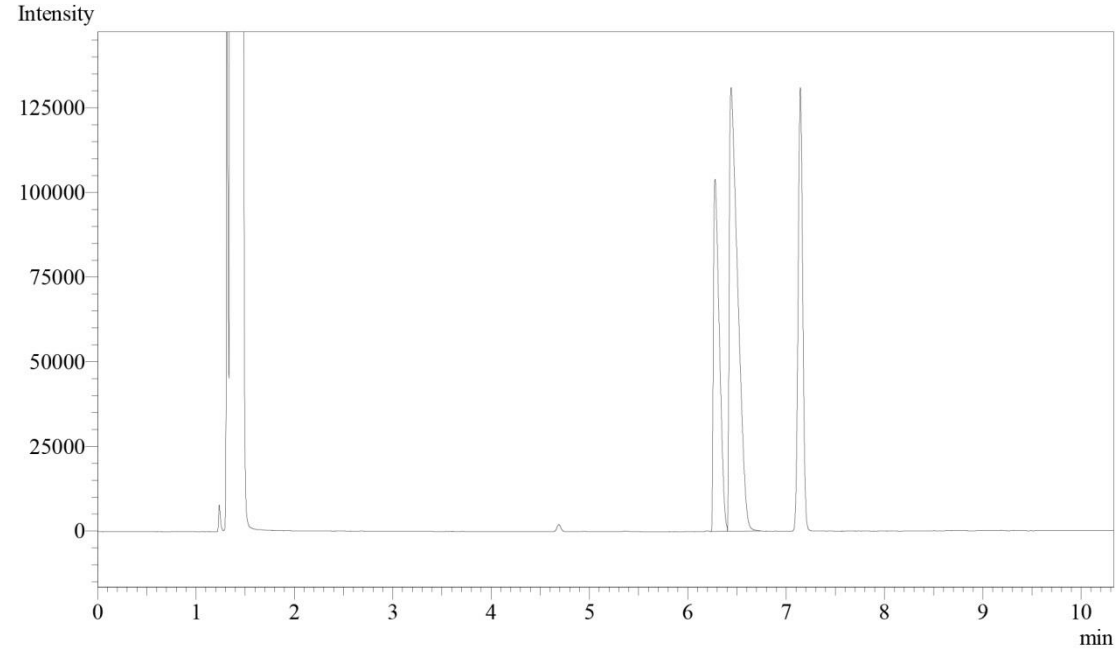

Peak#	Ret.Time	Area%
1	6,278	35,8993
2	6,441	64,1007
Total		100,0000

Figure S6. Kinetic Resolution of (*RS*)-1-Phenylethanol. Experimental conditions: *rac*-1-Phenylethanol (1mmol, 122mg), vinyl acetate (1eqv) as acyl donor, and 18mg (15%w/w) of SP_C0_1 in cyclohexane (3 mL) for 2 h at 60°C.

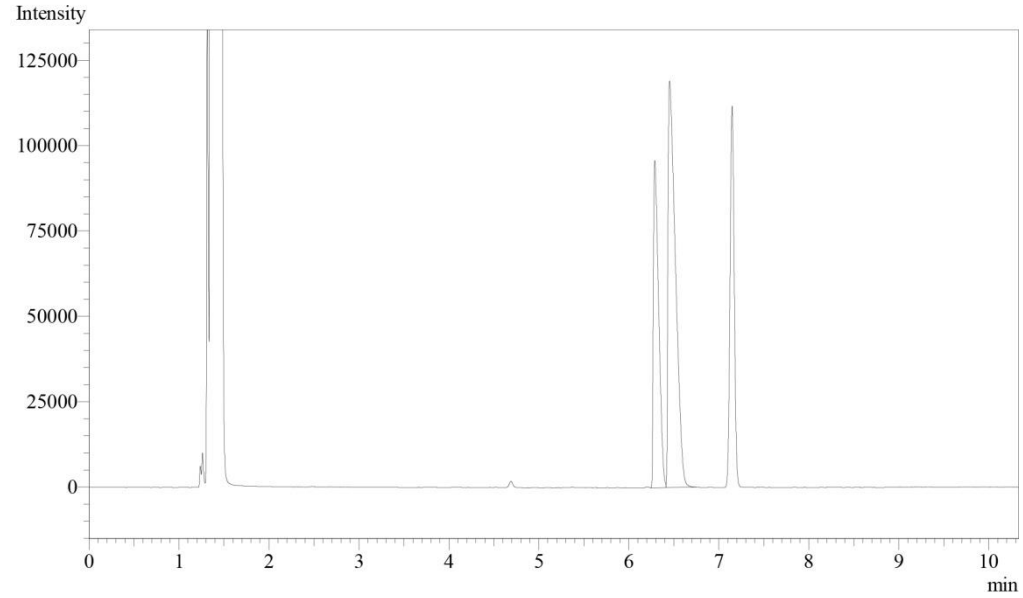

Peak#	Ret.Time	Area%
1	6,289	36,3866
2	6,453	63,6134
Total		100,0000

Figure S7. Figure S5. Kinetic Resolution of (*RS*)-1-Phenylethanol. Experimental conditions: *rac*-1-Phenylethanol (1mmol, 122mg), vinyl acetate (1eqv) as acyl donor, and 18mg (15%w/w) of SP_C2 in cyclohexane (3 mL) for 2 h at 60°C.

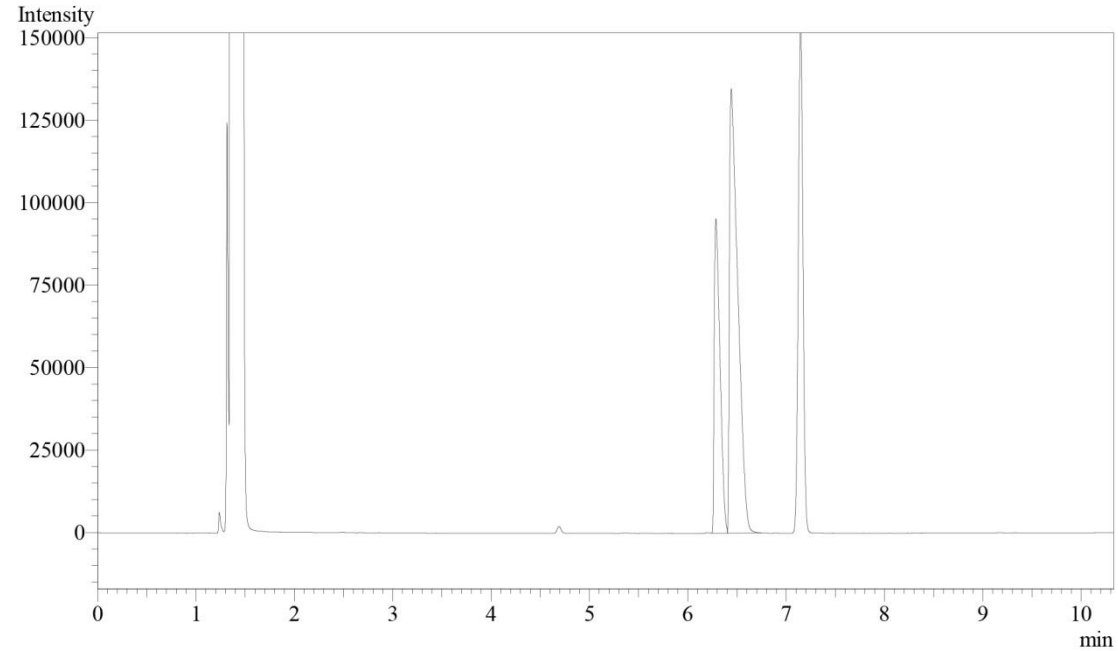

Peak#	Ret.Time	Area%
1	6,286	32,5755
2	6,443	67,4245
Total		100,0000

Figure S8. Kinetic Resolution of (*RS*)-1-Phenylethanol. Experimental conditions: *rac*-1-Phenylethanol (1mmol, 122mg), vinyl acetate (1eqv) as acyl donor, and 18mg (15%w/w) of SP_C4 in cyclohexane (3 mL) for 2 h at 60°C.

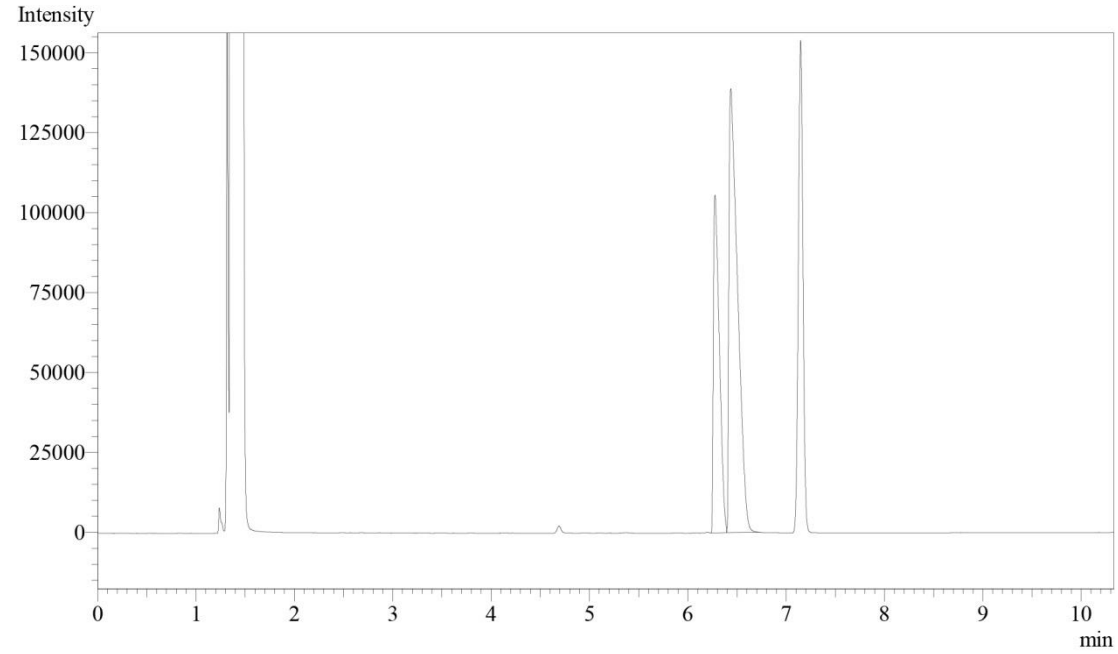

Peak#	Ret.Time	Area%
1	6,277	34,3998
2	6,438	65,6002
Total		100,0000

Figure S9. Kinetic Resolution of (*RS*)-1-Phenylethanol. Experimental conditions: *rac*-1-Phenylethanol (1mmol, 122mg), vinyl acetate (1eqv) as acyl donor, and 18mg (15%w/w) of SP_C6 in cyclohexane (3 mL) for 2 h at 60°C.

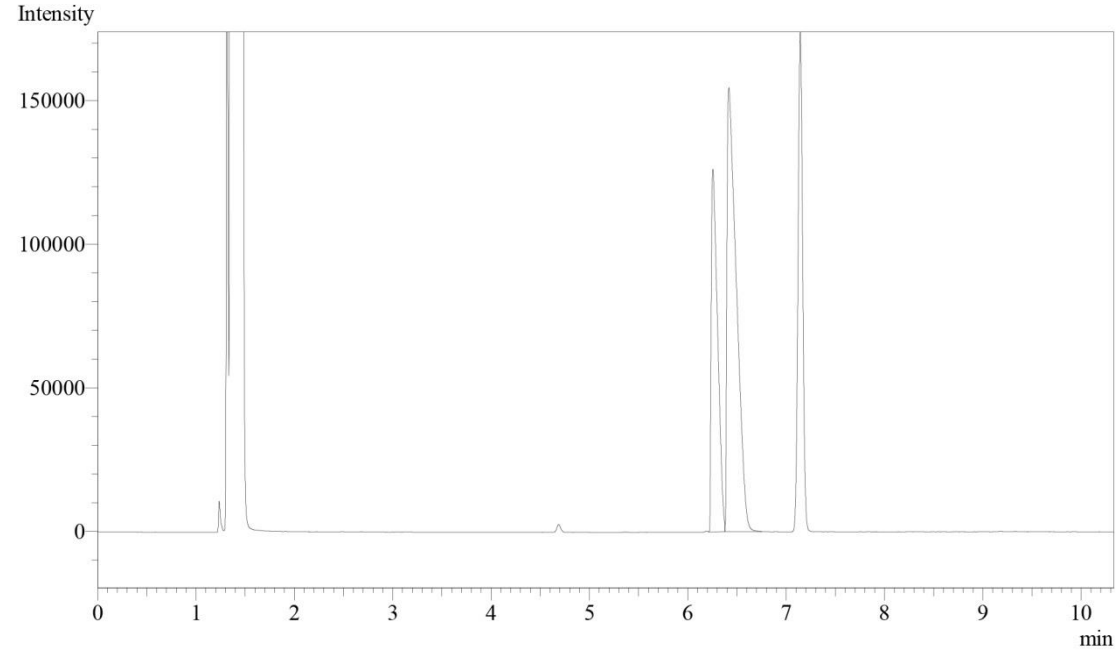

Peak#	Ret.Time	Area%
1	6,257	35,5382
2	6,419	64,4618
Total		100,0000

Figure S10 Kinetic Resolution of (*RS*)-1-Phenylethanol. Experimental conditions: *rac*-1-Phenylethanol (1mmol, 122mg), vinyl acetate (1eqv) as acyl donor, and 18mg (15%w/w) of SP_C6_1 in cyclohexane (3 mL) for 2 h at 60°C.

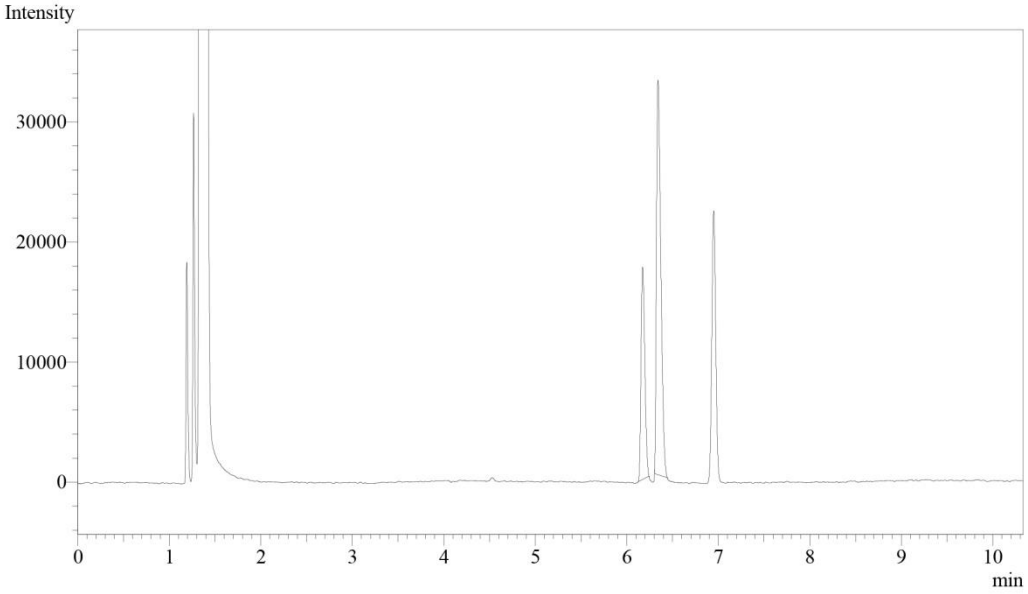

Peak#	Ret.Time	Area%
1	6,173	31,9261
2	6,341	68,0739
Total		100,0000

Figure S11 Kinetic Resolution of (*RS*)-1-Phenylethanol. Experimental conditions: *rac*-1-Phenylethanol (1mmol, 122mg), vinyl acetate (1eqv) as acyl donor, and 18mg (15%w/w) of SP_C6_2 in cyclohexane (3 mL) for 2 h at 60°C.

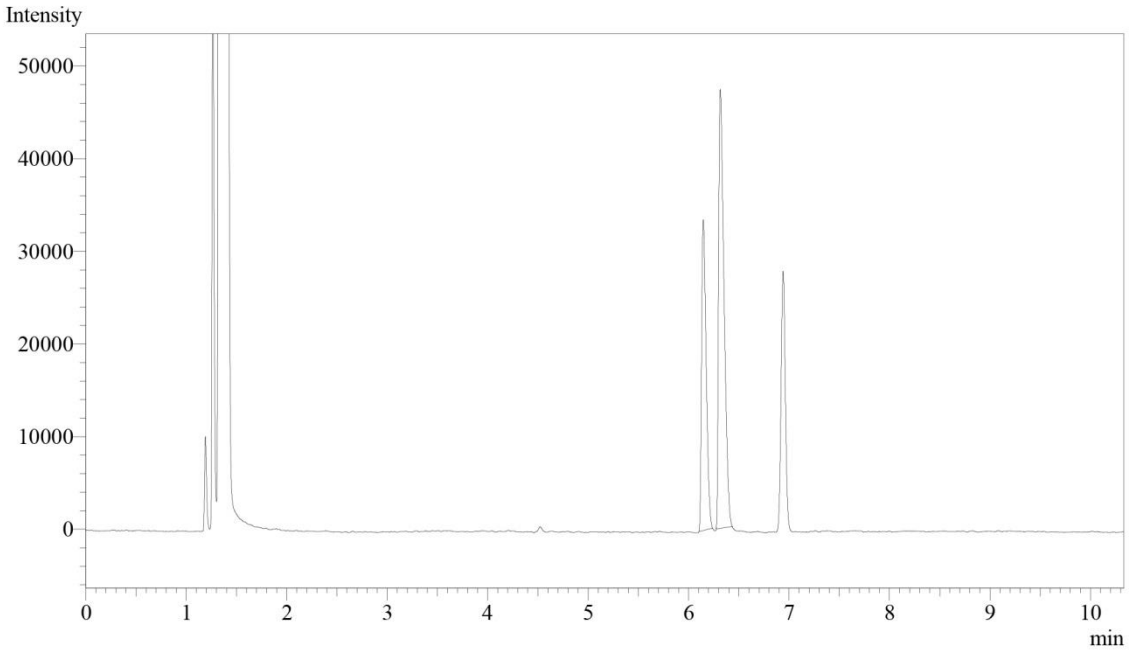

Peak#	Ret.Time	Area%
1	6,147	37,4113
2	6,316	62,5887
Total		100,0000

Figure S12 Kinetic Resolution of (*RS*)-1-Phenylethanol. Experimental conditions: *rac*-1-Phenylethanol (1mmol, 122mg), vinyl acetate (1eqv) as acyl donor, and 18mg (15%w/w) of SP_C6_3 in cyclohexane (3 mL) for 2 h at 60°C.

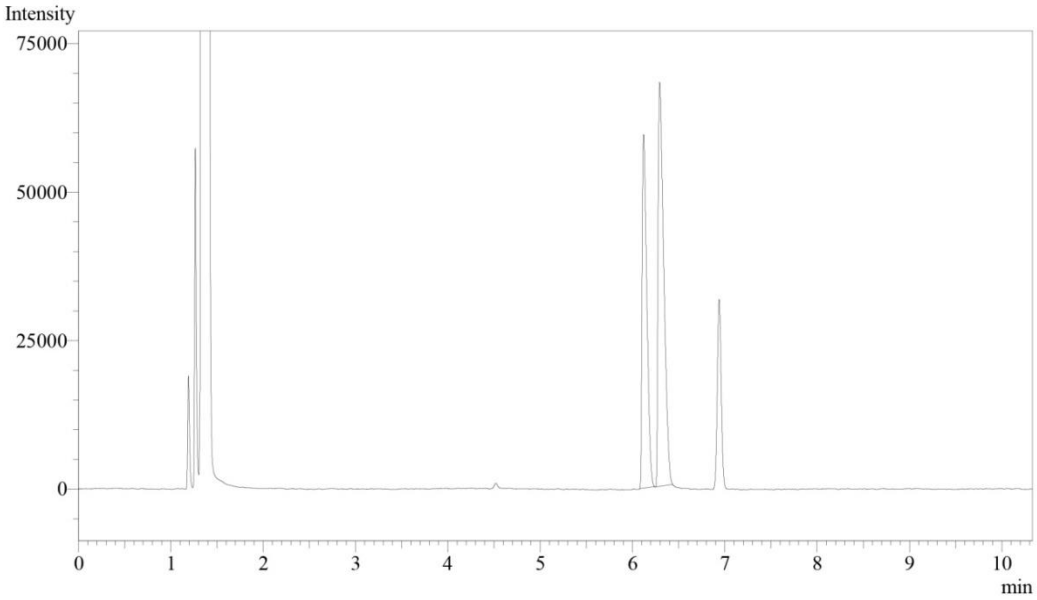

Peak#	Ret.Time	Area%
1	6,121	42,1983
2	6,295	57,8017
Total		100,0000

Figure S13. Kinetic Resolution of (*RS*)-1-Phenylethanol. Experimental conditions: *rac*-1-Phenylethanol (1mmol, 122mg), vinyl acetate (1eqv) as acyl donor, and 18mg (15%w/w) of SP_C6_4 in cyclohexane (3 mL) for 2 h at 60°C.

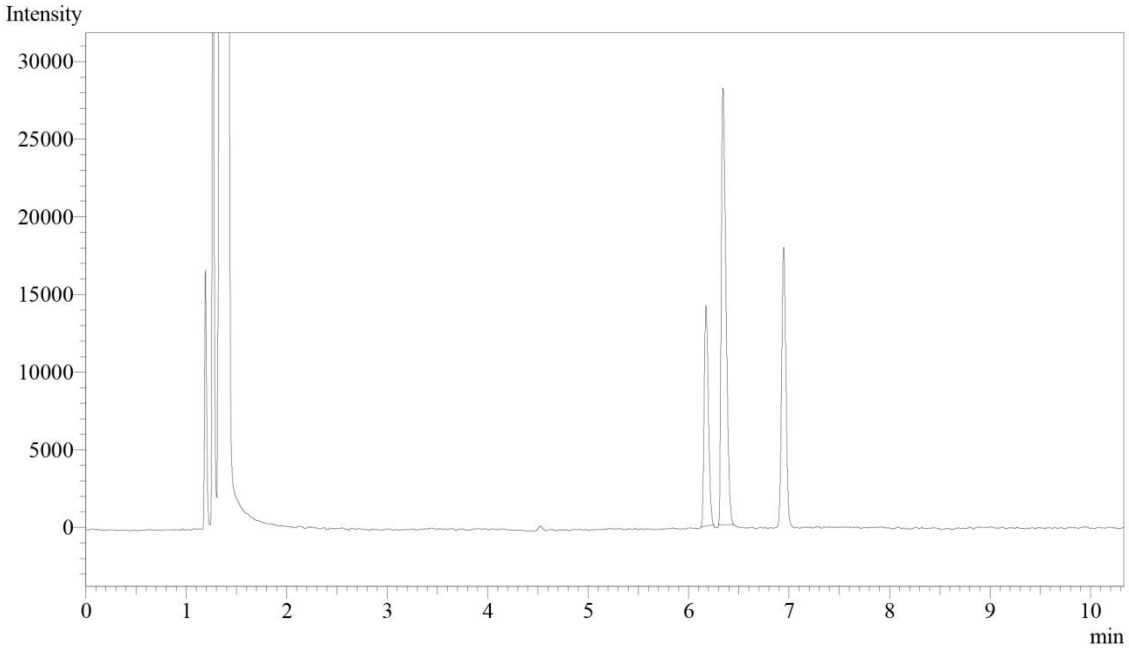

Peak#	Ret.Time	Area%
1	6,173	30,9184
2	6,342	69,0816
Total		100,0000

Figure S14. Kinetic Resolution of (*RS*)-1-Phenylethanol. Experimental conditions: *rac*-1-Phenylethanol (1mmol, 122mg), vinyl acetate (1eqv) as acyl donor, and 18mg (15%w/w) of SP_C8 in cyclohexane (3 mL) for 2 h at 60°C.

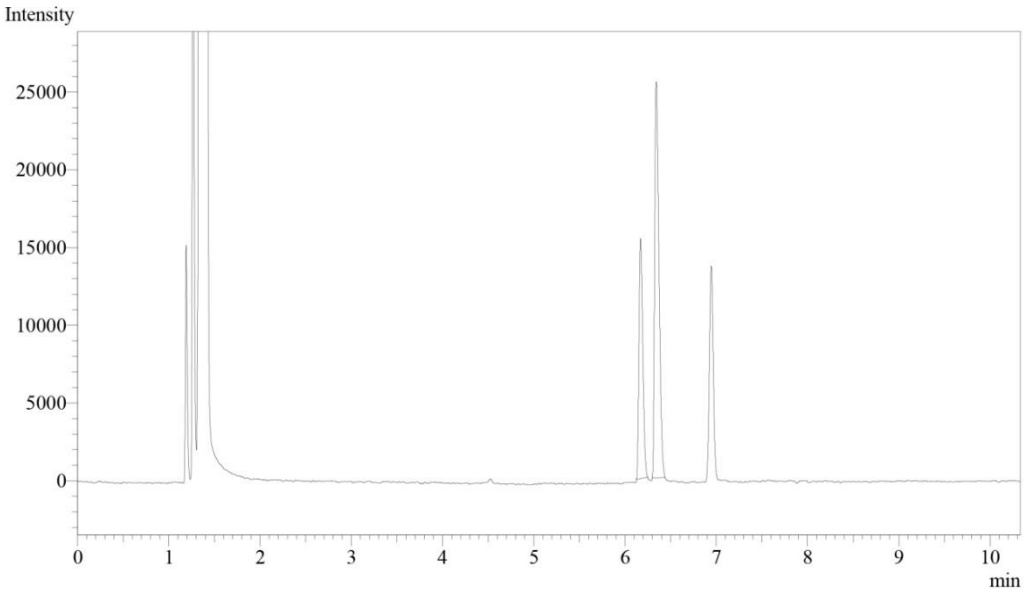

Peak#	Ret.Time	Area%
1	6,170	35,2308
2	6,343	64,7692
Total		100,0000

Figure S15. Kinetic Resolution of (*RS*)-1-Phenylethanol. Experimental conditions: *rac*-1-Phenylethanol (1mmol, 122mg), vinyl acetate (1eqv) as acyl donor, and 18mg (15%w/w) of SP_C10 in cyclohexane (3 mL) for 2 h at 60°C.

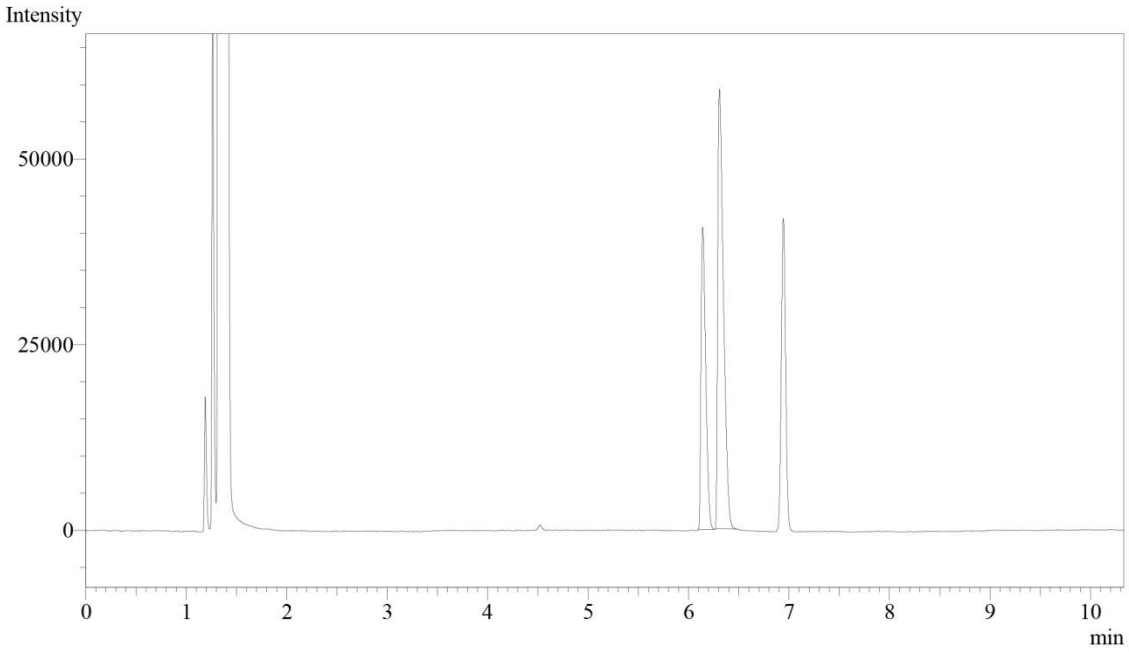

Peak#	Ret.Time	Area%
1	6,141	35,9938
2	6,308	64,0062
Total		100,0000

Figure S16. Kinetic Resolution of (*RS*)-1-Phenylethanol. Experimental conditions: *rac*-1-Phenylethanol (1mmol, 122mg), vinyl acetate (1eqv) as acyl donor, and 18mg (15%w/w) of SP_C12 in cyclohexane (3 mL) for 2 h at 60°C.

2.1.2 - Chromatograms of Kinetic Resolution in 4 Hours of Reaction

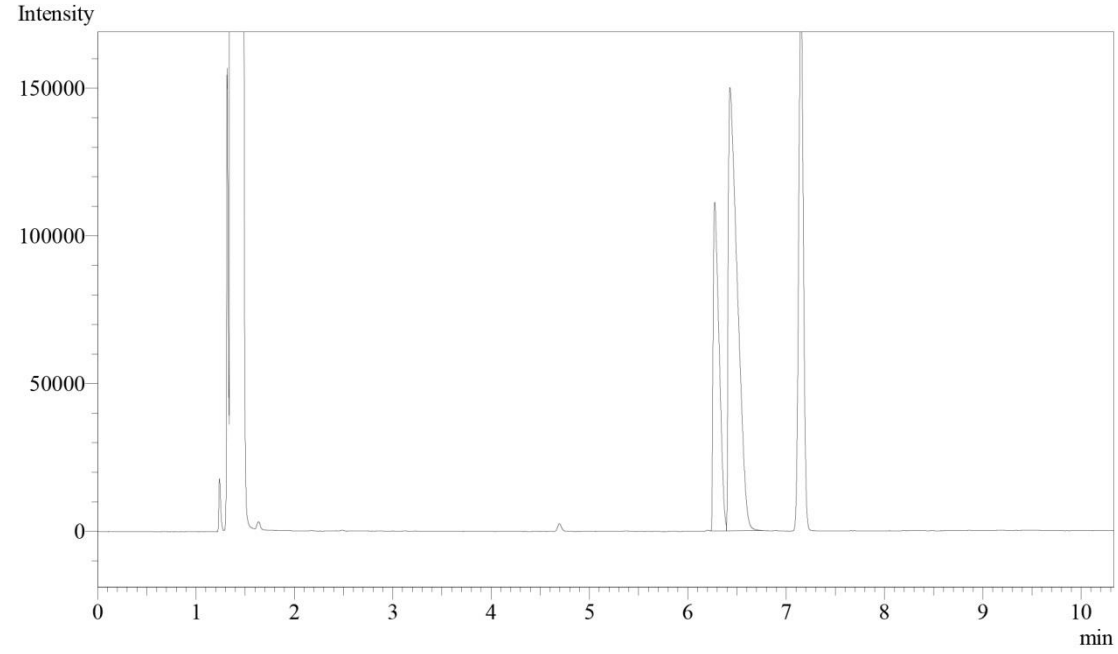

Peak#	Ret.Time	Area%
1	6,275	32,7918
2	6,431	67,2082
Total		100,0000

Figure S18. Kinetic Resolution of (*RS*)-1-Phenylethanol. Experimental conditions: *rac*-1-Phenylethanol (1mmol, 122mg), vinyl acetate (1eqv) as acyl donor, and 18mg (15%w/w) of SP_C0 in cyclohexane (3 mL) for 4 h at 60°C.

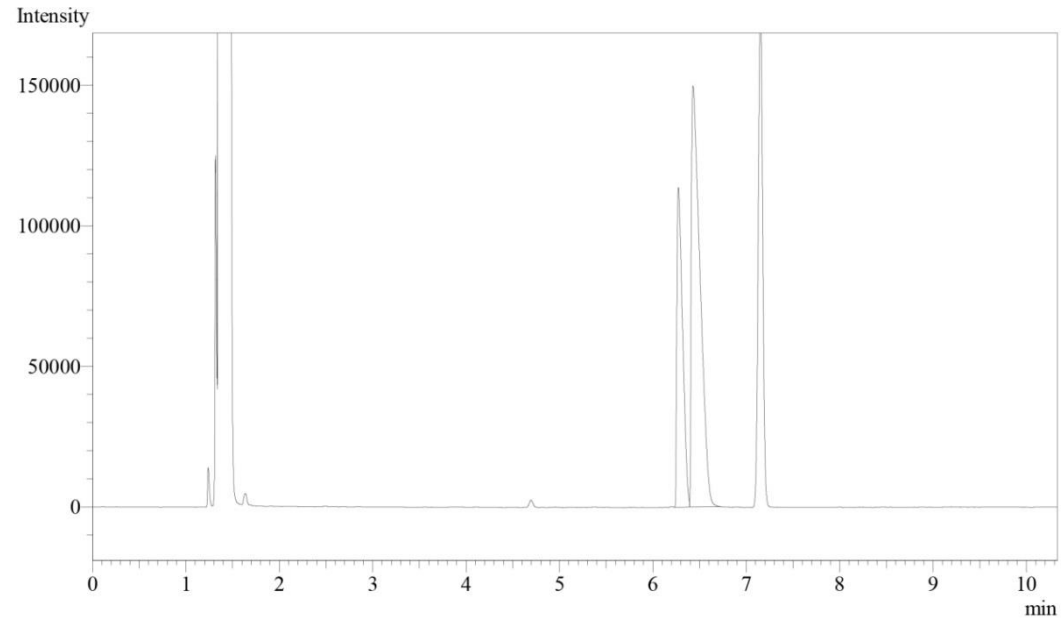

Peak#	Ret.Time	Area%
1	6,274	33,3930
2	6,432	66,6070
Total		100,0000

Figure S19. Kinetic Resolution of (*RS*)-1-Phenylethanol. Experimental conditions: *rac*-1-Phenylethanol (1mmol, 122mg), vinyl acetate (1eqv) as acyl donor, and 18mg (15%w/w) of SP_C0_1 in cyclohexane (3 mL) for 4 h at 60°C.

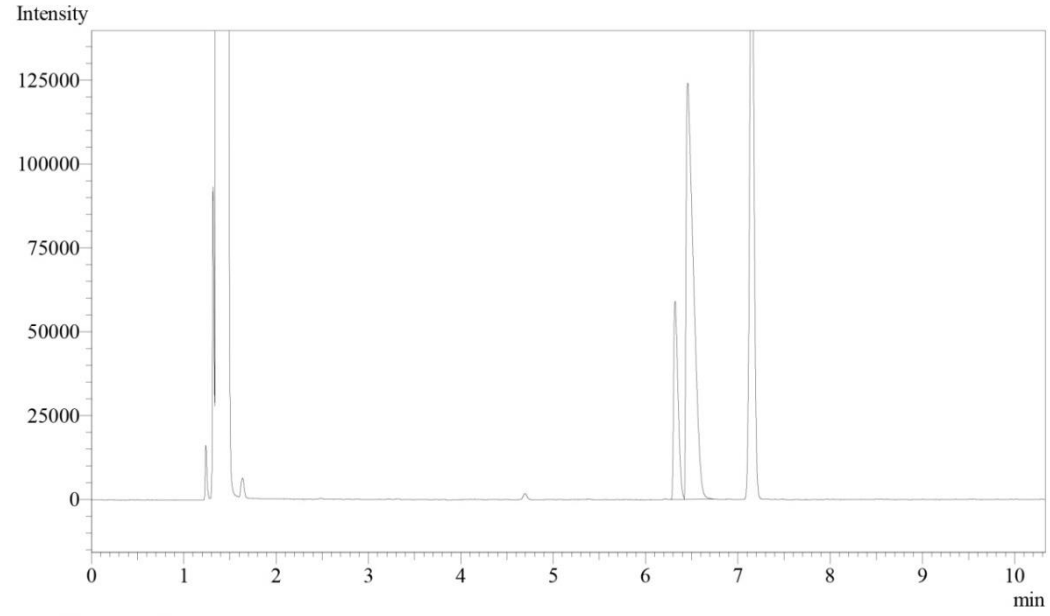

Peak#	Ret.Time	Area%
1	6,322	21,9844
2	6,459	78,0156
Total		100,0000

Figure S20. Kinetic Resolution of (*RS*)-1-Phenylethanol. Experimental conditions: *rac*-1-Phenylethanol (1mmol, 122mg), vinyl acetate (1eqv) as acyl donor, and 18mg (15%w/w) of SP_C2 in cyclohexane (3 mL) for 4 h at 60°C.

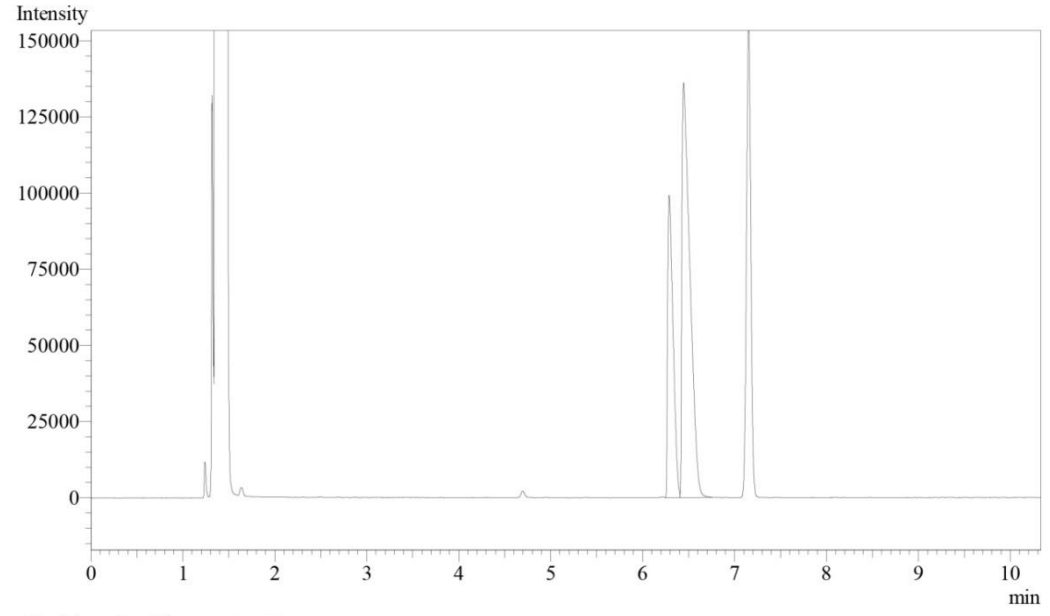

Peak#	Ret.Time	Area%
1	6,290	33,0351
2	6,447	66,9649
Total		100,0000

Figure S21. Kinetic Resolution of (*RS*)-1-Phenylethanol. Experimental conditions: *rac*-1-Phenylethanol (1mmol, 122mg), vinyl acetate (1eqv) as acyl donor, and 18mg (15%w/w) of SP_C4 in cyclohexane (3 mL) for 4 h at 60°C.

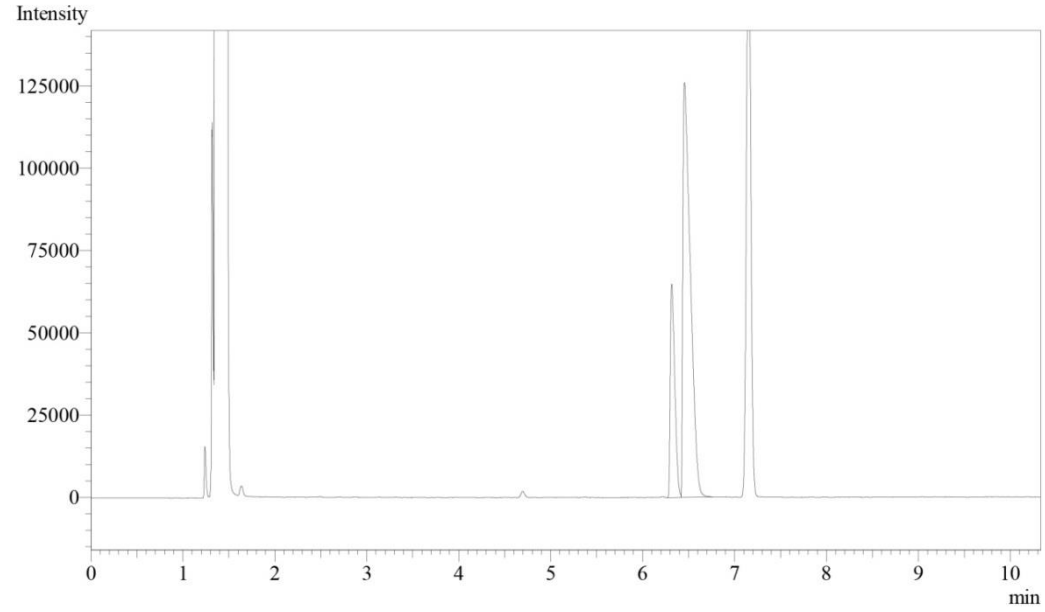

Peak#	Ret.Time	Area%
1	6,318	23,6289
2	6,457	76,3711
Total		100,0000

Figure S22. Kinetic Resolution of (*RS*)-1-Phenylethanol. Experimental conditions: *rac*-1-Phenylethanol (1mmol, 122mg), vinyl acetate (1eqv) as acyl donor, and 18mg (15%w/w) of SP_C6 in cyclohexane (3 mL) for 4 h at 60°C.

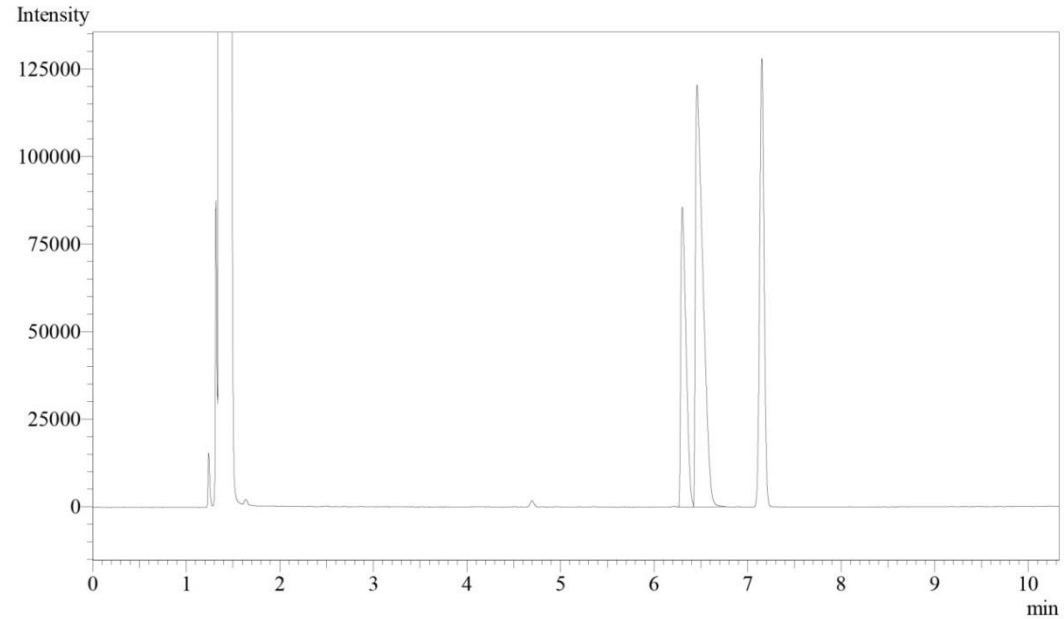

Peak#	Ret.Time	Area%
1	6,303	33,0417
2	6,460	66,9583
Total		100,0000

Figure S23. Kinetic Resolution of (*RS*)-1-Phenylethanol. Experimental conditions: *rac*-1-Phenylethanol (1mmol, 122mg), vinyl acetate (1eqv) as acyl donor, and 18mg (15%w/w) of SP_C6_1 in cyclohexane (3 mL) for 4 h at 60°C.

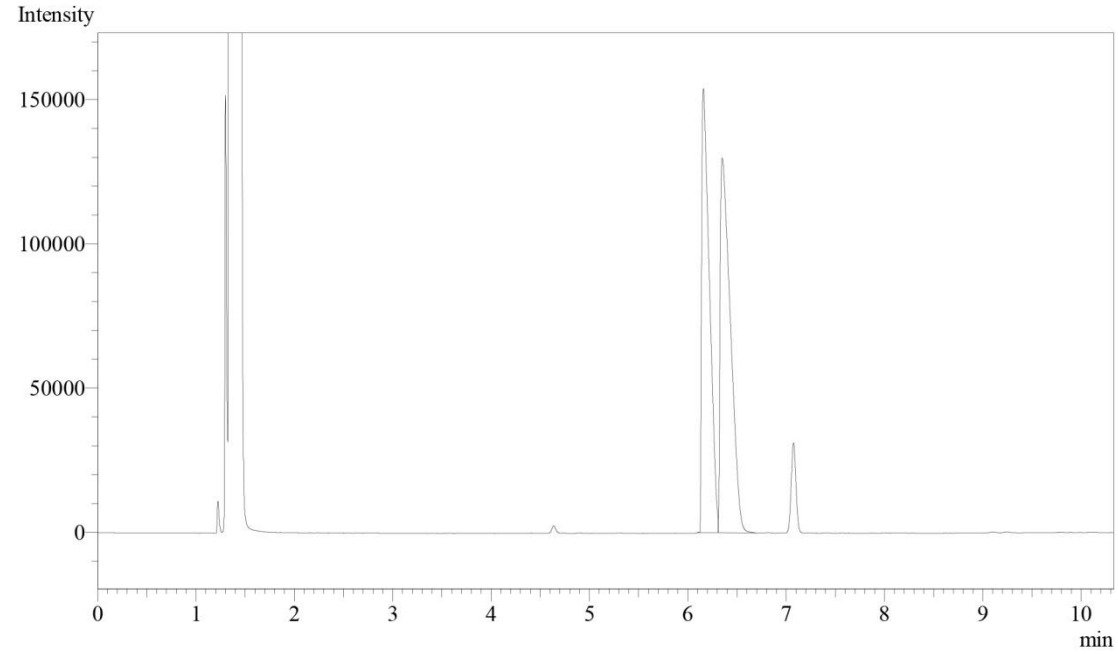

Peak#	Ret.Time	Area%
1	6,160	47,4015
2	6,352	52,5985
Total		100,0000

Figure S24. Kinetic Resolution of (*RS*)-1-Phenylethanol. Experimental conditions: *rac*-1-Phenylethanol (1mmol, 122mg), vinyl acetate (1eqv) as acyl donor, and 18mg (15%w/w) of SP_C0_1 in cyclohexane (3 mL) for 4 h at 60°C.

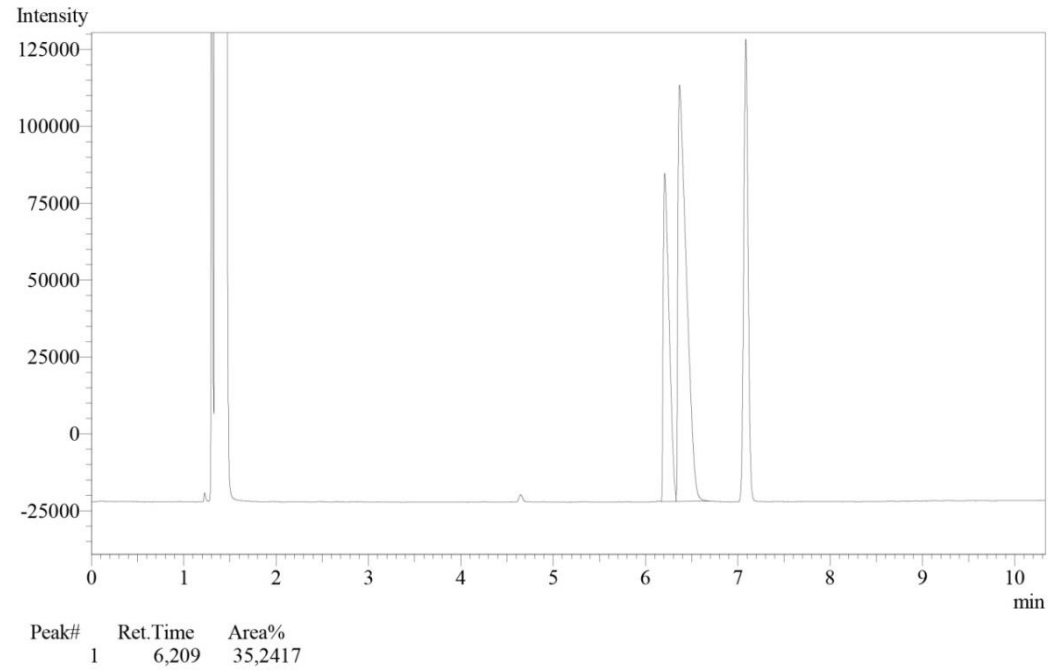

Peak#	Ret.Time	Area%
1	6,209	35,2417
2	6,370	64,7583
Total		100,0000

Figure S25. Kinetic Resolution of (*RS*)-1-Phenylethanol. Experimental conditions: *rac*-1-Phenylethanol (1mmol, 122mg), vinyl acetate (1eqv) as acyl donor, and 18mg (15%w/w) of SP_C6_1 in cyclohexane (3 mL) for 4 h at 60°C.

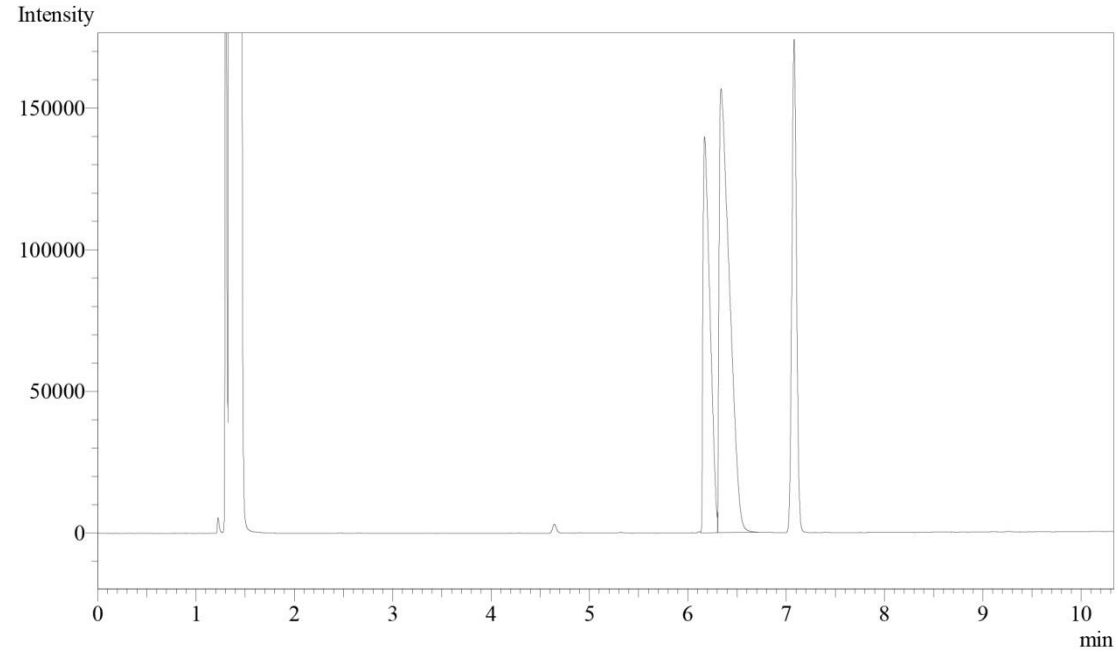

Peak#	Ret.Time	Area%
1	6,173	37,5437
2	6,340	62,4563
Total		100,0000

Figure S26. Kinetic Resolution of (*RS*)-1-Phenylethanol. Experimental conditions: *rac*-1-Phenylethanol (1mmol, 122mg), vinyl acetate (1eqv) as acyl donor, and 18mg (15%w/w) of SP_C6_2 in cyclohexane (3 mL) for 4 h at 60°C.

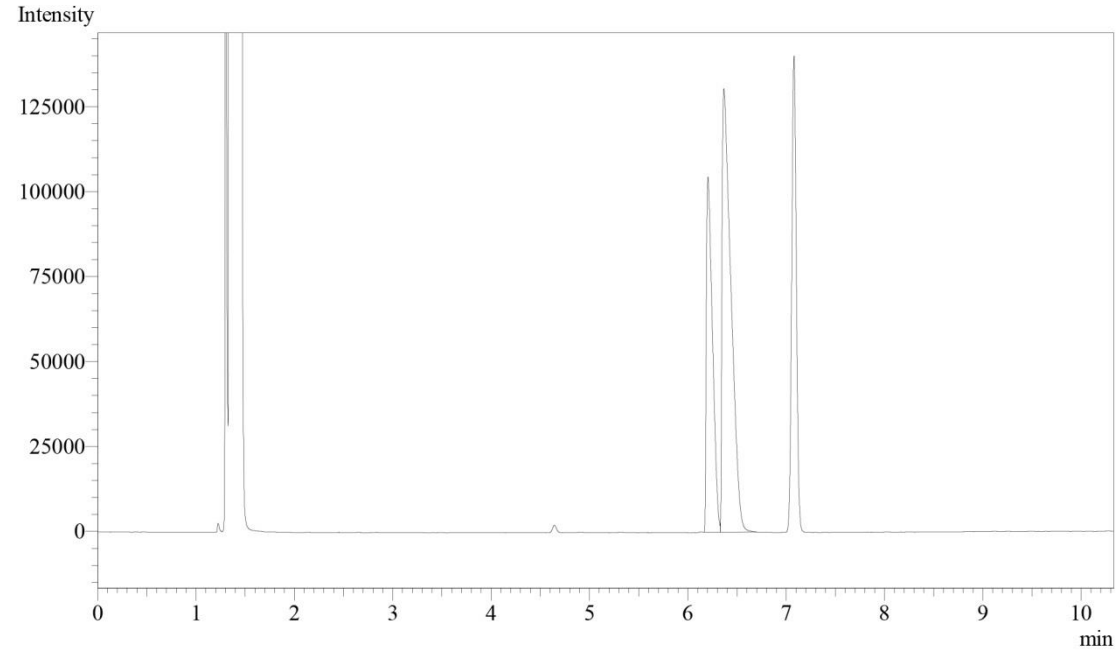

Peak#	Ret.Time	Area%
1	6,206	35,6143
2	6,367	64,3857
Total		100,0000

Figure S27. Kinetic Resolution of (*RS*)-1-Phenylethanol. Experimental conditions: *rac*-1-Phenylethanol (1mmol, 122mg), vinyl acetate (1eqv) as acyl donor, and 18mg (15%w/w) of SP_C6_3 in cyclohexane (3 mL) for 4 h at 60°C.

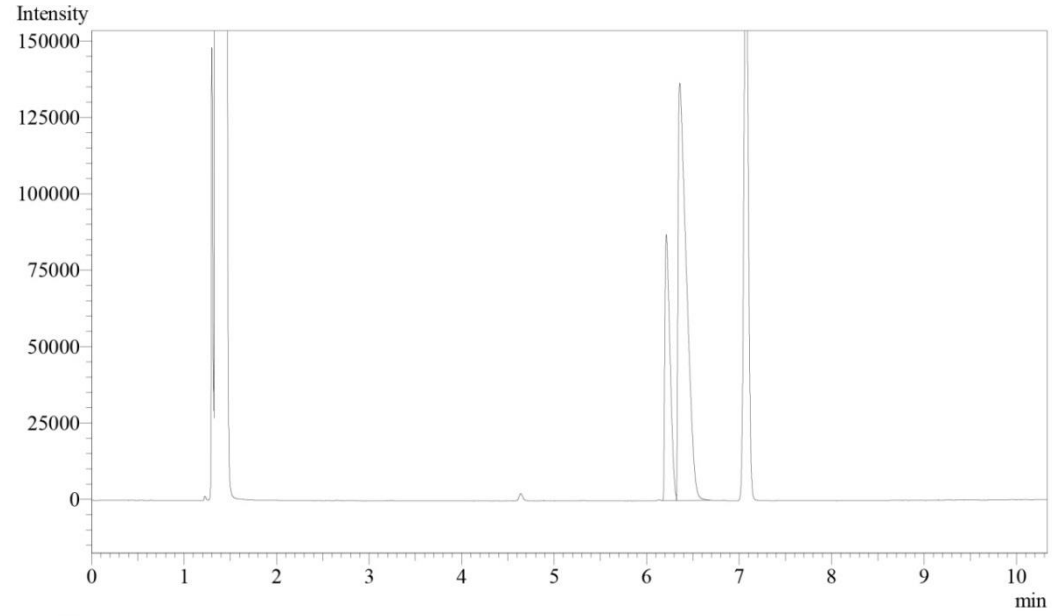

Peak#	Ret.Time	Area%
1	6,214	28,2448
2	6,360	71,7552
Total		100,0000

Figure S28. Kinetic Resolution of (*RS*)-1-Phenylethanol. Experimental conditions: *rac*-1-Phenylethanol (1mmol, 122mg), vinyl acetate (1eqv) as acyl donor, and 18mg (15%w/w) of SP_C6_4 in cyclohexane (3 mL) for 4 h at 60°C.

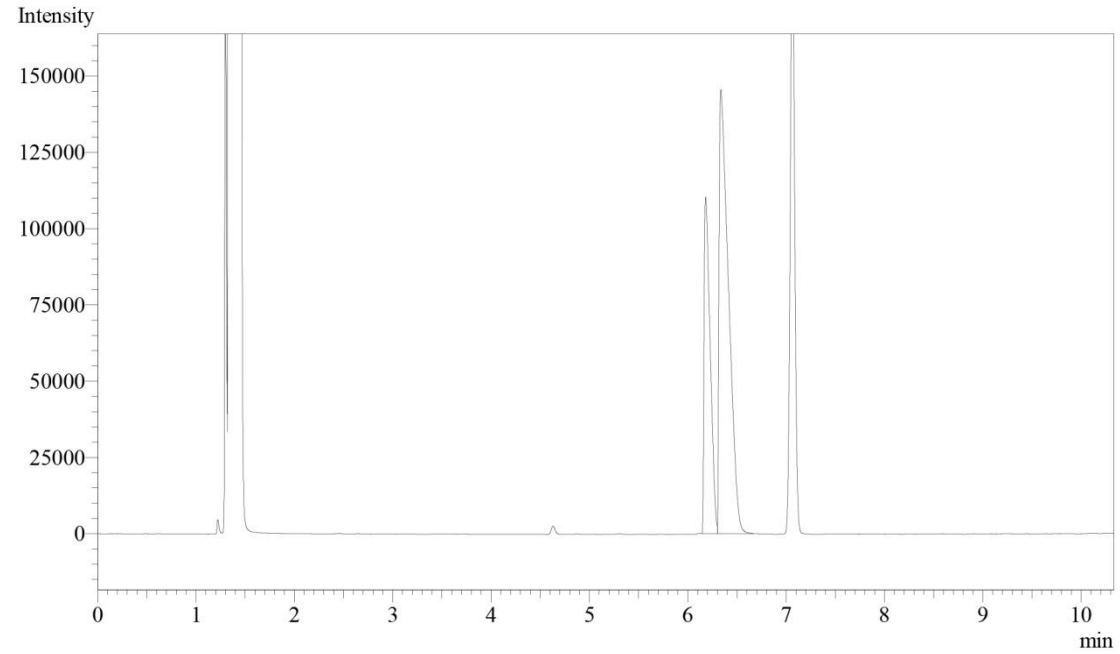

Peak#	Ret.Time	Area%
1	6,183	32,8927
2	6,337	67,1073
Total		100,0000

Figure S29. Kinetic Resolution of (*RS*)-1-Phenylethanol. Experimental conditions: *rac*-1-Phenylethanol (1mmol, 122mg), vinyl acetate (1eqv) as acyl donor, and 18mg (15%w/w) of SP_C8 in cyclohexane (3 mL) for 4 h at 60°C.

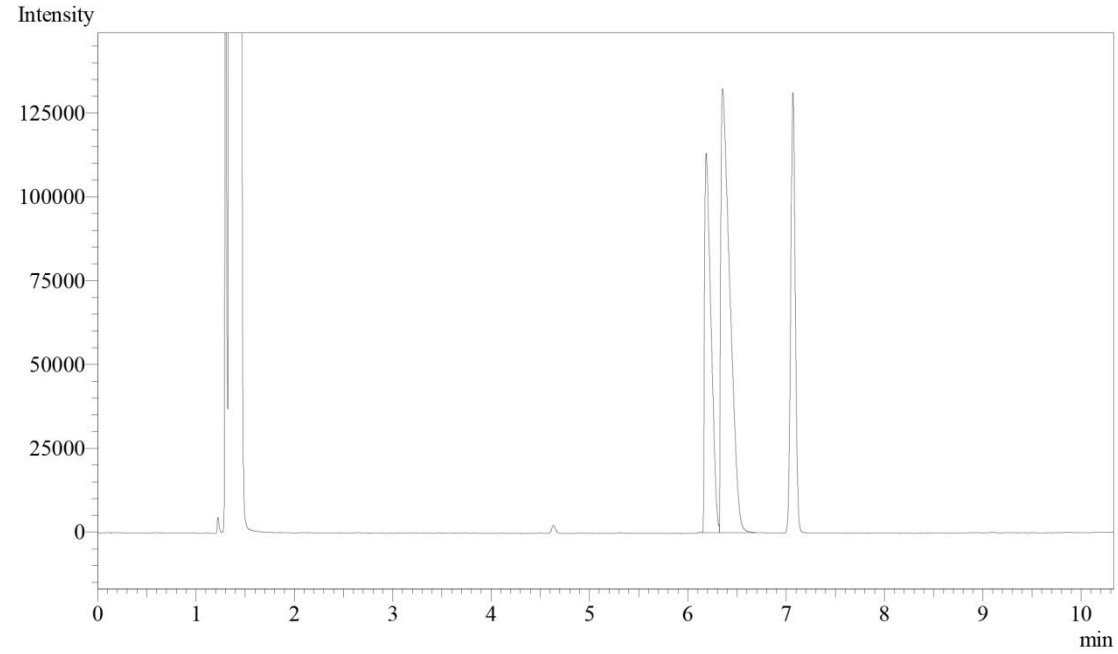

Peak#	Ret.Time	Area%
1	6,188	37,5959
2	6,355	62,4041
Total		100,0000

Figure S30. Kinetic Resolution of (*RS*)-1-Phenylethanol. Experimental conditions: *rac*-1-Phenylethanol (1mmol, 122mg), vinyl acetate (1eqv) as acyl donor, and 18mg (15%w/w) of SP_C10 in cyclohexane (3 mL) for 4 h at 60°C.

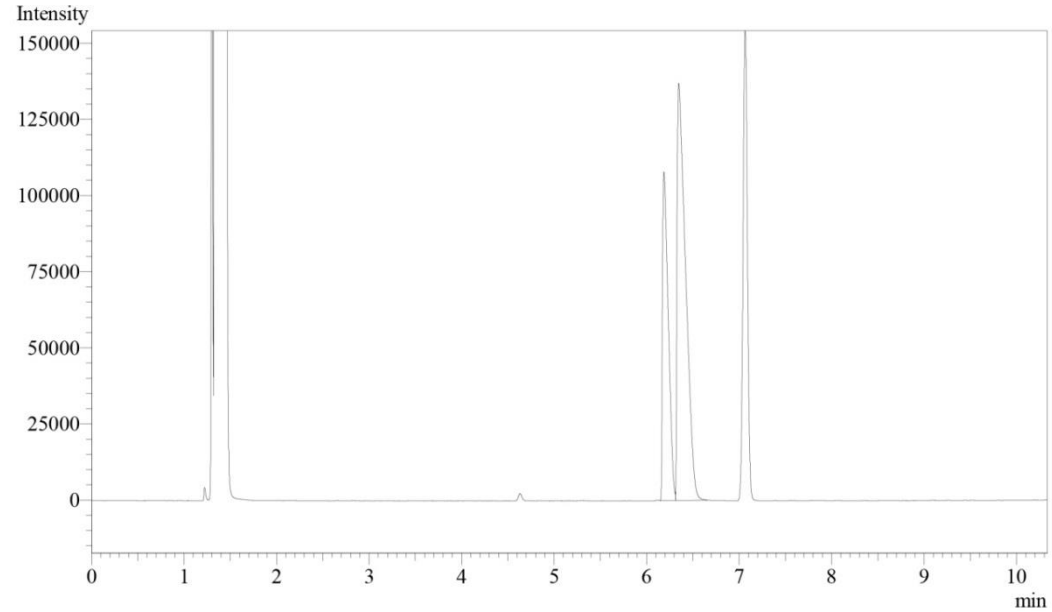

Peak#	Ret.Time	Area%
1	6,189	34,9665
2	6,349	65,0335
Total		100,0000

Figure S31. Kinetic Resolution of (*RS*)-1-Phenylethanol. Experimental conditions: *rac*-1-Phenylethanol (1mmol, 122mg), vinyl acetate (1eqv) as acyl donor, and 18mg (15%w/w) of SP_C12 in cyclohexane (3 mL) for 4 h at 60°C.

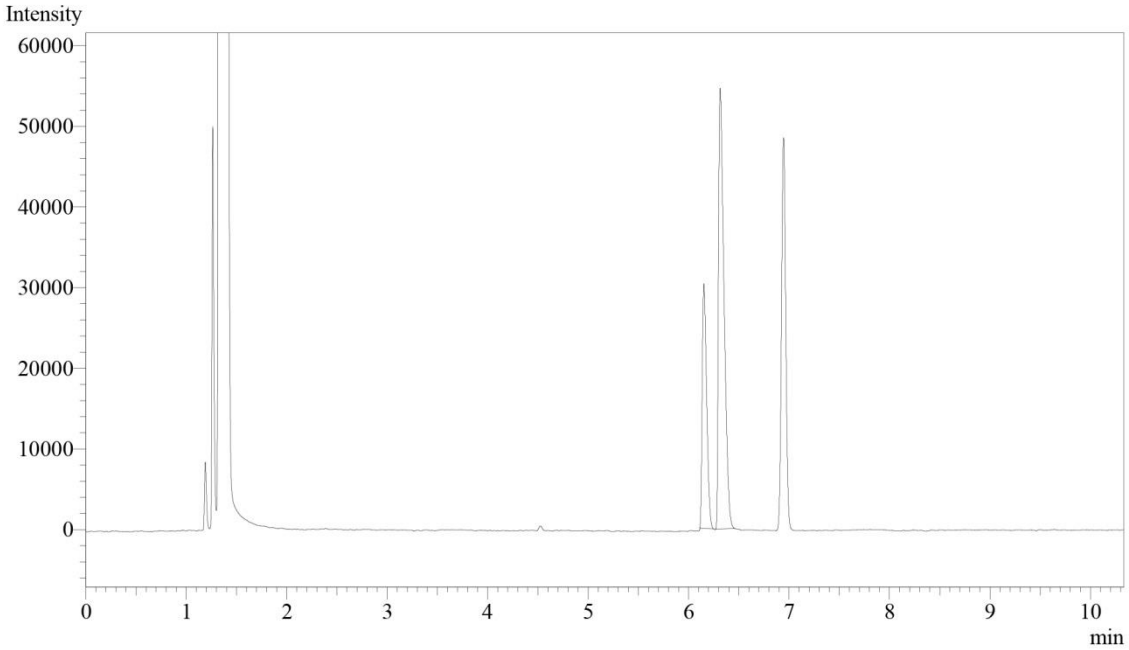

Peak#	Ret.Time	Area%
1	6,153	30,7305
2	6,315	69,2695
Total		100,0000

Figure S32. Kinetic Resolution of (*RS*)-1-Phenylethanol. Experimental conditions: *rac*-1-Phenylethanol (1mmol, 122mg), vinyl acetate (1eqv) as acyl donor, and 18mg (15%w/w) of SP_C6_1 in cyclohexane (3 mL) for 4 h at 60°C.

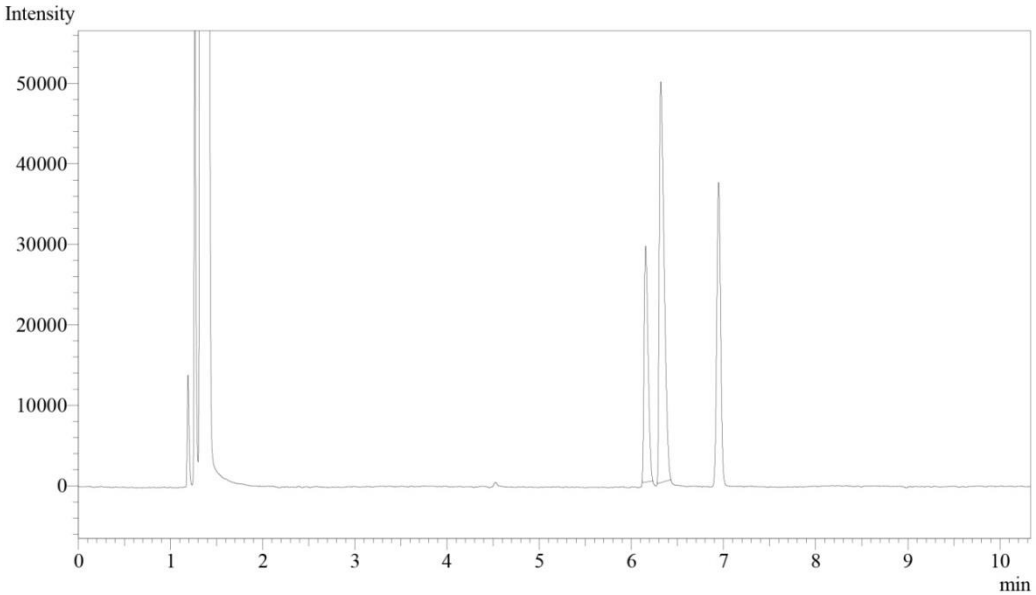

Peak#	Ret.Time	Area%
1	6,155	32,4597
2	6,320	67,5403
Total		100,0000

Figure S33. Kinetic Resolution of (*RS*)-1-Phenylethanol. Experimental conditions: *rac*-1-Phenylethanol (1mmol, 122mg), vinyl acetate (1eqv) as acyl donor, and 18mg (15%w/w) of SP_C6_2 in cyclohexane (3 mL) for 4 h at 60°C.

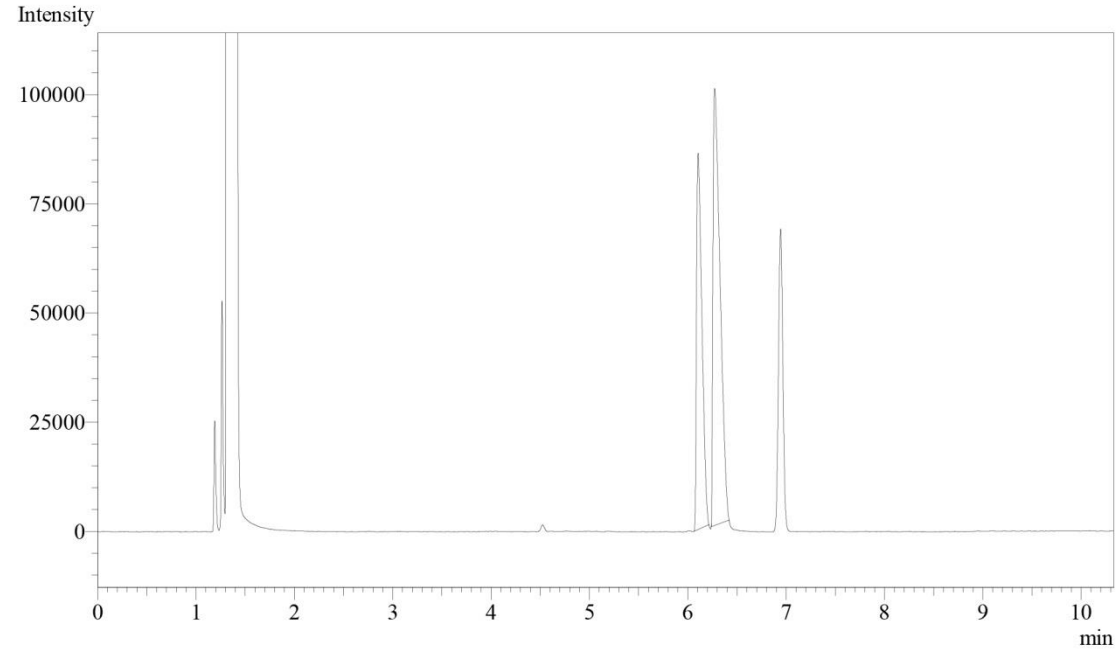

Peak#	Ret.Time	Area%
1	6,106	39,6712
2	6,275	60,3288
Total		100,0000

Figure S34. Kinetic Resolution of (*RS*)-1-Phenylethanol. Experimental conditions: *rac*-1-Phenylethanol (1mmol, 122mg), vinyl acetate (1eqv) as acyl donor, and 18mg (15%w/w) of SP_C6_3 in cyclohexane (3 mL) for 4 h at 60°C.

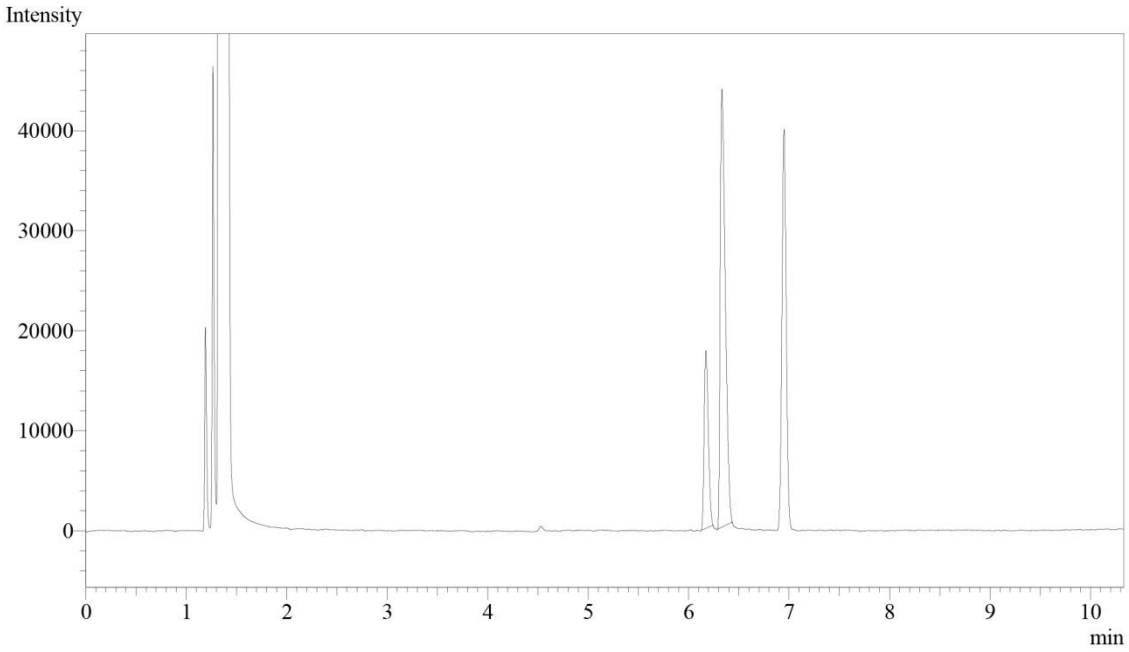

Peak#	Ret.Time	Area%
1	6,172	24,9957
2	6,332	75,0043
Total		100,0000

Figure S35. Kinetic Resolution of (*RS*)-1-Phenylethanol. Experimental conditions: *rac*-1-Phenylethanol (1mmol, 122mg), vinyl acetate (1eqv) as acyl donor, and 18mg (15%w/w) of SP_C8 in cyclohexane (3 mL) for 4 h at 60°C.

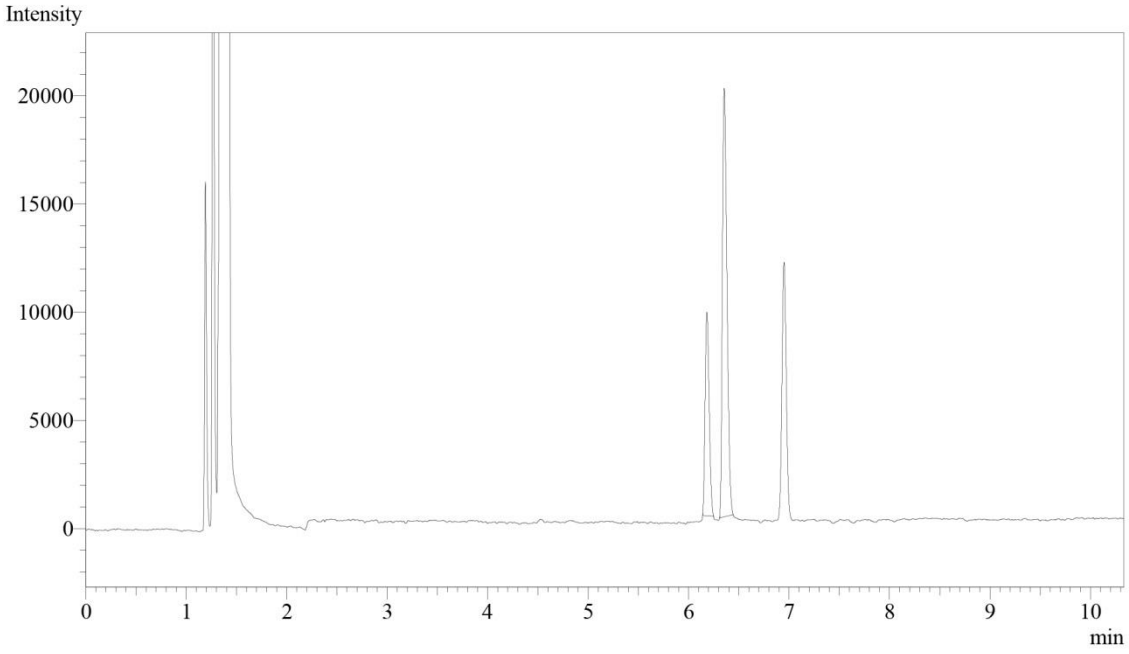

Peak#	Ret.Time	Area%
1	6,182	29,6973
2	6,355	70,3027
Total		100,0000

Figure S36. Kinetic Resolution of (*RS*)-1-Phenylethanol. Experimental conditions: *rac*-1-Phenylethanol (1mmol, 122mg), vinyl acetate (1eqv) as acyl donor, and 18mg (15%w/w) of SP_C10 in cyclohexane (3 mL) for 4 h at 60°C.

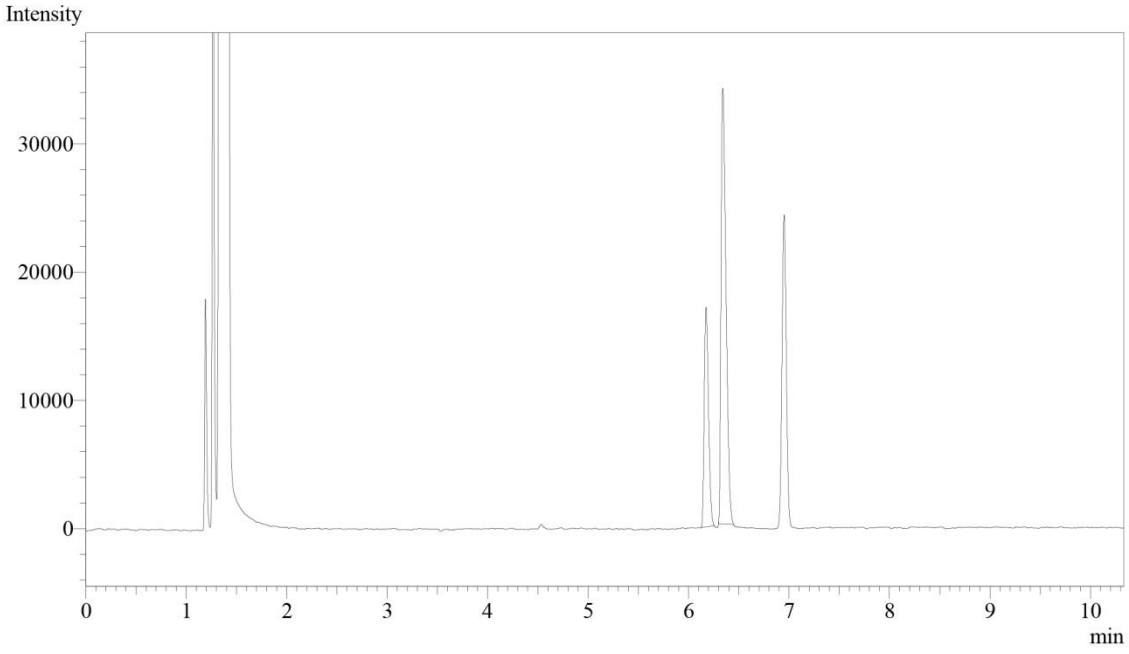

Peak#	Ret.Time	Area%
1	6,174	30,3342
2	6,341	69,6658
Total		100,0000

Figure S37. Kinetic Resolution of (*RS*)-1-Phenylethanol. Experimental conditions: *rac*-1-Phenylethanol (1mmol, 122mg), vinyl acetate (1eqv) as acyl donor, and 18mg (15%w/w) of SP_C12 in cyclohexane (3 mL) for 4 h at 60°C.

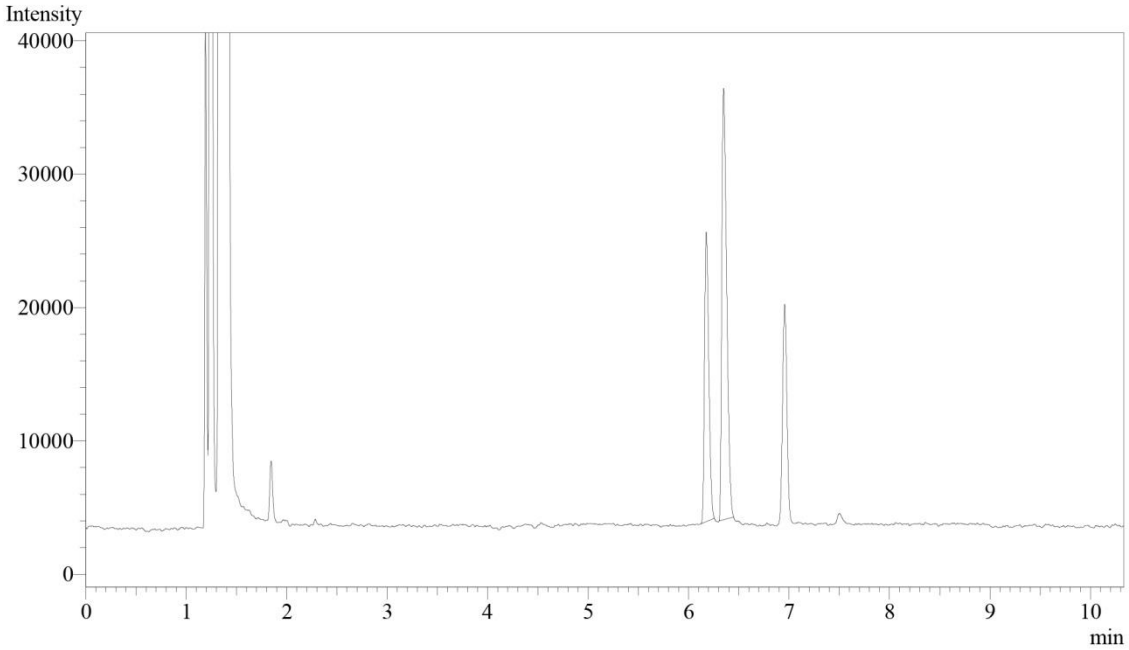

Peak#	Ret.Time	Area%
1	6,176	37,0422
2	6,349	62,9578
Total		100,0000

Figure S38. Kinetic Resolution of (*RS*)-1-Phenylethanol. Experimental conditions: *rac*-1-Phenylethanol (1mmol, 122mg), vinyl acetate (1eqv) as acyl donor, and 18mg (15%w/w) of SP_C6_4 in cyclohexane (3 mL) for 4 h at 60°C.

- 2.1.3 - Chromatograms of Kinetic Resolution in 5 Hours of Reaction

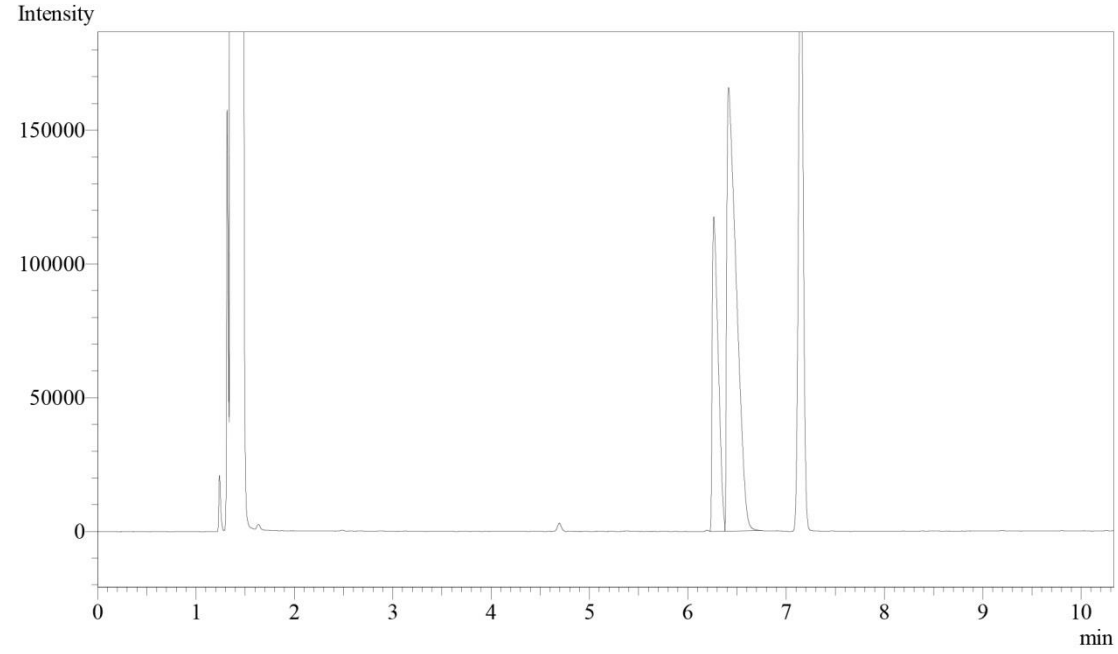

Peak#	Ret.Time	Area%
1	6,266	30,6020
2	6,417	69,3980
Total		100,0000

Figure S39. Kinetic Resolution of (*RS*)-1-Phenylethanol. Experimental conditions: *rac*-1-Phenylethanol (1mmol, 122mg), vinyl acetate (1eqv) as acyl donor, and 18mg (15%w/w) of SP_C0 in cyclohexane (3 mL) for 5 h at 60°C.

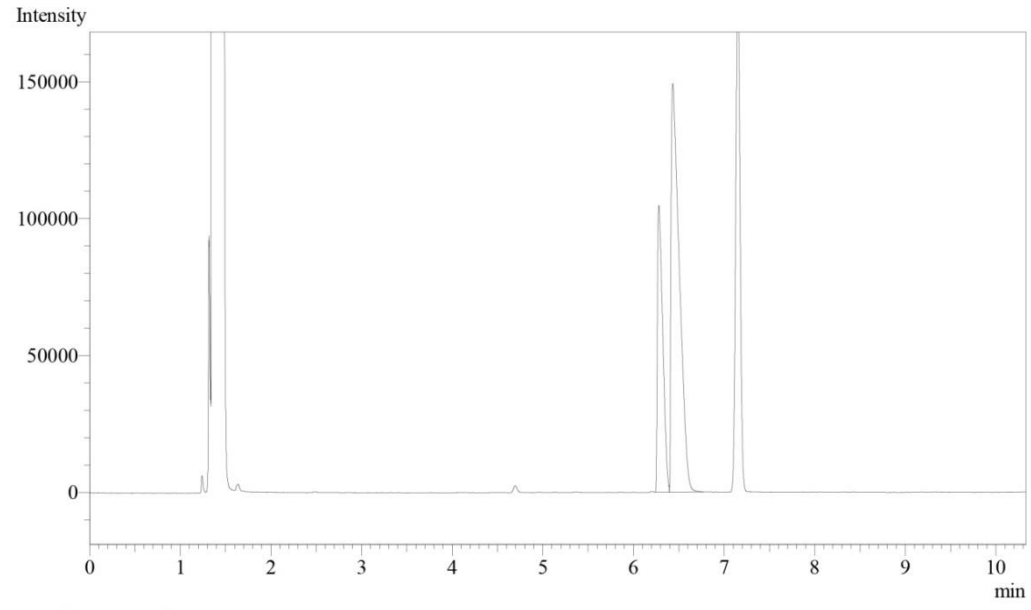

Peak#	Ret.Time	Area%
1	6,281	31,2580
2	6,435	68,7420
Total		100,0000

Figure S40. Kinetic Resolution of (*RS*)-1-Phenylethanol. Experimental conditions: *rac*-1-Phenylethanol (1mmol, 122mg), vinyl acetate (1eqv) as acyl donor, and 18mg (15%w/w) of SP_C0_1 in cyclohexane (3 mL) for 5 h at 60°C.

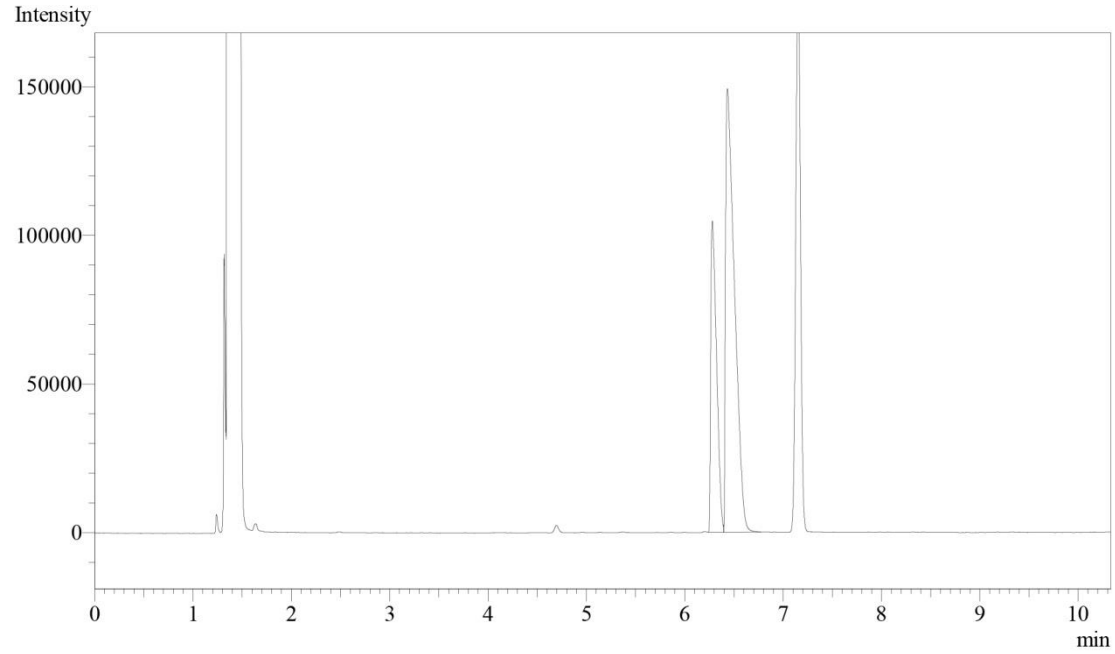

Peak#	Ret.Time	Area%
1	6,281	31,2580
2	6,435	68,7420
Total		100,0000

Figure S41. Kinetic Resolution of (*RS*)-1-Phenylethanol. Experimental conditions: *rac*-1-Phenylethanol (1mmol, 122mg), vinyl acetate (1eqv) as acyl donor, and 18mg (15%w/w) of SP_C2 in cyclohexane (3 mL) for 5 h at 60°C.

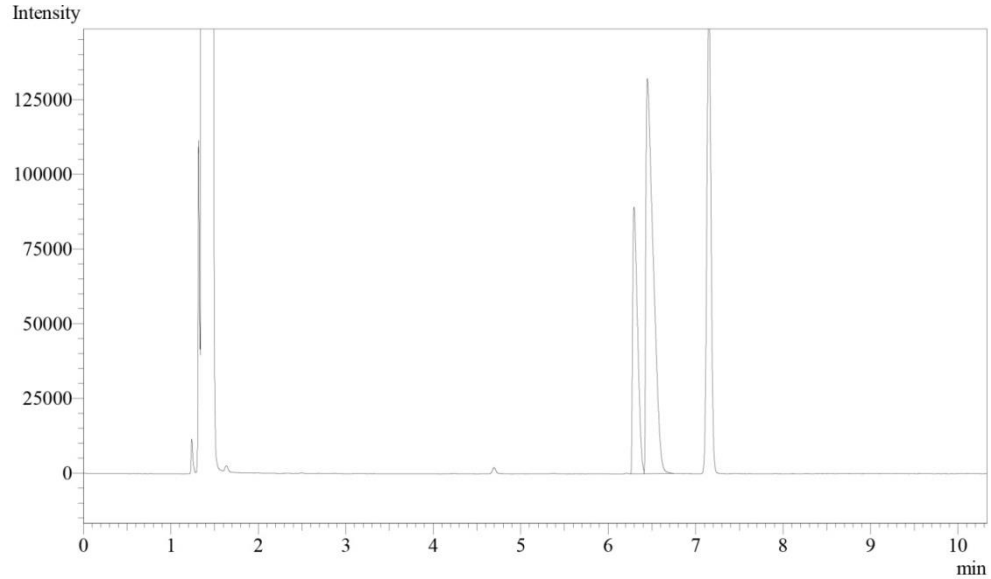

Peak#	Ret.Time	Area%
1	6,297	30,9141
2	6,450	69,0859
Total		100,0000

Figure S42. Kinetic Resolution of (*RS*)-1-Phenylethanol. Experimental conditions: *rac*-1-Phenylethanol (1mmol, 122mg), vinyl acetate (1eqv) as acyl donor, and 18mg (15%w/w) of SP_C4 in cyclohexane (3 mL) for 5 h at 60°C.

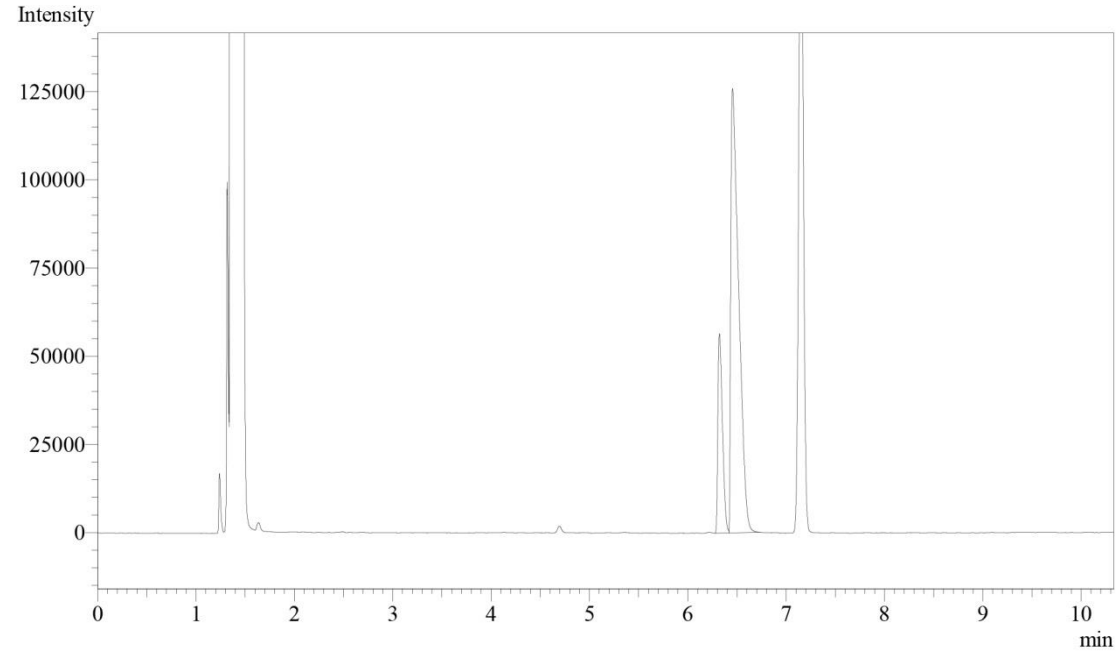

Peak#	Ret.Time	Area%
1	6,323	20,6618
2	6,456	79,3382
Total		100,0000

Figure S43. Kinetic Resolution of (*RS*)-1-Phenylethanol. Experimental conditions: *rac*-1-Phenylethanol (1mmol, 122mg), vinyl acetate (1eqv) as acyl donor, and 18mg (15%w/w) of SP_C6 in cyclohexane (3 mL) for 5 h at 60°C.

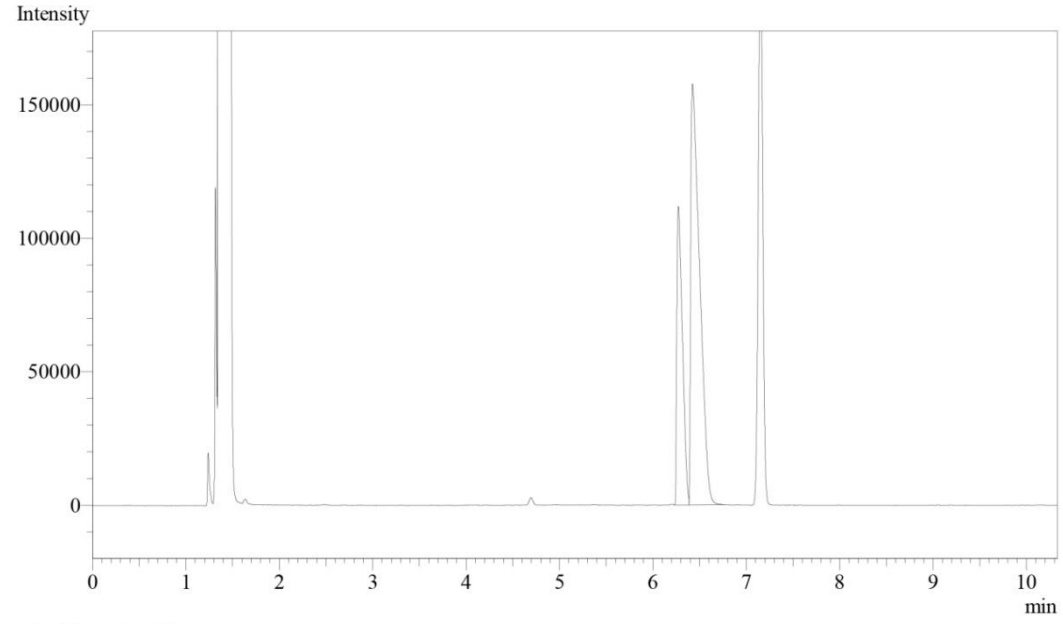

Peak#	Ret.Time	Area%
1	6,274	30,9972
2	6,426	69,0028
Total		100,0000

Figure S44. Kinetic Resolution of (*RS*)-1-Phenylethanol. Experimental conditions: *rac*-1-Phenylethanol (1mmol, 122mg), vinyl acetate (1eqv) as acyl donor, and 18mg (15%w/w) of SP_C6_1 in cyclohexane (3 mL) for 5 h at 60°C.

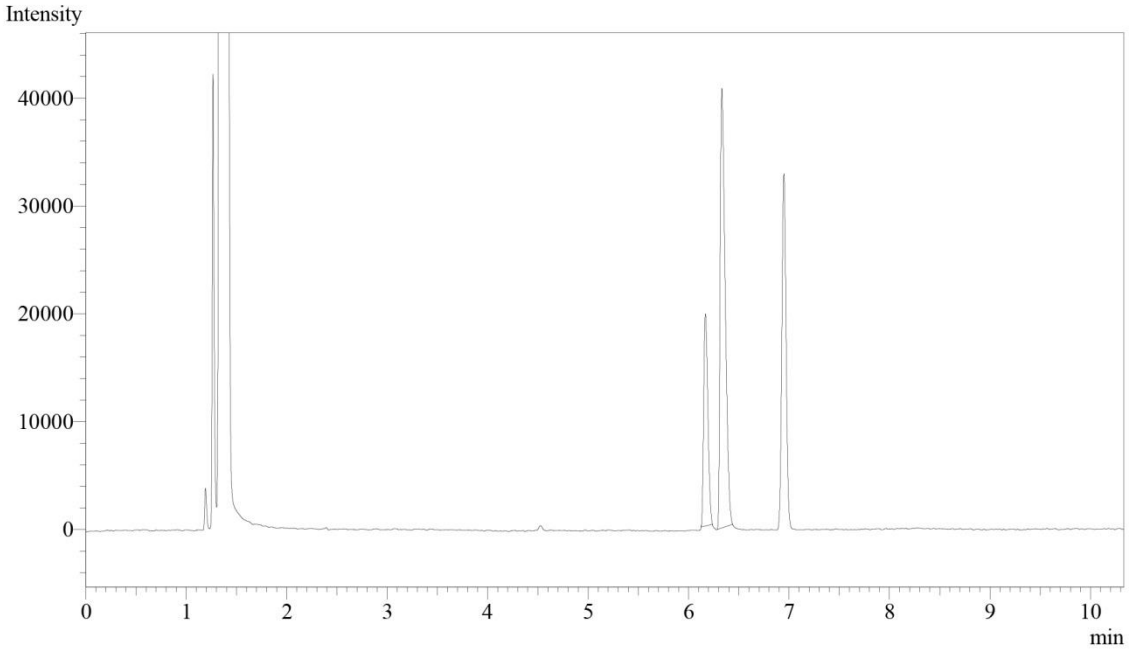

Peak#	Ret.Time	Area%
1	6,168	28,4761
2	6,331	71,5239
Total		100,0000

Figure S45. Kinetic Resolution of (*RS*)-1-Phenylethanol. Experimental conditions: *rac*-1-Phenylethanol (1mmol, 122mg), vinyl acetate (1eqv) as acyl donor, and 18mg (15%w/w) of SP_C6_1 in cyclohexane (3 mL) for 5 h at 60°C.

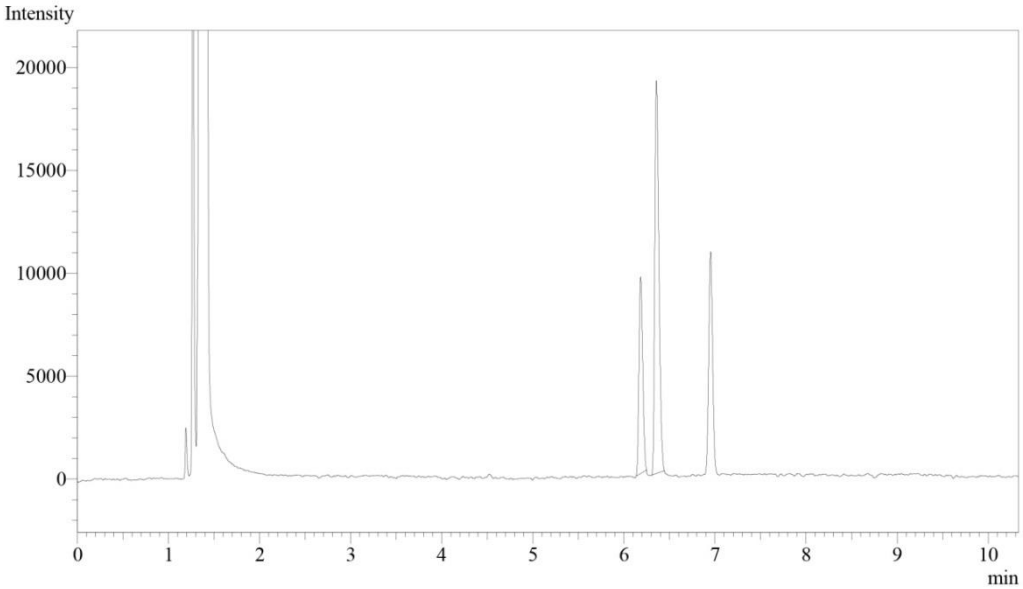

Peak#	Ret.Time	Area%
1	6,184	31,3357
2	6,357	68,6643
Total		100,0000

Figure S46. Kinetic Resolution of (*RS*)-1-Phenylethanol. Experimental conditions: *rac*-1-Phenylethanol (1mmol, 122mg), vinyl acetate (1eqv) as acyl donor, and 18mg (15%w/w) of SP_C6_2 in cyclohexane (3 mL) for 5 h at 60°C.

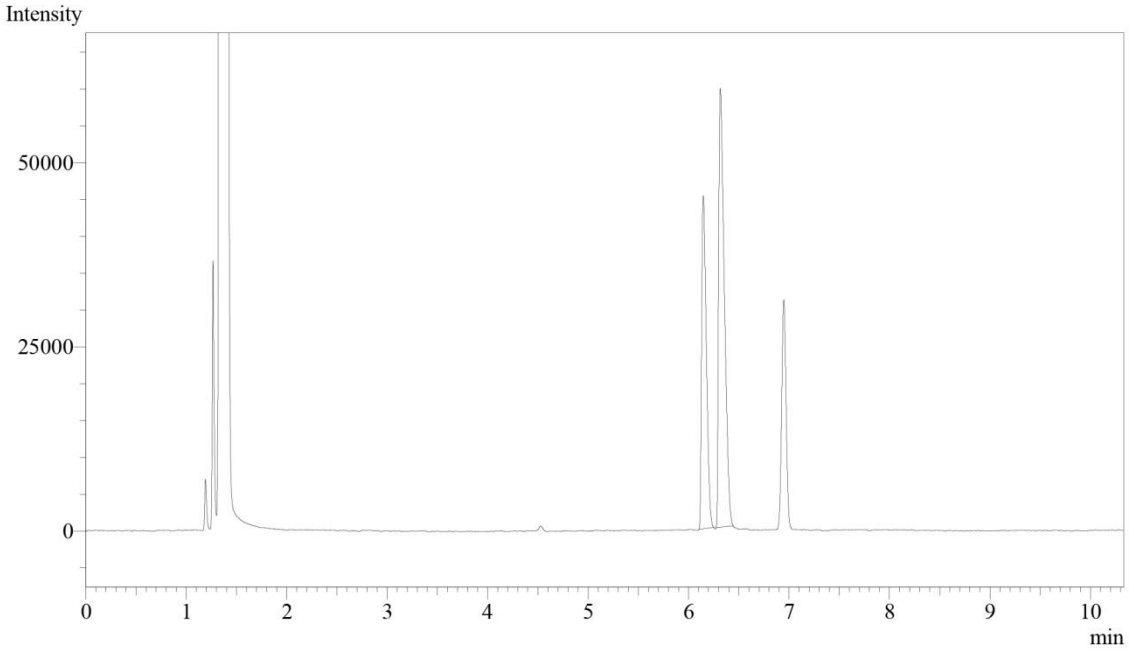

Peak#	Ret.Time	Area%
1	6,147	38,4891
2	6,317	61,5109
Total		100,0000

Figure S47. Kinetic Resolution of (*RS*)-1-Phenylethanol. Experimental conditions: *rac*-1-Phenylethanol (1mmol, 122mg), vinyl acetate (1eqv) as acyl donor, and 18mg (15%w/w) of SP_C6_3 in cyclohexane (3 mL) for 5 h at 60°C.

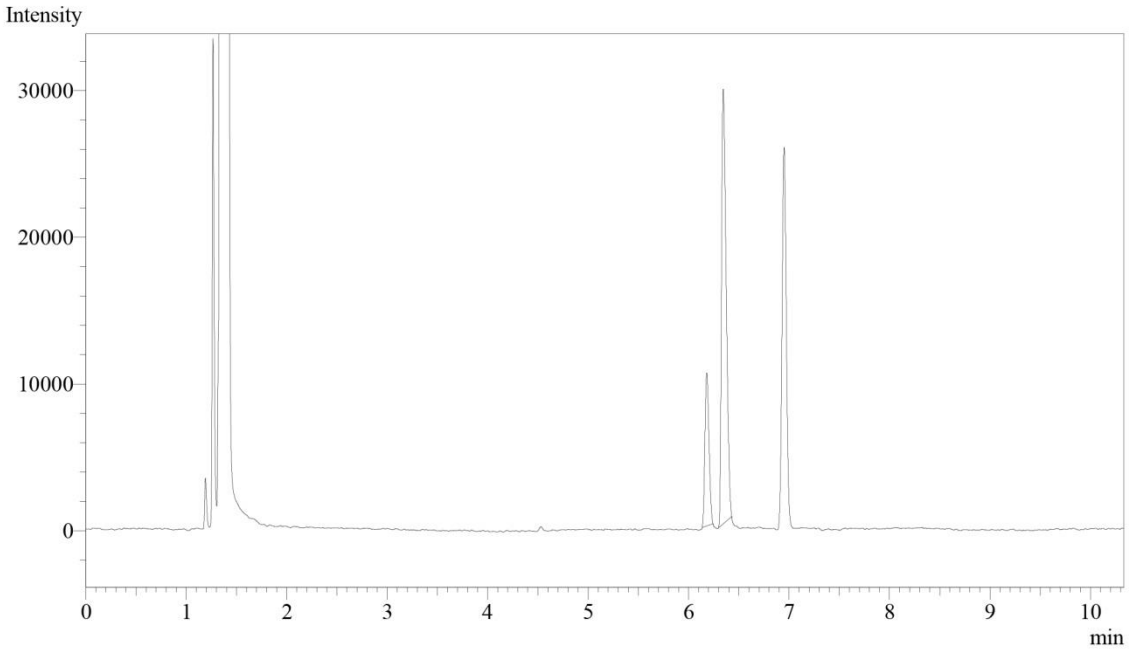

Peak#	Ret.Time	Area%
1	6,181	23,4442
2	6,345	76,5558
Total		100,0000

Figure S48. Kinetic Resolution of (*RS*)-1-Phenylethanol. Experimental conditions: *rac*-1-Phenylethanol (1mmol, 122mg), vinyl acetate (1eqv) as acyl donor, and 18mg (15%w/w) of SP_C8 in cyclohexane (3 mL) for 5 h at 60°C.

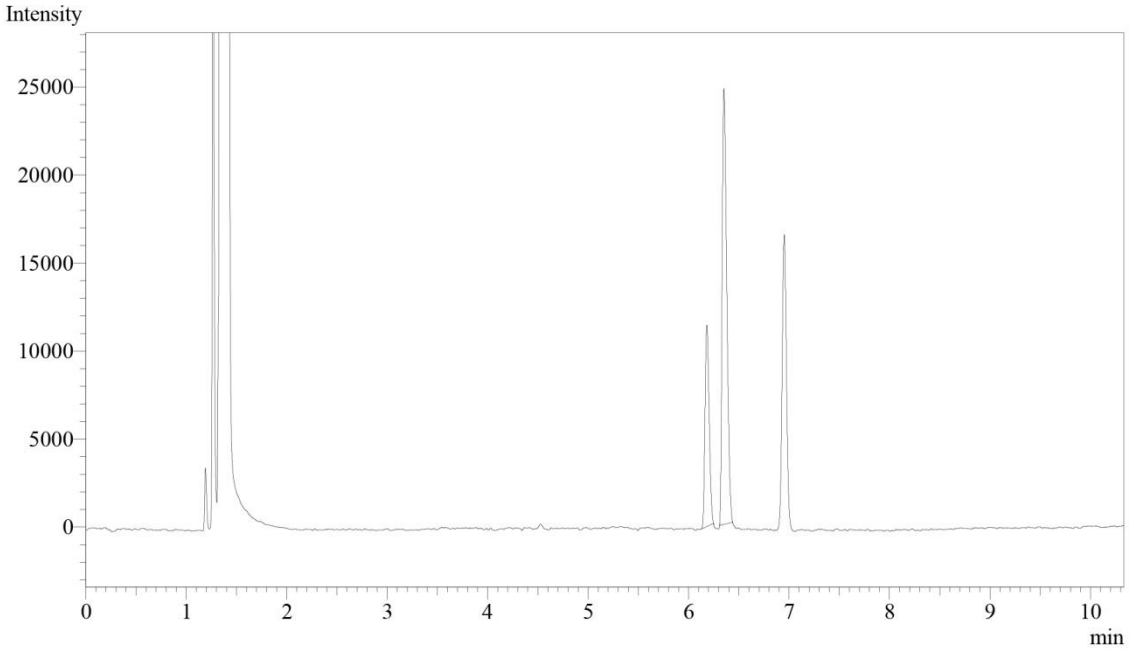

Peak#	Ret.Time	Area%
1	6,182	29,3116
2	6,352	70,6884
Total		100,0000

Figure S49. Kinetic Resolution of (*RS*)-1-Phenylethanol. Experimental conditions: *rac*-1-Phenylethanol (1mmol, 122mg), vinyl acetate (1eqv) as acyl donor, and 18mg (15%w/w) of SP_C10 in cyclohexane (3 mL) for 5 h at 60°C.

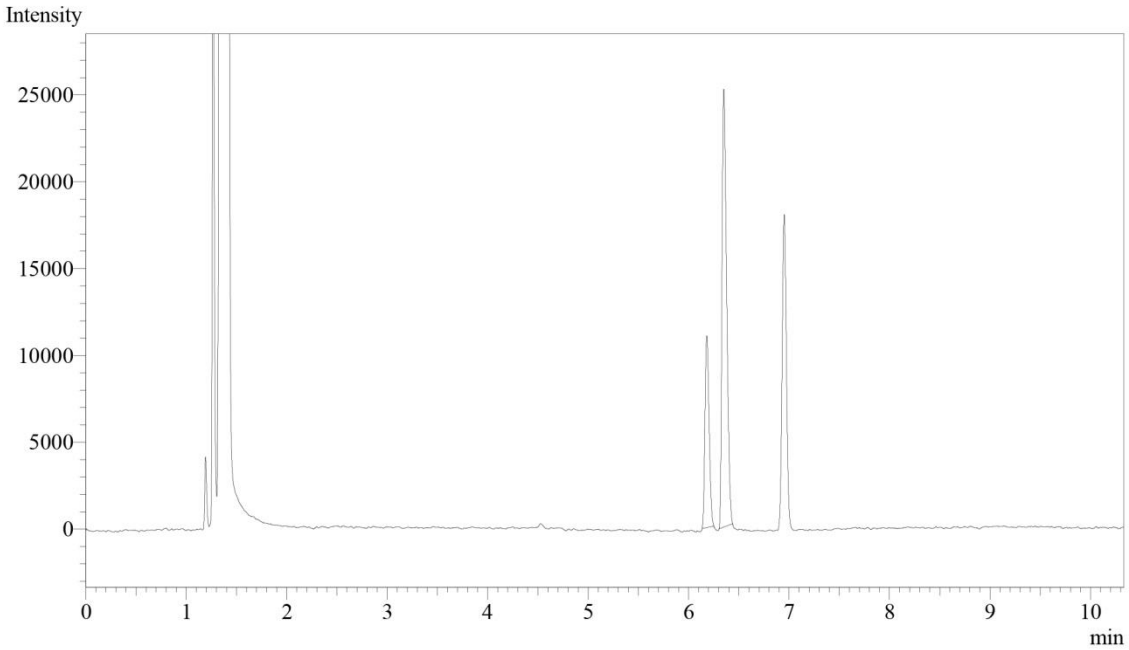

Peak#	Ret.Time	Area%
1	6,181	28,1157
2	6,350	71,8843
Total		100,0000

Figure S50. Kinetic Resolution of (*RS*)-1-Phenylethanol. Experimental conditions: *rac*-1-Phenylethanol (1mmol, 122mg), vinyl acetate (1eqv) as acyl donor, and 18mg (15%w/w) of SP_C12 in cyclohexane (3 mL) for 5 h at 60°C.

Figure 1. SP_C12

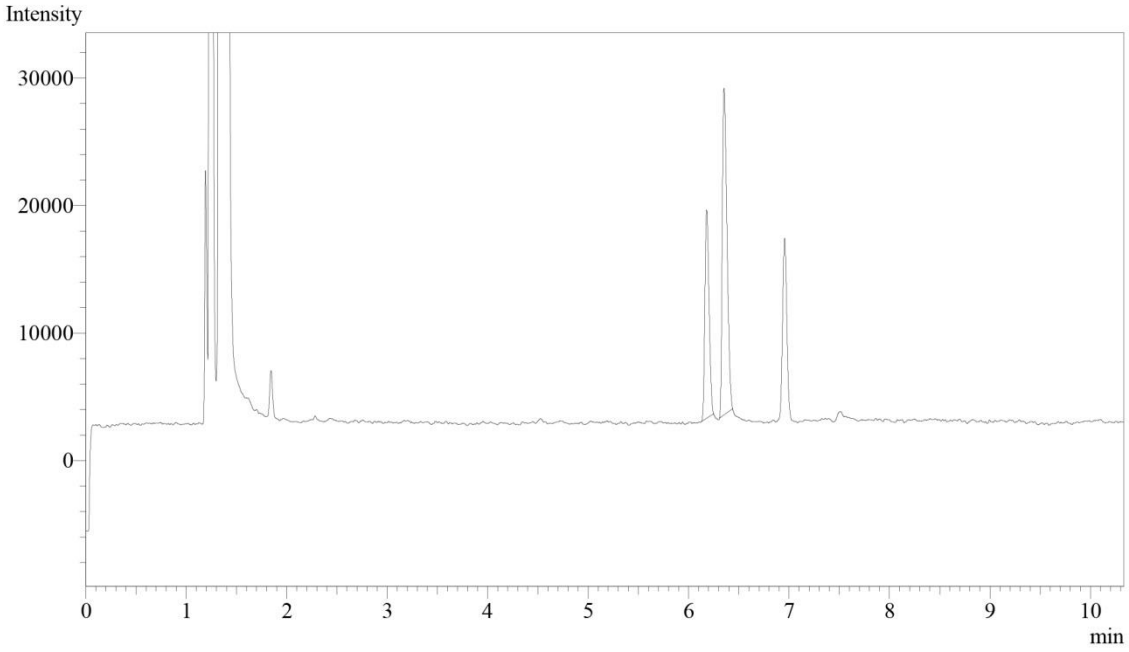

Peak#	Ret.Time	Area%
1	6,180	36,0336
2	6,353	63,9664
Total		100,0000

Figure S51. Kinetic Resolution of (*RS*)-1-Phenylethanol. Experimental conditions: *rac*-1-Phenylethanol (1mmol, 122mg), vinyl acetate (1eqv) as acyl donor, and 18mg (15%w/w) of SP_C6_4 in cyclohexane (3 mL) for 5 h at 60°C.

3. Scanning Electronic Microscopy (SEM) - sporopollenin

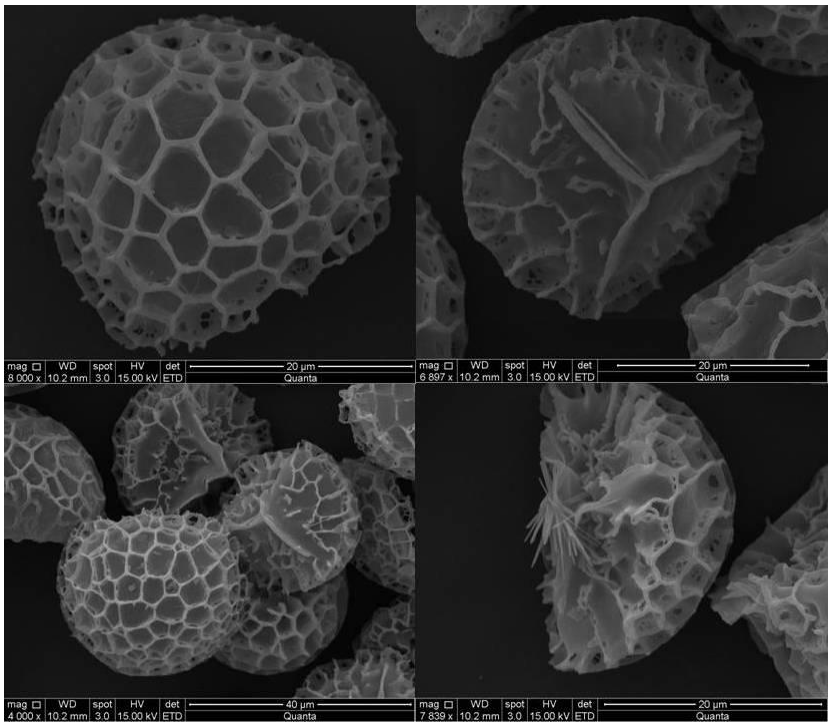

Figure S52: SEM of a sporopollenin before immobilization. Experimental Conditions: 1mg of sample metallized by gold under vacuum, and alanysed in a Zeiss EVO® 50H microscopy.

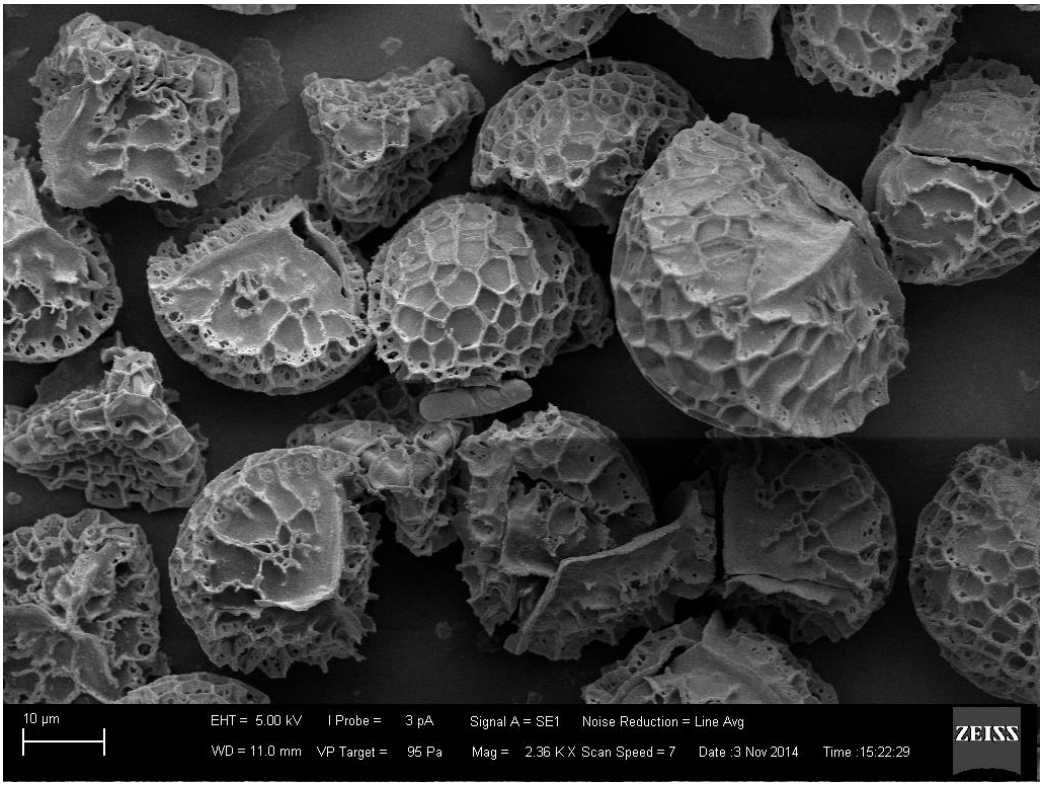

Figure S53: SEM of SP_C0_1 biocatalyst. Experimental Conditions: 1mg of sample metallized by gold under vacuum, and alanysed in a Zeiss EVO® 50H microscopy

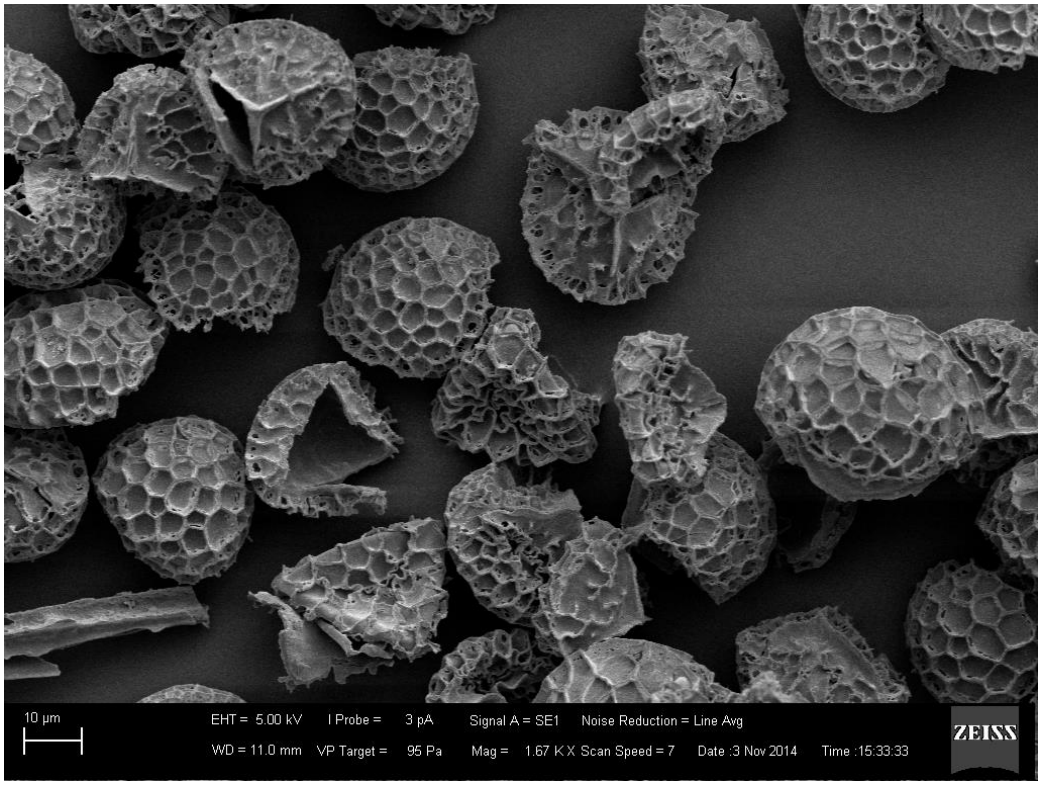

Figure S54: SEM of SP_C2 biocatalyst. Experimental Conditions: 1mg of sample metallized by gold under vacuum, and alanysed in a Zeiss EVO® 50H microscopy

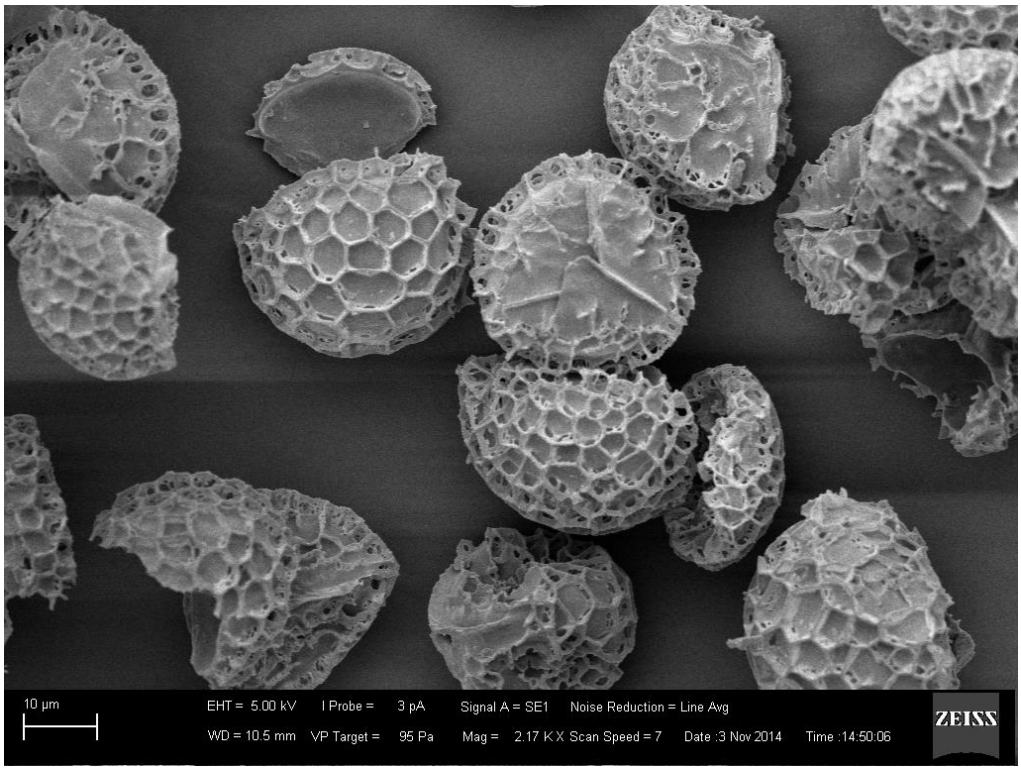

Figure S55: SEM of SP_C6 biocatalyst. Experimental Conditions: 1mg of sample metallized by gold under vacuum, and alanysed in a Zeiss EVO® 50H microscopy

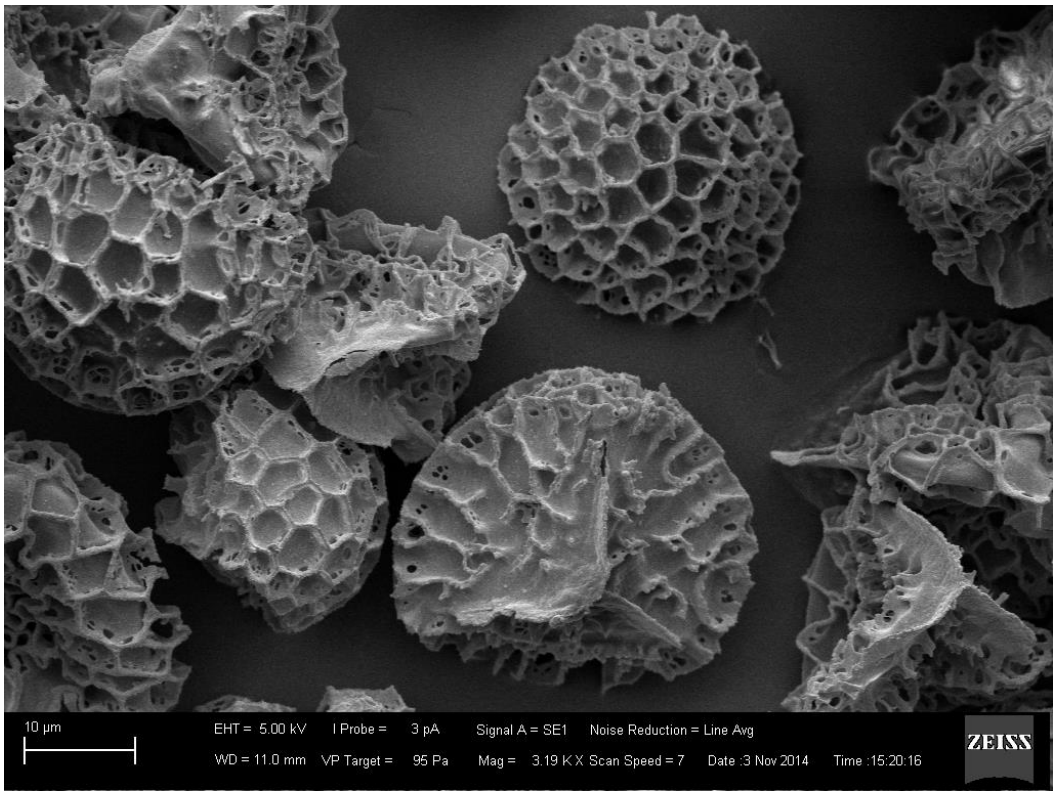

Figure S56: SEM of SP_C6_1 biocatalyst. Experimental Conditions: 1mg of sample metallized by gold under vacuum, and alanysed in a Zeiss EVO® 50H microscopy.

Figure S57: SEM of SP_C8 biocatalyst. Experimental Conditions: 1mg of sample metallized by gold under vacuum, and alanysed in a Zeiss EVO® 50H microscopy

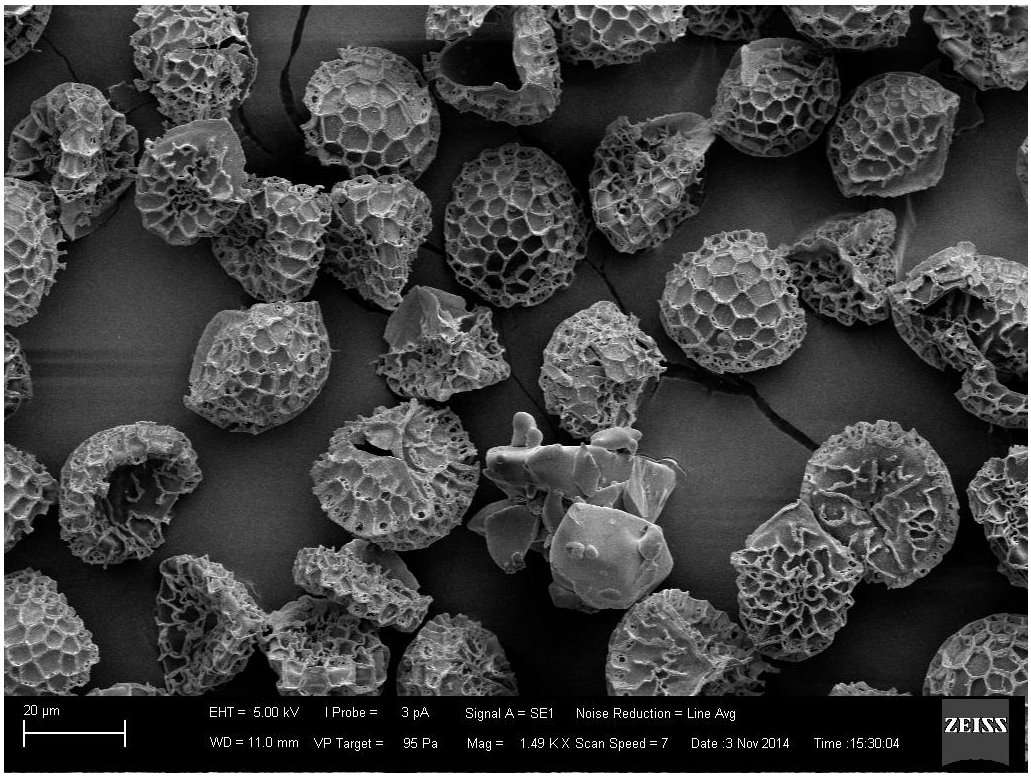

Figure S58: SEM of SP_C10 biocatalyst. Experimental Conditions: 1mg of sample metallized by gold under vacuum, and alanysed in a Zeiss EVO® 50H microscopy

4. IF-RT Spectra

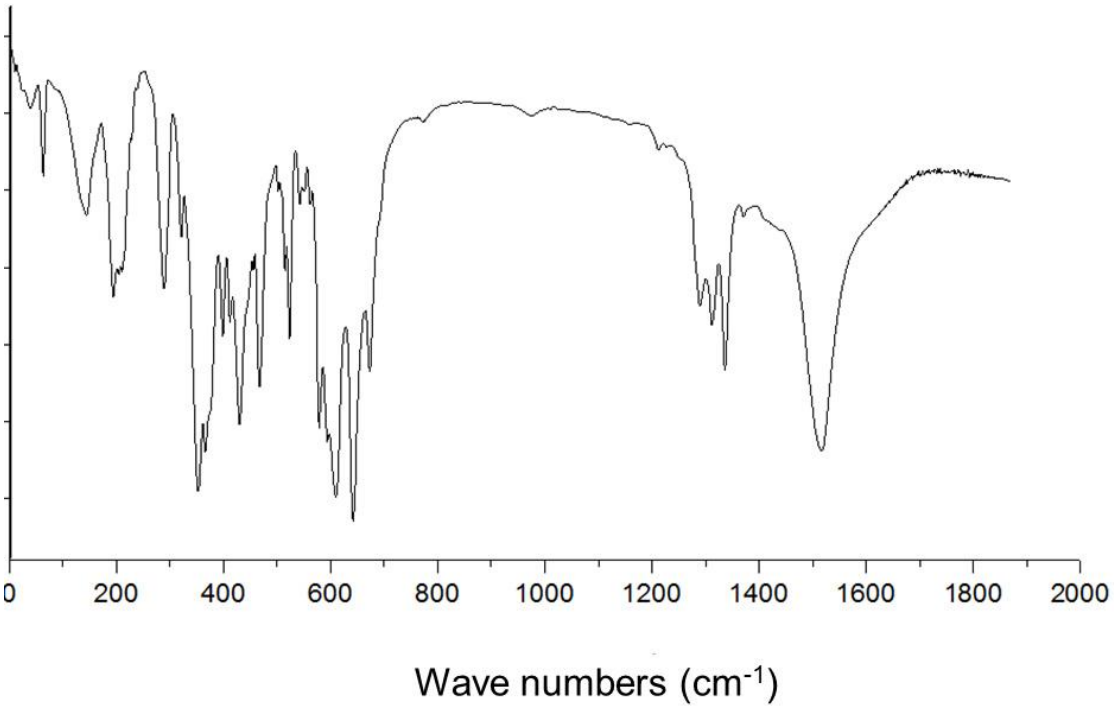

Figure S59: IR-RT spectra of SP_C8 biocatalyst.

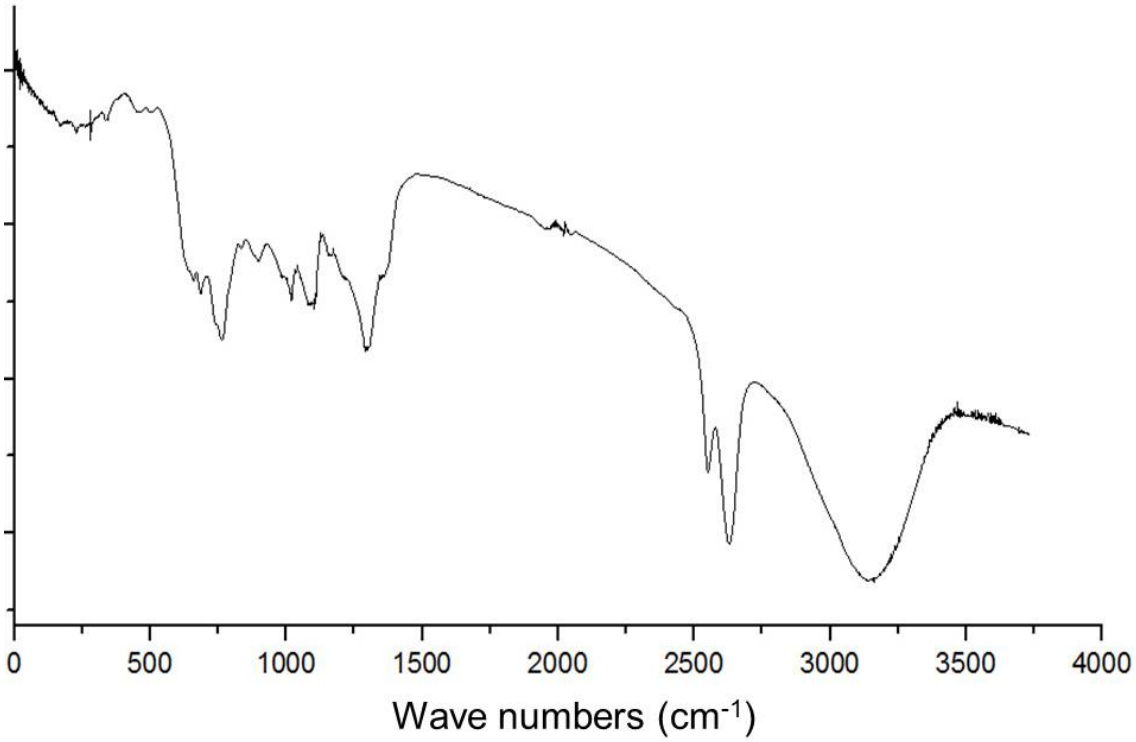

Figure S60: IR-RT spectra of SP_C0 biocatalyst.

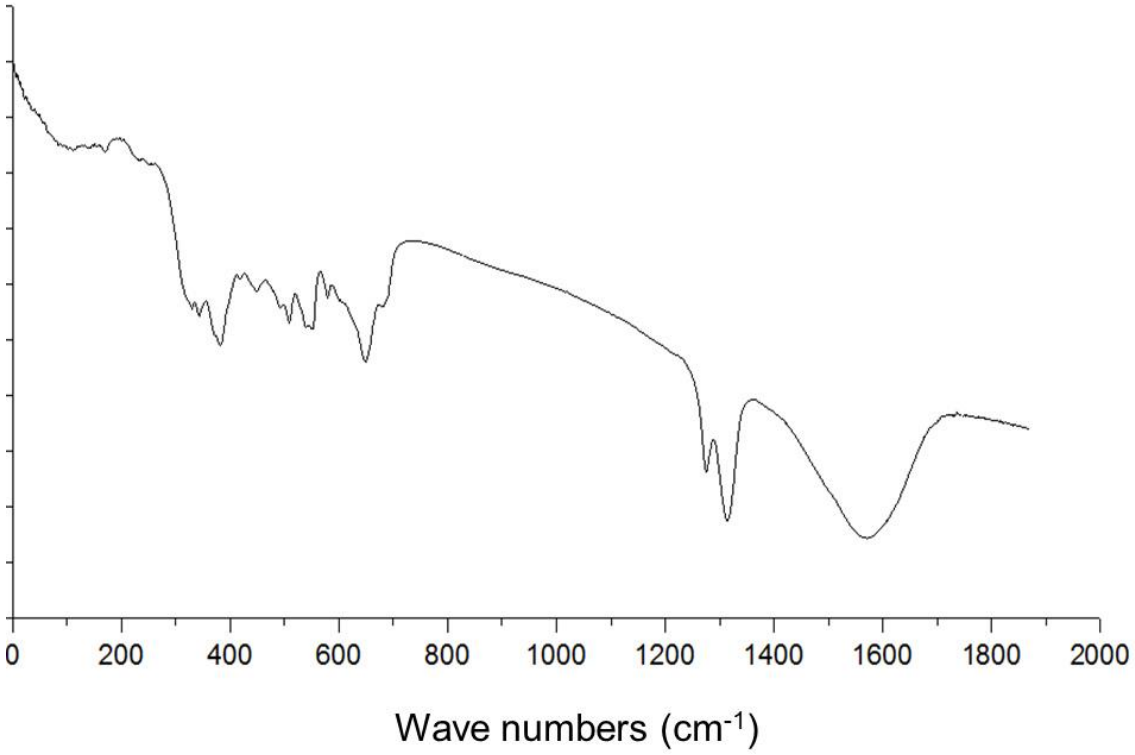

Figure S61: IR-RT spectra of SP_C6_1 biocatalyst.

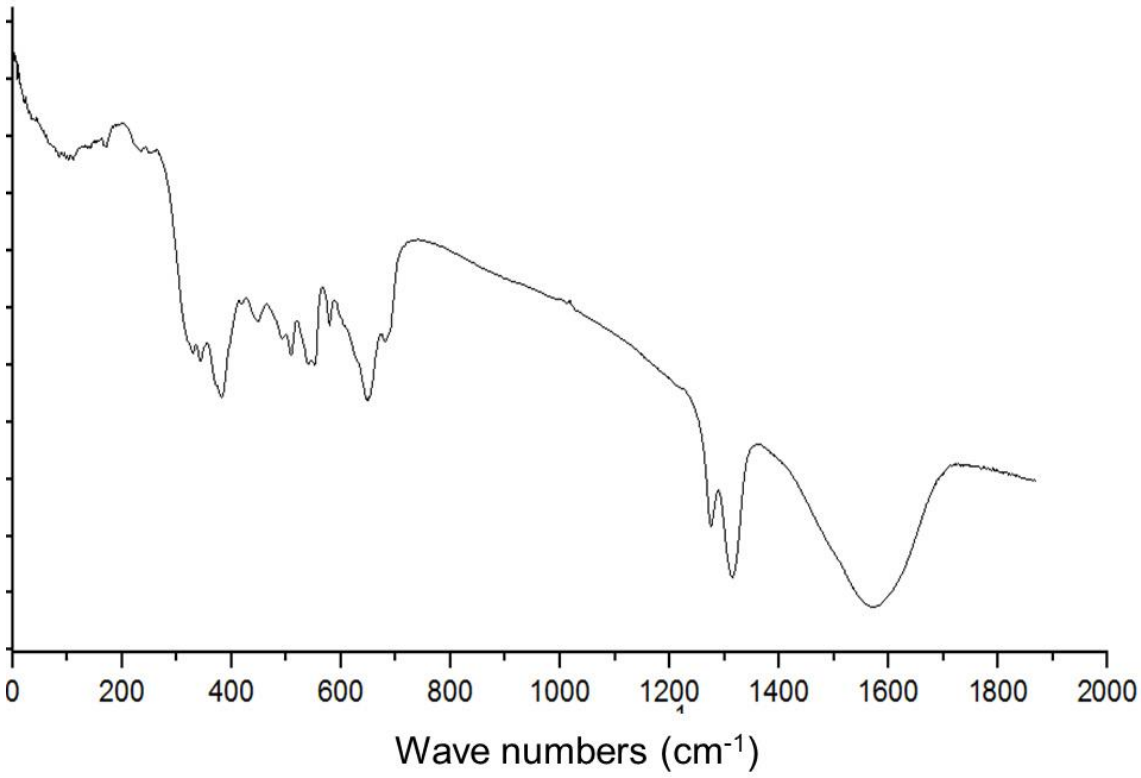

Figure S62: IR-RT spectra of SP_C0_1 biocatalyst.

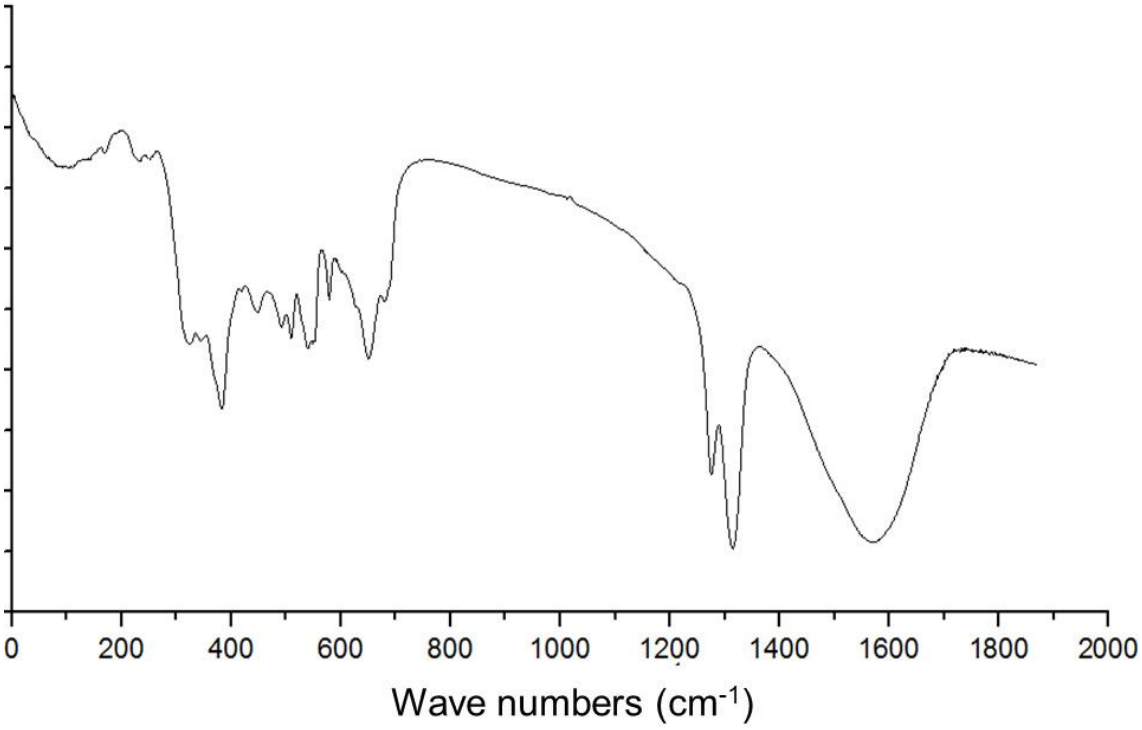

Figure S63: IR-RT spectra of SP_C6_3 biocatalyst.

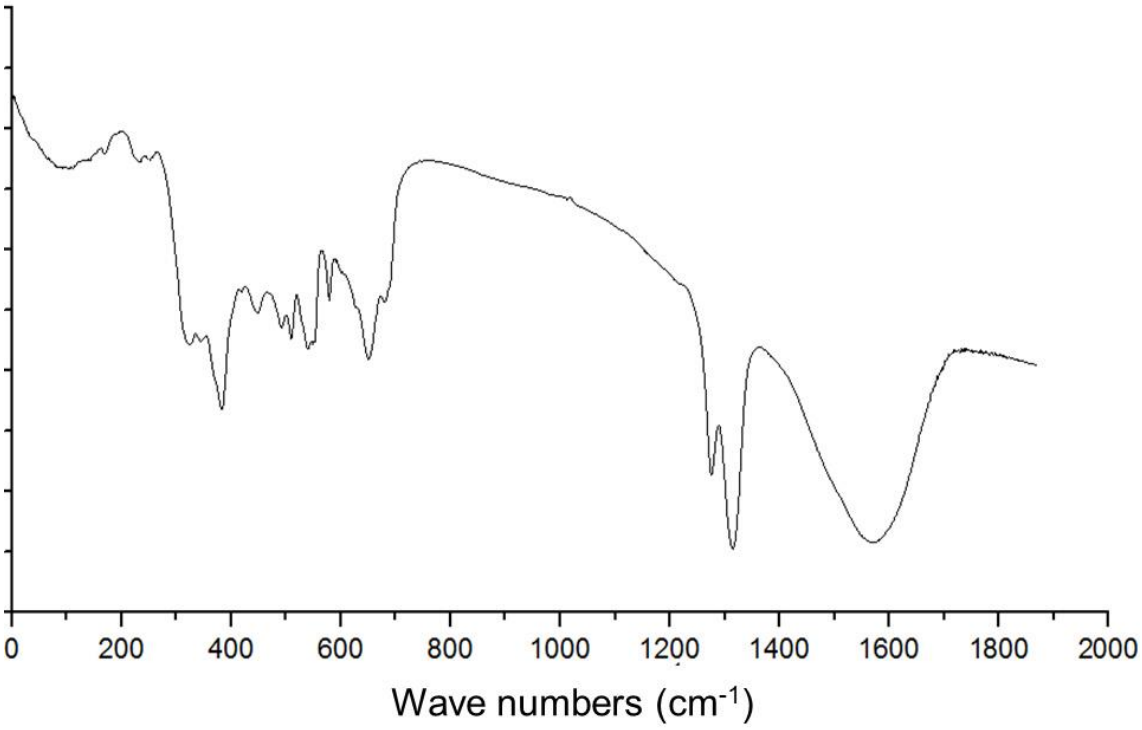

Figure S64: IR-RT spectra of SP_C6_2 biocatalyst.

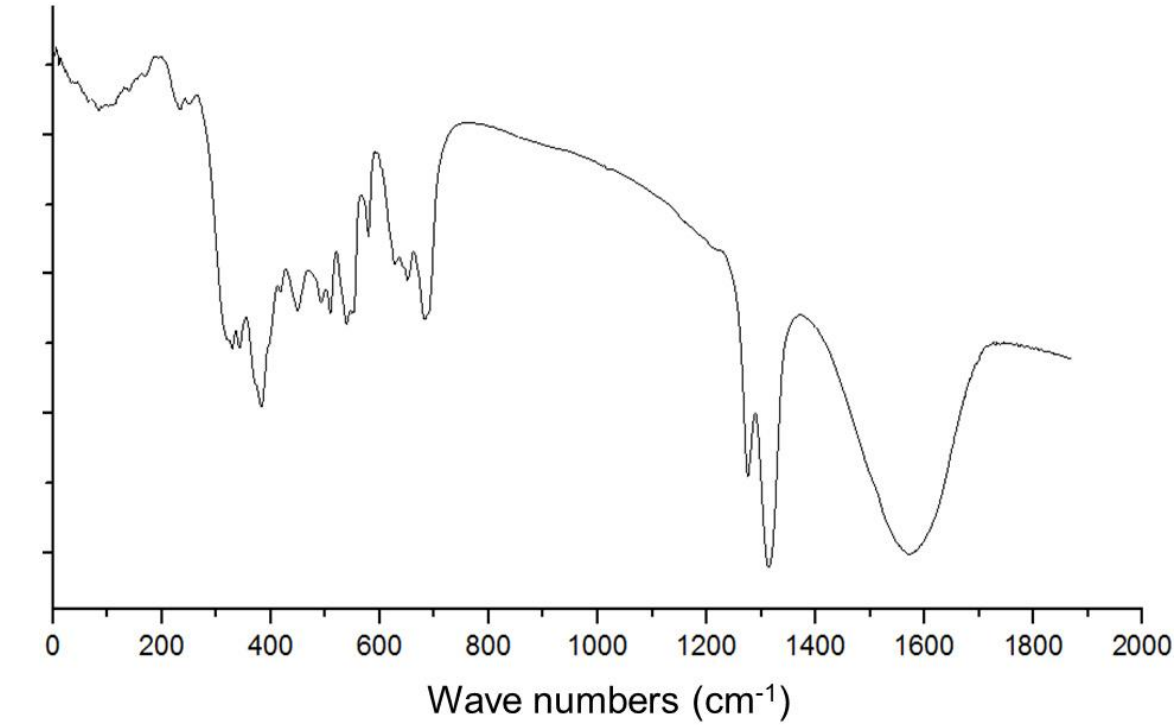

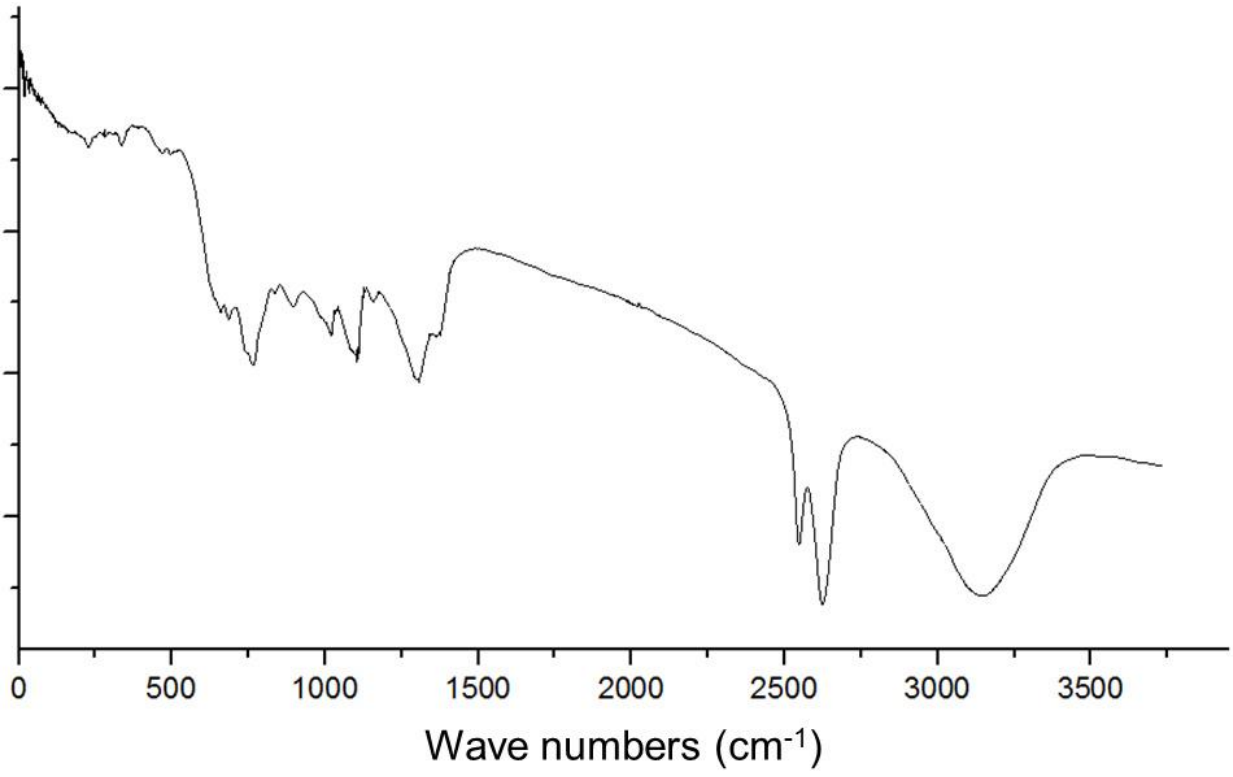

Figure S65: IR-RT spectra of SP_C2 biocatalyst.

Figure S66: IR-RT spectra of SP_C4 biocatalyst.

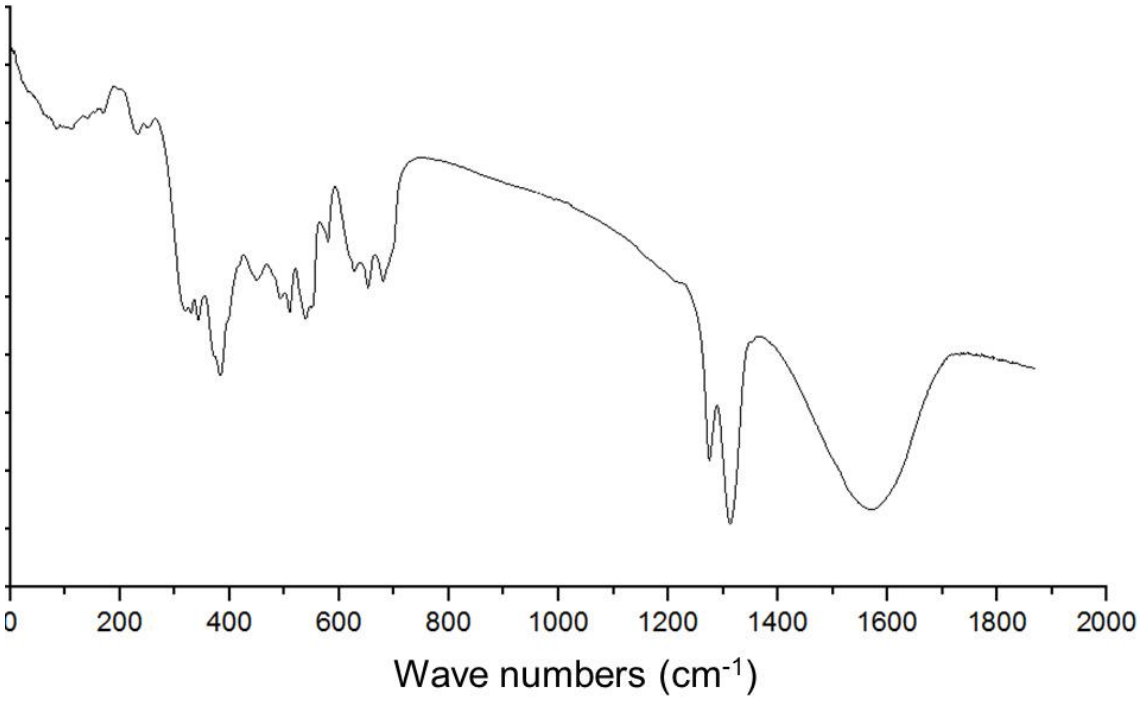

Figure S67: IR-RT spectra of SP_C6_4 biocatalyst.

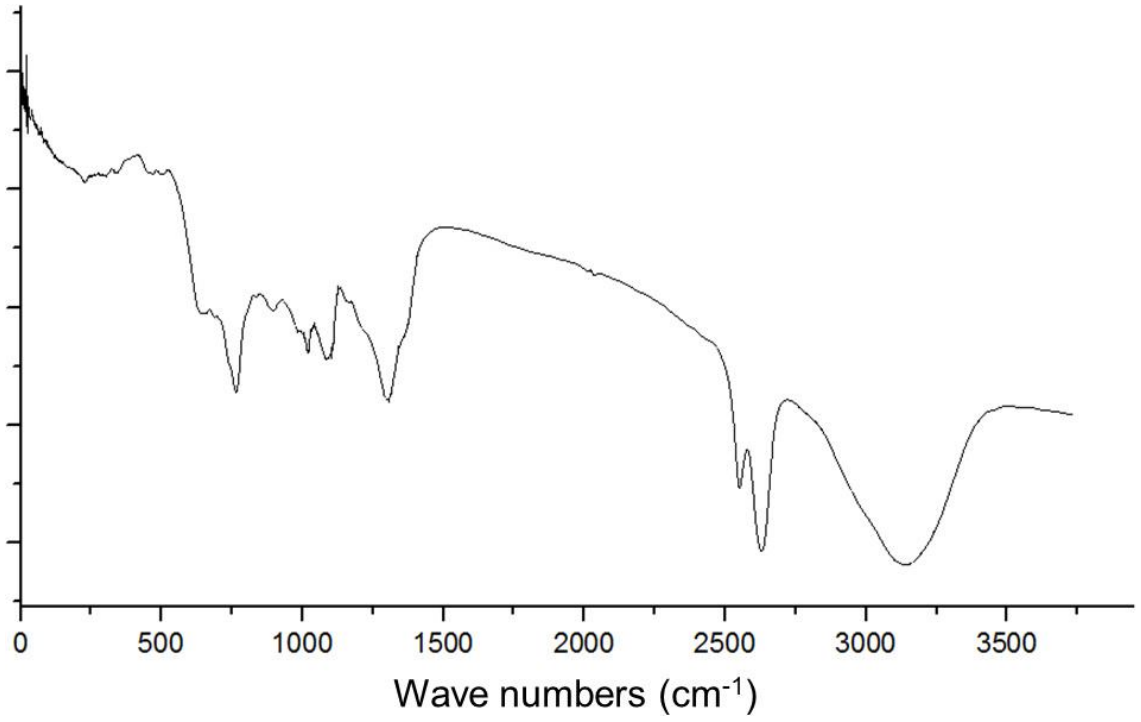

Figure S68: IR-RT spectra of SP_C6 biocatalyst.

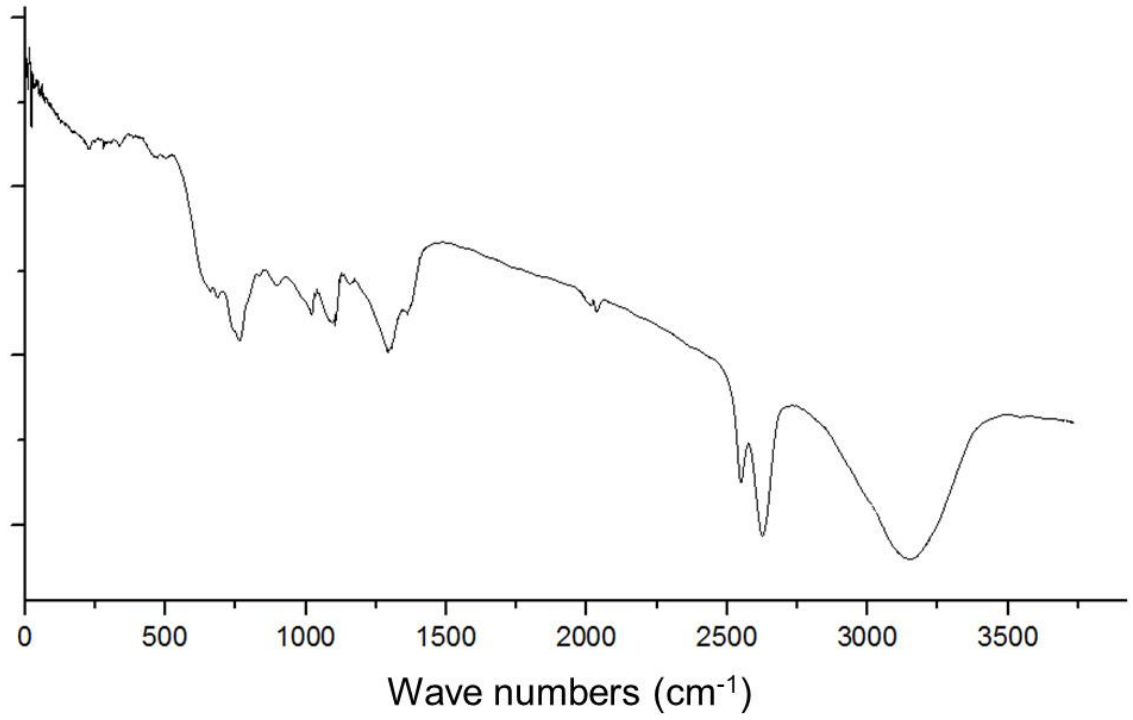

Figure S69: IR-RT spectra of SP_C6_1 biocatalyst.

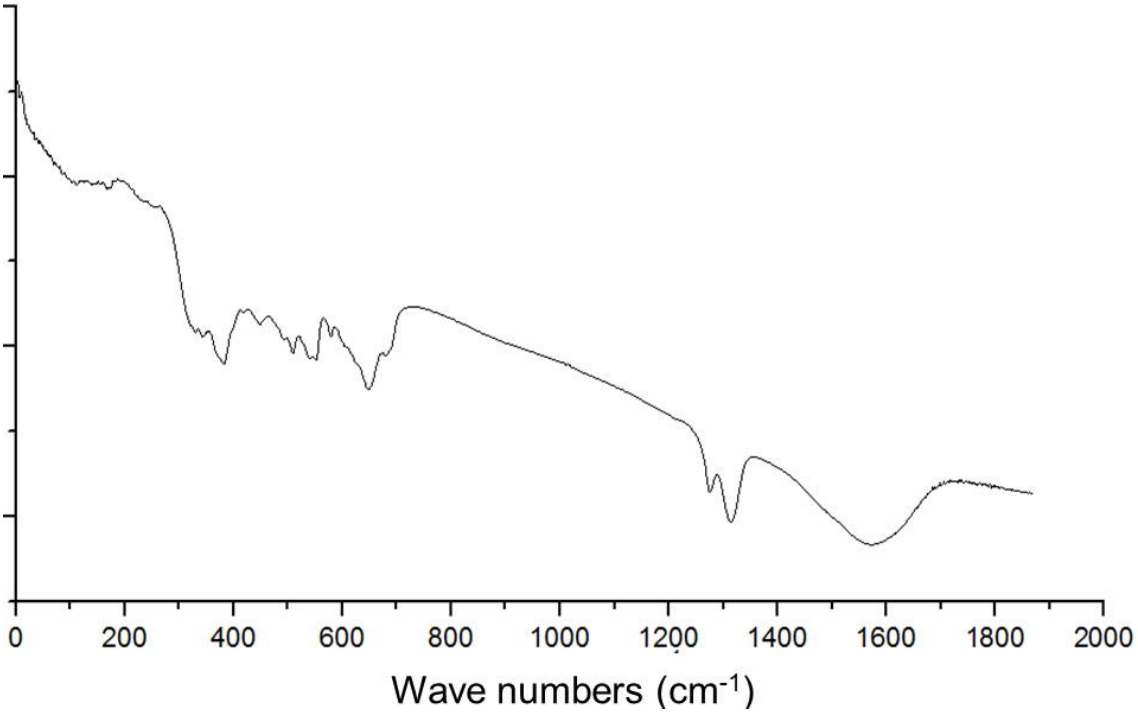

Figure S70: IR-RT spectra of SP_C8 biocatalyst

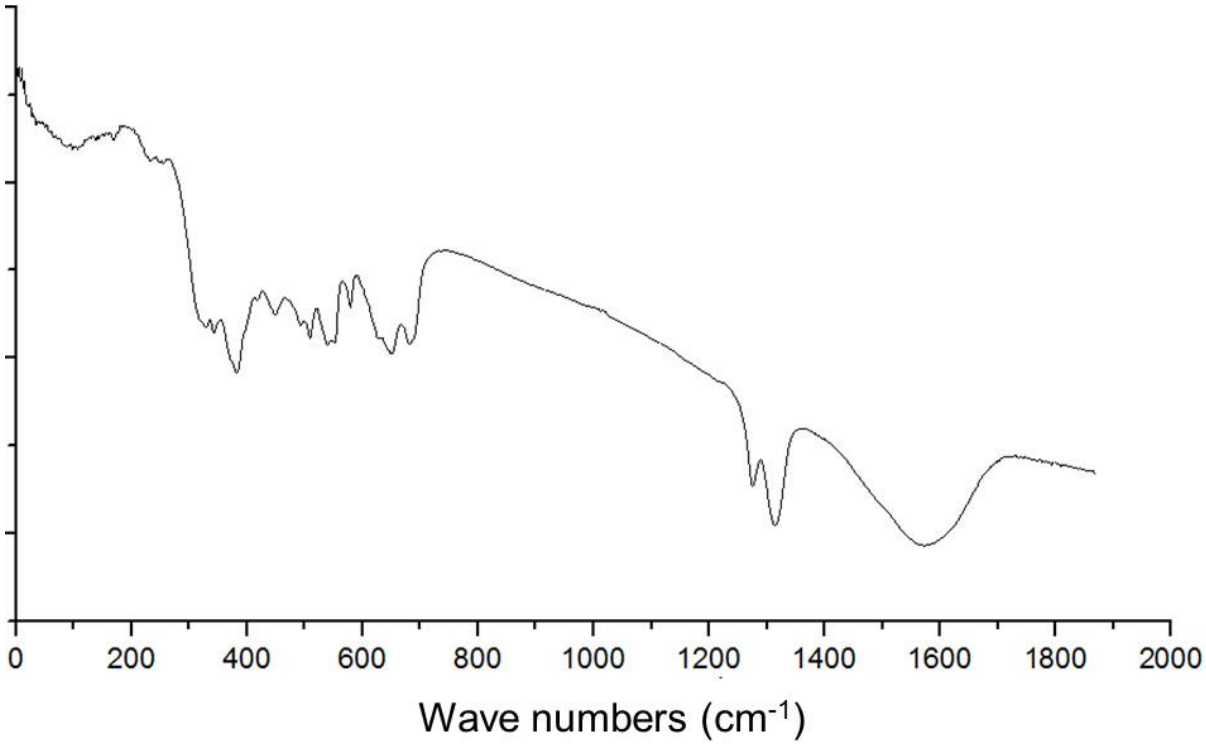

Figure S71: IR-RT spectra of SP_C10 biocatalyst.

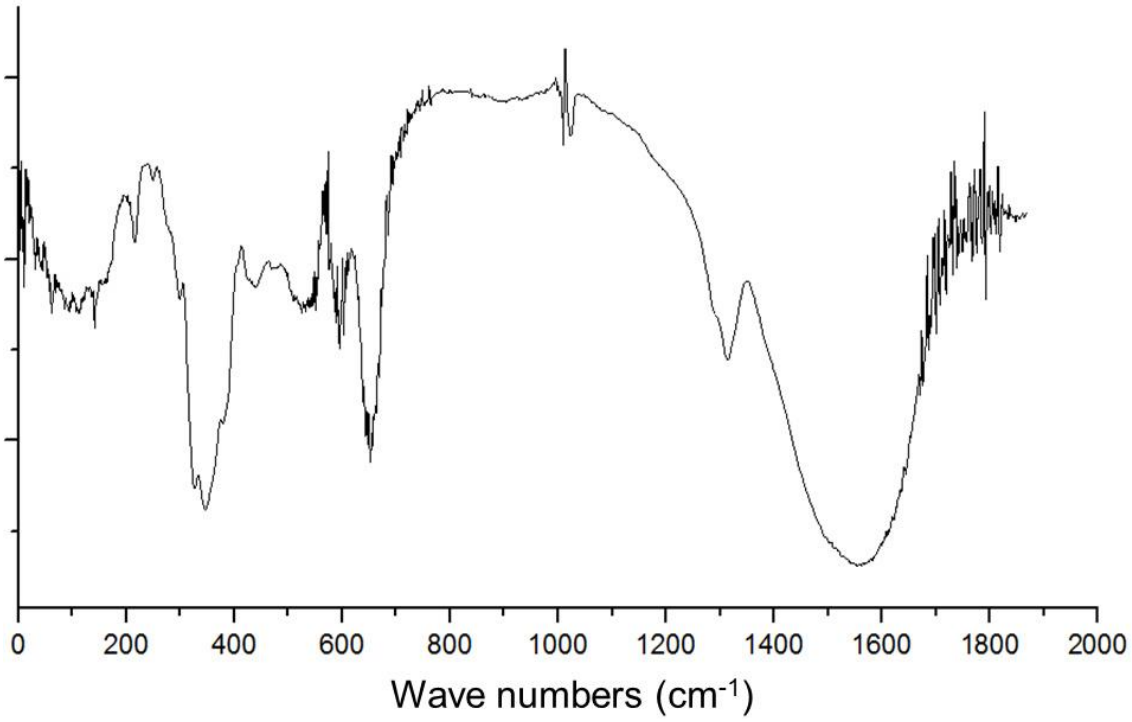

Figure S72: IR-RT spectra of Novozyme 435 biocatalyst.